



HAL
open science

Etude expérimentale des régimes de combustion d'un feu de compartiment dans des conditions de sous-ventilation

Anthony Edwin Pearson

► To cite this version:

Anthony Edwin Pearson. Etude expérimentale des régimes de combustion d'un feu de compartiment dans des conditions de sous-ventilation. Energie électrique. Université de Poitiers, 2007. Français. NNT: . tel-00259507

HAL Id: tel-00259507

<https://theses.hal.science/tel-00259507>

Submitted on 28 Feb 2008

HAL is a multi-disciplinary open access archive for the deposit and dissemination of scientific research documents, whether they are published or not. The documents may come from teaching and research institutions in France or abroad, or from public or private research centers.

L'archive ouverte pluridisciplinaire **HAL**, est destinée au dépôt et à la diffusion de documents scientifiques de niveau recherche, publiés ou non, émanant des établissements d'enseignement et de recherche français ou étrangers, des laboratoires publics ou privés.

THÈSE

pour l'obtention du grade de

DOCTEUR de l'UNIVERSITÉ de POITIERS

École Nationale Supérieure de Mécanique et d'Aérotechnique

&

Faculté des Sciences Fondamentales et Appliquées

(Diplôme National – Arrêté du 7 août 2006)

École Doctorale Sciences pour l'Ingénieur et Aéronautique

Secteur de Recherche : Énergie, Thermique, Combustion

Présentée par :

Anthony Edwin PEARSON

ÉTUDE EXPÉRIMENTALE DES RÉGIMES DE COMBUSTION D'UN FEU DE COMPARTIMENT DANS DES CONDITIONS DE SOUS-VENTILATION

EXPERIMENTAL STUDY OF THE COMBUSTION REGIMES OF A COMPARTMENT FIRE UNDER CONDITIONS OF UNDERVENTILATION

Directeurs de thèse : Jean-Michel MOST et David Douglas DRYSDALE

Soutenue le 6 Février 2007
devant la Commission d'Examen

- JURY -

M. F. PENOT
M. A. COPPALLE
M. B. KARLSSON
M. D. DRYSDALE
M. J.-M. MOST
M. P. ROUSSEAUX

Directeur de Recherche CNRS au LET, Poitiers
Professeur au CORIA, Rouen
Professeur à l'Université d'Islande, Reykjavik
Professeur à l'Université d'Edimbourg, Ecosse
Directeur de Recherche CNRS au LCD, Poitiers
Professeur à l'Université de Poitiers

*Président
Rapporteur
Rapporteur*

THÈSE

pour l'obtention du grade de

DOCTEUR de l'UNIVERSITÉ de POITIERS

École Nationale Supérieure de Mécanique et d'Aérotechnique

&

Faculté des Sciences Fondamentales et Appliquées

(Diplôme National – Arrêté du 7 août 2006)

École Doctorale Sciences pour l'Ingénieur et Aéronautique

Secteur de Recherche : Énergie, Thermique, Combustion

Présentée par :

Anthony Edwin PEARSON

ÉTUDE EXPÉRIMENTALE DES RÉGIMES DE COMBUSTION D'UN FEU DE COMPARTIMENT DANS DES CONDITIONS DE SOUS-VENTILATION

Directeurs de thèse : Jean-Michel MOST et David Douglas DRYSDALE

Soutenue le 6 Février 2007
devant la Commission d'Examen

- JURY -

M. F. PENOT
M. A. COPPALLE
M. B. KARLSSON
M. D. DRYSDALE
M. J.-M. MOST
M. P. ROUSSEUX

Directeur de Recherche CNRS au LET, Poitiers
Professeur au CORIA, Rouen
Professeur à l'Université d'Islande, Reykjavik
Professeur à l'Université d'Edimbourg, Ecosse
Directeur de Recherche CNRS au LCD, Poitiers
Professeur à l'Université de Poitiers

Président
Rapporteur
Rapporteur

Acknowledgements

Any PhD project relies on a triangular relationship between the student, the supervisors and the financiers.

I have had a rather high turnover rate of supervisors during the years I have been working towards the creation of this thesis. Prof Dougal Drysdale from the University of Edinburgh has been with the project from the outset, providing the benefit of his experience, unflappability, optimism and wide-ranging knowledge on all aspects of fire safety engineering and science. Doctor Asif Usmani accompanied me for the first few months as co-supervisor, acting as a second source of patience and optimism. After growth and restructuring of the Fire Safety Research Group at the University of Edinburgh, the role of co-supervisor was passed to Prof José Torero, a seemingly endless fountain of knowledge and important source of moral support. Prof Bill Easson was added to the team, officially only as “Supervision Assistant”, but that description that does not do justice to the technical aid and tuition he provided. The French Connection in the project was directed by Dr Jean-Michel Most, providing the benefit of his constant availability whenever help was needed, his experience in writing reports and papers and his generosity (not to mention his cooking).

As for the financial support, I am indebted to my parents not only for the moral support that one comes to take for granted, but also for a five-digit sum of hard currency. To their relief, I had the fortune to receive a grant from the US National Fire Protection Association and then later obtain funding from the Firenet research network financed by the European Union – a project which not only provided a generous grant, but also much opportunity to collaborate with other key people in the field of fire safety research. In particular, valuable help was gained via the network from Profs Colomba di Blasi, Mike Delichatsios and Jennifer Wen, and Drs

Remerciements

Tout projet de thèse est basé sur une relation triangulaire entre l'étudiant, les encadrants et les financiers.

Mon taux d'usage d'encadrants était assez haut pendant les années où j'ai travaillé sur ce projet. Prof Dougal Drysdale de l'Université d'Edimbourg a suivi le projet dès le début, et j'ai pu profiter de son expérience, son imperturbabilité, son optimisme et son savoir vaste sur l'ensemble du domaine de la sécurité incendie. Dr Asif Usmani m'a accompagné pendant les premiers mois comme co-directeur de thèse, et était une deuxième source de tranquillité et d'optimisme. Suite à l'élargissement et à la réorganisation de l'équipe de recherche de sécurité incendie à l'Université d'Edimbourg, le rôle de co-directeur est passé au Prof José Torero, une source, comme il semble, inexhaustible de savoir et une source importante de soutien moral. Prof Bill Easson a été ajouté à l'équipe, officiellement comme « Assistant de Direction », mais cette description ne rend pas compte à l'aide technique et la formation qu'il m'a offertes. Le côté français du projet a été dirigé par Dr Jean-Michel Most, qui m'a fait profiter de sa disponibilité quasiment constante quand il y avait besoin d'aide, de son expérience dans l'écriture des rapports et des articles et de sa générosité (sans parler de sa cuisine).

Pour le soutien financier, je suis redevable à mes parents, non seulement pour le soutien moral dont on profite sans demander, mais aussi pour une somme d'argent de cinq chiffres. J'ai ensuite eu la chance de recevoir une bourse de la National Fire Protection Association aux Etats-Unis, et plus tard j'ai obtenu une bourse par le réseau Firenet, financée par l'Union Européenne. Ce réseau ne m'a pas seulement offert une bourse généreuse, mais également beaucoup d'opportunités de collaborer avec des personnes dans le cadre mondial de la recherche sur la sécurité incendie. En particulier, j'ai reçu de l'aide importante par le réseau des

Carmen Branca, Andrej Horvat and Yehuda Sinai

I would like to thank Profs Alexis Coppalle, Björn Karlsson and Patrick Rousseaux, and Dr François Penot for accepting the task of reviewing and judging my work.

An experimental project as complicated as the one described in this document would not get very far without assistance from the technical staff who provide many ideas, but whose names rarely figure in the lists of authors of any reports. I would like to thank Neil Wood and Jacques Baillargeat for retaining their humour when faced with requests to do the impossible, Jean-Paul Bigeau for his patience after the countless times I broke the fruits of his labour, Pascal Grelier for finding better ways of constructing the objects I asked him to build, Alain Claverie for ensuring that I did not repeat the operational errors of an anonymous student in Edinburgh which were behind my being moved to France, Cécile Losier for being a rich source of ideas, and Kevin Anderson, Véronique Bertin, Daniel Falaise and Yves Foy for their skilled work in their respective fields.

The advice of people who previously worked on a project is of course also invaluable; Drs Davoud Ahmadyar, Mickaël Coutin, Gérard Débenest and Jean-Marc Rousset provided the benefit of their experience. I am also indebted to Dr Bertrand Poireault and to Gilles Bertin and Jérôme Ricola: although I have not had the honour to meet these gentlemen, the reports they left behind describing the work they performed at the LCD before I arrived aided my understanding of the history of the project.

During the first months in Poitiers I had the good fortune to work alongside Yann Beaumin, who provided many an idea and for whose presence during the initial experimental work aided the assurance of safe working practice (No I wasn't trying to kill you when I singed your hair).

Profs Colomba di Blasi, Mike Delichatsios et Jennifer Wen, et des Drs Carmen Branca, Andrej Horvat et Yehuda Sinai.

J'aimerais remercier les Profs Alexis Copalle, Björn Karlsson et Patrick Rousseaux, et Dr François Penot pour avoir accepté de relire et de juger mon travail.

Un projet expérimental si complexe que celui décrit dans ce document ne serait pas possible sans l'aide du personnel technique qui fournit beaucoup d'idées mais qui ne figure que rarement dans les listes d'auteurs de rapports. J'aimerais remercier Neil Wood et Jacques Baillargeat pour avoir gardé leur humour quand je leur ai passé des demandes pour faire l'impossible, Jean-Paul Bigeau pour avoir gardé sa patience après toutes les fois où j'ai cassé ses constructions, Pascal Grelier pour avoir trouvé de meilleurs façons de construire les pièces que je lui ai demandées de produire, Alain Claverie pour avoir assuré que je n'ai pas répété les erreurs d'un étudiant anonyme à Edimbourg qui sont la raison pourquoi je suis venu en France, Cécile Losier pour ses idées, et Kevin Anderson, Véronique Bertin, Daniel Falaise et Yves Foy pour leur travail de spécialiste.

Les conseils des gens ayant déjà travaillé sur un projet sont bien sûr aussi très précieux. Drs Davoud Ahmadyar, Mickaël Coutin, Gérard Debenest et Jean-Marc Rousset m'ont fait profiter de leur expérience. Je suis également redevable de Dr Bertrand Poireault et de Ms. Gilles Bertin et Jérôme Ricola ; je n'ai jamais rencontré ces messieurs, mais les rapports qu'ils ont laissés de leurs travaux avant mon arrivée au LCD m'ont aidé à comprendre la trame de fond du projet.

Pendant mes premiers mois à Poitiers, j'ai eu la chance de travailler à côté de Yann Beaumin, qui a fourni beaucoup d'idées et qui a aidé à assurer un fonctionnement sécurisé dans la salle d'expérience (quand je t'ai brûlé les cheveux, ce n'était pas une tentative pour te tuer).

La collaboration internationale pendant

The international collaboration which was set up during the project provided unusual challenges to the administrative staff. The secretaries, particularly Ruth Khan and Jocelyne Bardeau, provided immeasurable practical help, moral support and humour. I owe more debt than most of the ENSMA's PhD students to Corinne Dutault and the *Scolarité* team at the ENSMA, to Martine Lafont and to Sylvie Perez and the *Scolarité* team at the faculty offices in Poitiers for their flexibility and humour in tackling whatever complications landed at their respective doors.

I would like to thank Profs Andrew Barry, Pascal Bauer, Yves Bertrand, Peter Grant, Francis Roger and Claude Templier, and Drs Michel Champion, Pierre Joulain and Henri-Noël Presles for their tireless work at the unrewarding task of getting the scientists in their respective institutions to work together as a team.

I would also like to express my gratitude to Dr Patrice Remaud and to François Baty-Sorel for providing much more than just lectures.

The people I met, too numerous to list, during the seminars, conferences and meetings I attended since starting the project were a source of inspiration and hope for the future of fire safety science.

The sanity of any PhD student depends heavily on the support he or she obtains from his or her fellow students. I owe my gratitude to all who have passed my way during the course of the project. The following deserve particular mention. Drs Jo Sherrat and Kuang Chung Tsai who shared their office with me in Edinburgh, showed me the ropes and pointed out that any problems I may experience are nothing compared to what they had had to deal with. Dr Tim Andzi Barhé took me under his wings during the first years at Poitiers and provided immeasurable moral support. Dr Philipp Bauer provided many an idea and useful technical and computing support. Dr Gabriel

le projet a donné des défis particuliers pour le personnel administratif. Les secrétaires, en particulier Ruth Khan et Jocelyne Bardeau, ont offert de l'aide pratique, du soutien moral et un humour incommensurable. Je dois beaucoup plus que le plupart des thésards de l'ENSMA à Corinne Dutault et l'équipe de la Scolarité à l'ENSMA, à Martine Lafont et à Sylvie Perez et l'équipe de la Scolarité de la Faculté SFA à Poitiers pour leur flexibilité et leur humour dans la résolution de toutes les complications qui leur sont tombées dessus.

J'aimerais exprimer ma gratitude envers les Profs Andrew Barry, Pascal Bauer, Yves Bertrand, Peter Grant, Francis Roger et Claude Templier, et les Drs Michel Champion, Pierre Joulain et Henri-Noël Presles pour leur travail dans la tâche ingrate de faire travailler comme collectif les scientifiques dans leurs institutions respectives.

J'aimerais également remercier Dr Patrice Remaud et François Baty-Sorel pour ne pas avoir que donné des cours.

Les personnes, trop nombreuses pour être citées ici, que j'ai rencontrées pendant les séminaires, conférences et réunions auxquelles j'ai assisté, ont été une source d'inspiration et d'espoir pour l'avenir de la science de sécurité incendie.

La santé mentale d'un thésard dépend fortement du soutien qu'il ou elle reçoit des autres étudiants. Je dois une gratitude à tous ceux qui ont croisé mon chemin pendant le projet. Les suivants méritent particulièrement d'être nommés : Drs Jo Sherrat et Kuang Chung Tsai qui ont partagé leur bureau à Edimbourg avec moi, qui m'ont introduit dans le travail de recherche et qui ont montré que tout problème que je pourrais avoir n'est rien comparé aux difficultés qu'ils ont eues. Dr Tim Andzi Barhé m'a accompagné pendant les premiers mois à Poitiers et m'a donné un soutien moral inestimable. Dr Philipp Bauer m'a fourni avec beaucoup d'idées et donné du soutien avec l'informatique. Dr Gabriel Canteins a joué un rôle

Canteins played a key part in bringing us students together to form a social group rather than remaining collection of individuals. Dr Rui Rego and soon-to-be-Dr Weylong SiauW provided invaluable support simply by showing that one can remain calm and composed despite all the hardships. Drs and not-yet-Drs Sébastien Bourgois, Bastien Boust, Fabien Chassagne, Yun Chi Chung, Max Clarke, Cony Dörich, Hazem El Rabii, Olivier Esnault, Sergio Ferraris, Andrès Fuentes, John Grondin, Georges Guigay, Vianney Guilly, Nicolas Henne-ton, Larbi Jabine, Stephen Johnson, Susan Lamont, Yu Ying Liu, Bernardo Martinez, Raphael Meyrand, Phu Khan Nguyen, Laurence Pagnanini, Scott Rodgers, Yussef Roudani, Jacques Tézanou, Piotr Tofilo, and Mmes Elena Chouteau and Ioana Magda all provided many an hour of company.

Finally, I owe a lot to those who provided me with space to escape occasionally from the ivory tower and communicate with the rest of humanity. The staff at the fire station in Jaunay Clan entertained me for many an hour and provided fascinating insight into the business side of fire safety in France. The Scout Association in the UK and the Eclaireuses Eclaireurs de France provided me with much support without which I don't know how I would have coped. I am convinced that the friendship, training, leadership experience and moral support I gained during my time in Scouting outweigh the benefit the Scout Movement received from me. I would like to thank everyone I met in Scouting for the experience and friendship, particularly the teams of the 75th, 85th, 98th and 139th Groups in Edinburgh, Blackford District Leadership, Edinburgh Area Leadership, the OASIS team in Edinburgh, the team of the Poitiers Group, Aquitaine-Poitou-Charentes Regional Leadership, but equally the Beavers, Cubs, Scouts, Venture Scouts, trainee Leaders and parents who allowed me the privilege of working with them. Particular mention is due to Chantal Cherrier, Dr Louise Fromard,

clé pour faire que nous étudiants formions un groupe social au lieu de rester une collection d'individus. Dr Rui Rego et bientôt-Dr Weylong SiauW m'ont donné du soutien tout simplement en montrant qu'il est possible de rester calme malgré les difficultés. Drs et pas-encore-Drs Sébastien Bourgois, Bastien Boust, Fabien Chassagne, Yun Chi Chung, Max Clarke, Cony Dörich, Hazem El Rabii, Olivier Esnault, Sergio Ferraris, Andrès Fuentes, John Grondin, Georges Guigay, Vianney Guilly, Nicolas Henne-ton, Larbi Jabine, Stephen Johnson, Susan Lamont, Yu Ying Liu, Bernardo Martinez, Raphael Meyrand, Phu Khan Nguyen, Laurence Pagnanini, Scott Rodgers, Yussef Roudani, Jacques Tézanou, Piotr Tofilo, et Mmes Elena Chouteau and Ioana Magda ont tous donné beaucoup d'heures de leur temps en ma compagnie.

Enfin, je dois beaucoup à ceux qui m'ont donné de l'espace pour sortir parfois de la tour d'ivoire et pour communiquer avec le reste de l'humanité. Le corps du centre de secours et d'incendie de Jaunay Clan m'a offert beaucoup d'heures de divertissement et m'a montré le fonctionnement du côté pratique de la sécurité incendie en France. La Scout Association en Grande-Bretagne et les Eclaireuses Eclaireurs de France m'ont apporté beaucoup de soutien, sans lequel je ne vois pas comment j'aurais pu aller au bout. Je suis convaincu que l'amitié, la formation, l'expérience et le soutien moral que j'ai reçus pendant le temps dans le Scoutisme valent plus que ce que le Mouvement Scout a reçu de moi. J'aimerais remercier tous ceux que j'ai rencontrés aux Scouts et Eclaireurs pour l'expérience et l'amitié, en particulier les équipes des 75^{me}, 85^{me}, 98^{me} et 139^{me} Groupes à Edimbourg, l'équipe de District de Blackford, l'équipe régionale d'Edimbourg, l'équipe du Groupe de Poitiers et l'équipe régional Aquitaine-Poitou-Charentes, mais aussi les Castors/Lutins, Louveteaux, Eclaireuses/eurs, Aîné(e)s, stagiaires en animation et parents qui m'ont donné le privilège de travailler

Edwin Maxwell, Wayne Pearson (no relation to the author), Frank Reynolds and Véro Sapin for the invaluable moral support they provided.

avec eux. Chantal Cherrier, Dr Louise Fromard, Edwin Maxwell, Wayne Pearson (aucune relation avec l'auteur), Frank Reynolds et Véro Sapin méritent particulièrement d'être cités pour le soutien moral inestimable qu'ils m'ont offert.

Table of Contents

Résumé	15
Symbols and Abbreviations.....	23
1 Introduction	27
1.1 Background	27
1.2 Literature Review	30
1.2.1 The Combustion Process.....	30
1.2.2 Fires in the Open	33
1.2.3 Compartment Fires.....	35
1.2.3.1 Fires in Very Well Ventilated Compartments.....	35
1.2.3.2 Fires in Compartments with “Normal” Ventilation	37
1.2.3.3 Underventilated Compartment Fires	47
1.2.3.4 Special Cases.....	50
1.2.4 Fires with Raised Fuel Sources	52
1.3 Aims	57
1.4 Contents of this Report.....	58
2 Experimental Apparatus	59
2.1 Compartments	60
2.1.1 Bertin Compartment.....	60
2.1.2 “Telephone Box”.....	63
2.2 Fuel Sources	64
2.2.1 Use of Gas Burners to Simulate Solid or Liquid Fuels	64
2.2.2 Burners used in the Study.....	66
2.2.2.1 Porous Burner.....	66
2.2.2.2 Line Burner	68
2.2.2.3 Sand-Bed Burner	68
2.2.3 Gas Supply	70
2.3 Measurements performed and Diagnostics used	71
2.3.1 Imaging of Flame	71
2.3.2 Velocity Measurements	72
2.3.2.1 Equipment	73
2.3.2.2 Velocity Field around the Burner.....	76
2.3.2.3 Velocity Field around the Edge of the Flame.....	78

2.3.2.4 Vent Flow Rate	80
2.3.3 Temperature Measurement.....	82
2.3.4 Chemical Analysis.....	83
2.3.5 Area Covered by the Flame.....	85
2.3.5.1 Aims and Concept.....	85
2.3.5.2 Technology used to measure the area covered by the flame	87
2.4 Operating Procedure.....	90
2.4.1 Ignition Procedure	90
2.4.2 Time to Steady State	91
3 Results and Discussion	97
3.1 Observation of Shape and Behaviour of the Flame.....	97
3.1.1 Overview	98
3.1.2 Flame Shape and Behaviour.....	98
3.1.2.1 Generalities	98
3.1.2.2 Blue Partial Interface Flames	102
3.1.2.3 Yellow Full Interface Flames	103
3.1.3 Extinction	104
3.2 Aerodynamics, Flame Structure and Stability.....	104
3.2.1 Velocity Field at the Exit of the Burner	105
3.2.2 Velocity Field around the Edge of the Flame.....	106
Motion of the Flame Edge.....	108
3.2.2.1 Velocity Field relative to the Flame.....	108
3.2.3 Temperature Field	110
3.2.3.1 Temperature Histories.....	110
3.2.3.2 Maps of Average Temperatures	112
3.2.4 Chemical Makeup of the Upper Layer	116
3.2.5 Tests with Methane as Fuel.....	118
3.2.6 Discussion	118
3.2.6.1 Flow Pattern	118
3.2.6.2 Flame Structure	120
3.2.6.3 Flame Stability	121
3.2.6.4 Presence of External Flaming	123
3.2.6.5 Influence of Fuel and Comparison with Morehart's Configuration.....	123
3.3 Analysis of the Area Covered by the Flame.....	124
3.4 Influence of the Ventilation on the Behaviour of the Flame	134

3.4.1 Description of the Behaviour	134
3.4.2 Layer Depth	137
3.4.3 Minimum Fuel Flow Rate	140
3.4.4 Temperatures	143
3.4.5 Vent Flow Rate.....	145
3.4.6 Discussion	151
3.4.6.1 Ventilation Regime	151
3.4.6.2 Extinction	153
4 Conclusion.....	163
References	167
Annexe – Estimate of the Heat Losses	171
Basic Assumptions and Input Values	171
Temperatures.....	171
Material Properties	172
Heat Losses through Walls.....	174
Convective Heat Transfer through the Vent.....	177
References	178

Résumé

1 Introduction

Lors des dernières décennies, un nombre important de recherches a été consacré aux feux libres ou confinés dans des compartiments. Ces études ont permis de faire évoluer les simulations numériques et d'obtenir des outils d'analyse de sûreté performants. Malgré cela, les incendies restent toujours synonymes de cause majeure de dégâts matériels et de pertes de vies humaines.

Les feux de compartiment présentent des comportements très variés qui dépendent principalement de la nature, de la position du combustible ainsi que de la ventilation de l'enceinte. Une partie de la chaleur dégagée par la flamme et des produits de combustion peut être piégée en dessous du plafond ce qui augmente le flux de chaleur vers les sources de combustible disponibles qui s'embrasent alors.

La plupart des recherches sur les feux de compartiment a porté sur des configurations dans lesquelles la source de combustible était positionnée sur, ou à proximité du sol. Par contre, peu d'informations sont disponibles sur le comportement d'un feu lorsque la source de combustible est dans une zone sous-ventilée. L'étude d'un tel scénario reste une priorité au Laboratoire de Combustion et de Détonique (LCD) dans le contexte du risque incendie dans les installations à ventilation contrôlée. De tels édifices posent des problèmes spécifiques quant à la sécurité d'incendie, la ventilation est réglée pour que les effluents, souvent polluants et toxiques, ne puissent être rejetés directement dans l'environnement.

Lors d'un précédent projet, des tests préliminaires ont été effectués en simulant partiellement, grâce à l'injection d'un hydrocarbure gazeux à travers un brûleur, la dégradation d'un combustible solide ou l'évaporation d'un combustible liquide. Cette simulation a permis à l'expérimentateur de décorréler le débit de combustible du flux de chaleur transmis des produits de combustion vers la source de combustible. Le dispositif expérimental consiste en une enceinte munie d'un linteau afin de piéger une couche chaude de fumées et de produits de combustion dans sa partie haute. Si le brûleur de simulation est en position basse dans l'enceinte, un panache de feu susceptible d'interagir avec la zone chaude se forme au-dessus du brûleur. Si le brûleur est placé en proximité de l'interface entre la couche supérieure de fumées et la couche d'air inférieure, l'entraînement d'air dans le panache ne va suffire que pour une combustion incomplète dans ce dernier, et par conséquent

du combustible imbrûlé va être transporter vers la couche supérieure, ce qui peut mener à l'apparition de flammes à l'interface entre les couches. Si le brûleur est maintenant placé dans la couche supérieure, et avec un faible débit de combustible, la flamme s'éteint. Pour de plus forts débits de gaz la flamme se détache du brûleur et se stabilise à l'interface entre les couches. Selon le débit de combustible, il est observé soit des flammes jaunes cellulaires couvrant toute l'interface, soit des flammes bleu-jaunes dont le taille fluctue sur une partie de l'interface.

Le but de ce travail de thèse est de compléter nos connaissances sur le comportement des feux quand la source de combustible est située dans la zone chaude piégée par le linteau. Les objectifs suivants ont été recherchés :

- l'identification des mécanismes qui permettent à la flamme de se stabiliser à l'interface entre les deux couches ;
- l'étude de l'influence du type de combustible, de son débit (et donc la puissance calorifique théoriquement dégagée), de la hauteur du linteau et de la taille de l'ouverture en dessous du linteau sur les régimes de flamme contrôlés par le débit de combustible ou par le débit d'air entrant.

2 Installation expérimentale

Cette recherche a été menée dans un compartiment à l'échelle de laboratoire (0.62 m de long, 0.84 m de haut, 0.40 m de large). Deux linteaux différents de hauteurs respectives 0.19 m et 0.34 m sont installés à tour de rôle au dessus de l'ouverture pour piéger une couche de fumées et de produits de combustion capable de rayonner et enflammer des cibles combustibles. Des panneaux isolants de différentes tailles sont utilisés pour modifier le facteur de ventilation F_V en changeant la forme et la surface de l'ouverture.

La surface de la flamme à l'interface des zones chaude et froide est considérée comme une grandeur représentative de régime de flamme. Pour permettre la détermination de cette surface et la comparaison de sa partie à l'intérieur avec sa partie à l'extérieur de l'enceinte, il faut que les deux parties soient horizontales pour que l'entraînement d'air dans les deux parties soit semblable. Pour affecter ceci, un canal horizontal, ouvert en partie inférieure, a été installé à la sortie de l'enceinte.

Des brûleurs à gaz alimentés en propane ou méthane sont utilisés pour introduire du combustible gazeux dans l'enceinte.

Plusieurs différentes techniques de diagnostique ont été utilisées pour décrire la flamme, son mode de stabilisation et son régime.

Des visualisations optiques et la capture d'images au moyen de caméscopes numériques ont permis d'enregistrer la dimension et la couleur des flammes ainsi que la taille des couches inférieure et supérieure. Avec l'aide d'une caméra numérique et d'un traitement des images, la surface couverte en moyenne par la flamme en fonction des paramètres a été déterminée.

Des mesures de champs de vitesse ont été effectuées à trois endroits différents par vélocimétrie d'images de particules (PIV). D'abord le champ aérodynamique dans la zone de l'orifice du brûleur a été enregistré. Ensuite des relevés ont été effectués près du bord d'attaque des flammes. Afin de pouvoir corrélérer l'écoulement avec la position de la flamme, le temps d'exposition de la caméra PIV a été réglé pour capturer à la fois la lumière du plan de laser diffusée par les particules d'ensemencement (diffusion de Mie) et la lumière de la flamme (émission spontanée). Finalement le champ de vitesse dans l'ouverture a été mesuré afin de calculer le débit d'air entrant dans l'enceinte.

Un peigne de thermocouples détermine le champ de température moyen dans l'enceinte.

Des prélèvements de gaz dans la zone supérieure de l'enceinte ont été effectués pour déterminer la composition chimique du milieu par une analyse chimique, soit par chromatographie en phase gazeuse, soit par des analyseurs en ligne pour les espèces stables majoritaires.

3 Résultats et Discussion

3.1 Observation de la forme et du comportement de la flamme

Dans le compartiment deux couches de produits différents sont bien identifiées : une couche d'air frais dans la partie basse, et une couche riche en combustible dilué dans des produits de combustion et pauvre en oxygène en partie haute piégée par le linteau.

Pour des débits de combustible \dot{m}_F importants ($> 0.65 \text{ g/s}$, ce qui correspond à une puissance calorifique \dot{H} de 30 kW), une flamme jaune cellulaire est observée, elle couvre toute

l'interface de l'enceinte entre les deux couches. Pour des débits de combustible plus faibles, la flamme se détache des parois et présente une taille fluctuante ; en même temps, elle change de couleur pour prendre un aspect complètement bleue pour des valeurs de \dot{m}_F inférieures à 0.27 g/s (13 kW). Si le débit de combustible est encore plus réduit, les fluctuations de taille deviennent plus importantes, jusque un seuil de 0.21 g/s, en dessous duquel la flamme ne peut pas être maintenue et s'éteint.

Dans l'enceinte les couches inférieure et supérieure sont thermiquement stables. Par contre, une instabilité thermique entre la flamme (plus chaude) et la couche supérieure moins chaude se manifeste à cause des pertes au travers des parois. Ceci explique l'aspect cellulaire de la flamme : à cause des effets de flottabilité, les gaz dans la zone de réaction sont entraînés vers le haut et une partie de ceux-ci pénètre dans la couche supérieure induisant un mouvement convectif.

3.2 Aérodynamique ; structure et stabilité de la flamme

Le champ de vitesse dans la zone à proximité de l'orifice du brûleur montre que le combustible sortant du brûleur s'écoule le long du plafond puis vers l'arrière de l'enceinte pendant que des gaz et des fumées de la couche viciée sont entraînés vers le haut et recirculent. On peut alors supposer que, dans ce vortex de recirculation, le combustible se mélange et se dilue dans des produits de combustion de la couche supérieure.

Le champ de vitesse en amont du liséré d'une flamme d'interface ne recouvrant pas la totalité de la surface, montre que le fluide aborde la flamme horizontalement, est ensuite dévié vers le haut, puis continue parallèlement à la flamme. La vitesse moyenne au bord d'attaque de la flamme est 0,3 m/s ce qui est de l'ordre de grandeur de la vitesse de propagation théorique d'une flamme de prémélange laminaire – la valeur exacte de la vitesse de propagation théorique ne peut pas être déterminée avec précision, car la température et la composition chimique en amont de la flamme sont inhomogènes et difficiles à mesurer.

La température dans la couche supérieure est dans l'ordre de 500°C. Pour un plus fort débit de combustible, la température dans la couche viciée augmente jusqu'à ce que la flamme couvre toute la surface de l'interface. La température devient alors indépendante du débit de combustible et de la taille de la ventilation.

L'analyse chimique dans la couche supérieure montre la forte dilution du combustible dans des produits de combustion : on obtient une concentration de 23 % en produits de combustion (CO_2 , H_2O), 6 % en combustibles divers et 2 % en oxygène. Les 69 % restant étaient de l'azote. En amont de la flamme, le combustible est donc dilué dans les produits de combustion.

Ces résultats indiquent que lorsque la flamme ne couvre que partiellement la surface de l'enceinte, un mécanisme de flamme triple stabilise la combustion – une zone de mélange se forme entre le combustible dilué dans des produits de combustion en partie supérieure et l'air en partie inférieure. Ce prémélange, à richesse variable, autoentretient la réaction chimique ; le front de flamme se propage à contre courant de l'écoulement vers le fond de l'enceinte. En aval de ce front la majorité des réactifs brûlent dans une flamme de diffusion.

La surface de la partie de la flamme à l'intérieur de l'enceinte et la stabilité de la combustion sont liées au rapport entre la vitesse l'écoulement en amont de la flamme, v_{gaz} , et la vitesse de propagation de la flamme de prémélange, S_L , vitesse caractéristique de la flamme laminaire. Si S_L est supérieure à v_{gaz} , la flamme se propage vers le fond de l'enceinte. Inversement, si S_L est inférieure à v_{gaz} , la surface de la flamme diminue. Une augmentation du débit de combustible mène à une augmentation de sa concentration dans les produits de combustion ainsi que de la température, et par conséquent à une augmentation de S_L : donc, la surface moyenne de la flamme augmente et la combustion devient plus stable. Les fluctuations de la surface de la flamme qui sont observées sont attribuées à des variations de concentrations, de température et de vitesse d'écoulement en amont du front. Au dessus d'un certain seuil de débit de combustible, l'équilibre entre les deux vitesses n'est plus atteint et la flamme recouvre toute la surface.

La couleur bleue de la flamme (émission des radicaux d'hydrocarbures) vient du fait que peu de suies sont formées. Si le débit de combustible augmente (forte dilution du combustible), la concentration en combustible dans la zone haute augmente ; la température de flamme augmente, d'où une production plus importante de suies.

3.3 Analyse de la surface couverte par la flamme

Il a été démontré que la surface couverte par la flamme n'est pas directement proportionnelle à la chaleur dégagée, mais qu'il faut considérer la surface en fonction du débit de combustible diminué du débit minimal pour assurer la combustion, $A_{fl}(\dot{m}_F - \dot{m}_{F-\min})$. La surface est par ailleurs liée à la chaleur convective \dot{Q}_{conv} , c'est à dire la chaleur dégagée diminuée des pertes thermiques $(\dot{Q} - \dot{Q}_{loss})$.

Tant que la combustion reste contrôlée par la disponibilité en combustible, la surface couverte par la flamme est indépendante du facteur de ventilation F_V . Ce critère sur la surface de flamme est quantifié pour le débit de combustible par unité de surface de flamme, qui relie alors le comportement de la combustion au flux de combustible moyen atteignant l'interface et brûlant dans la flamme d'interface.

Pour qu'une extinction se produise, c'est-à-dire l'impossibilité de maintenir la combustion, arrive, au moins un des deux critères suivants doit être rempli :

- que la vitesse de propagation du front de prémélange S_L soit inférieure à la vitesse de l'écoulement amont,
- que la concentration de combustible soit insuffisante pour maintenir une flamme de diffusion.

Pour pouvoir prédire le comportement dans des telles configurations, mais à d'autres échelles, il est important de trouver des paramètres caractéristiques qui lient les valeurs critiques du débit de combustible avec la géométrie. Une comparaison des observations faites avec le compartiment utilisé lors de la présente étude et des données d'une installation plus grande indiquent que le rapport entre le débit de combustible et la surface de l'enceinte – quasiment un flux de combustible – est une grandeur utile pour caractériser le seuil minimum pour permettre la combustion et le seuil minimum pour que la flamme couvre toute l'interface. Ces seuils dépendent néanmoins également de la hauteur du linteau H_S . Des valeurs suivantes ont été trouvées :

	$H_S = 0.19 \text{ m}$	$H_S = 0.34 \text{ m}$
seuil pour permettre la combustion	$0,75 \text{ kg/m}^2$	$0,82 \text{ kg/m}^2$
seuil pour flamme sur toute l'interface	$1,4 \text{ kg/m}^2$	$2,6 \text{ kg/m}^2$

Si le brûleur est rapproché soit de la paroi du fond, soit de l'avant du compartiment, un plus grand débit de combustible est nécessaire pour maintenir la combustion. Ce phénomène

s'explique parce que le vortex de recirculation est plus difficile à former, donc une combustion plus instable.

3.4 Influence de la ventilation sur le comportement de la flamme

L'épaisseur de la zone viciée augmente lorsque l'on restreint l'ouverture. Si cette dernière est réduite à moins de 12 % de sa taille initiale, la zone de fumée remplit l'intégralité du compartiment.

Le débit d'air entrant par l'ouverture, calculé à partir des mesures de vitesse par PIV, montre une corrélation de celui-ci avec la puissance un-tiers du débit de combustible (\propto la chaleur dégagée) tant que celui-ci est inférieur au seuil conduisant à des flammes recouvrant toute la surface. Pour les plus forts débits de combustible, le débit d'aération reste constant.

Si le facteur de ventilation F_V est réduit, le débit d'air mesuré se réduit proportionnellement à la puissance deux-tiers de F_V . On observe que pour des tailles d'ouverture en dessous de 12 % de la largeur de l'enceinte, donc en dessous de la valeur à laquelle la zone de fumée remplit toute l'enceinte, le débit d'air tombe en dessous de la valeur nécessaire pour une combustion complète du combustible. Lorsque la source de combustible est sur le sol, un tel comportement est associé à la transition du régime contrôlé par la disponibilité du combustible vers le régime contrôlé par la ventilation. La taille d'ouverture de 12 % correspond également à celle en dessous de laquelle la théorie pour des configurations avec la source de combustible sur le sol prédit la transition du régime contrôlé par la disponibilité du combustible vers celui contrôlé par la ventilation, $\dot{m}_F \Delta h_c = 1500 \text{ kW/m}^{2.5} F_V$. Ces résultats indiquent que la transition ainsi que le comportement du feu pour le régime contrôlé par la ventilation obéissent aux mêmes lois quel que soit la position du brûleur dans l'enceinte.

4 Conclusion

Ce travail a permis de prédire les régimes de combustion susceptibles de se stabiliser lorsqu'un combustible est introduit dans une zone non oxygénée (non ventilée). Des grandeurs caractéristiques ont été dégagées, en particulier le flux de combustible introduit dans la flamme pour prédire la stabilité de la combustion ou l'extinction. Ce travail constitue une réelle avancée dans la compréhension de la combustion de réactifs dilués préchauffés à haute température avant leur mise en contact et leur combustion.

Symbols and Abbreviations

A	[m ²]	Area
A_{fl}	[m ²]	Area covered by the flame
A_{fl-in}	[m ²]	Area covered by internal part of the flame
A_{fl-out}	[m ²]	Area covered by external part of the flame
A_V	[m ²]	Area of a vent
BRE		(UK) <i>Building Research Establishment</i>
ϕ		Constant
c_p	[J/kg K]	Specific heat capacity at constant pressure
C_d		Orifice coefficient
CCD		Charge coupled device (digital camera)
CNRS		<i>Centre Nationale de Recherche Scientifique</i> (French National Scientific Research Council)
CP		Combustion products
d	[m]	Diameter (of wire)
D	[m]	Diameter
EdF		<i>Électricité de France</i>
ENSMA		<i>Ecole Nationale Supérieure de Mécanique et d'Aérotechnique</i> (French National College for Mechanical Aerotechnical Engineering, Poitiers)
EU		European Union
F_V	[m ^{2.5}]	Ventilation factor = $A_V H_V^{0.5}$
FC		Fuel-control
Fr	[-]	Froude number = $\frac{v^2}{gD}$
g	= 9.81 m/s ²	Acceleration due to earth gravity
H	[m]	(Compartment) height
H_f	[m]	Flame height
H_V	[m]	Effective height of a vent (in the case of two vent arranged vertically one above the other, the effective height is the height difference between the upper edge of the upper vent and the lower edge of the lower vent)
HRR	[W]	Heat release rate
IFE		<i>Institution of Fire Engineers</i>
IRSN		<i>Institut pour Radioprotection et Sécurité Nucléaire</i> (French Institute for Radiological Protection and Nuclear Safety)
k	[W/m K]	Thermal conductivity
KDP		Potassiumdiphosphate
L	[m]	(Compartment) length
LCD		<i>Laboratoire de Combustion et de Détonique</i> (Laboratory for Combustion and Detonics, Poitiers, France)
m	[kg]	Mass
\dot{m}	[kg/s]	Mass flow rate
\dot{m}''	[kg/m ² s]	Mass flux
M	[kg/kmol]	Molar mass
N	[kmol]	Molar count

NFPA	(US) <i>National Fire Protection Association</i>
Nu [-]	Nusselt number $= \frac{\alpha L}{k}$
p [Pa]	Pressure
PIV	Particle imaging velocimetry
q [J/kg]	specific heat, heat per mass
q_L [J/kg]	specific latent heat of gasification
Q [J]	Heat
\dot{Q} [W]	Heat release rate
	Heat transfer rate
\dot{Q}'' [W/m ²]	Heat flux
Q^* [-]	Nondimensional heat release rate $= \frac{\dot{Q}}{\rho_\infty c_p T_\infty \sqrt{g} D^{2.5}}$
Q_{prod} [J]	Heat produced during combustion
r [-]	Stoichiometric ratio
$R = 8310$ kJ/kg K	Ideal gas constant
Re [-]	Reynolds number $= \frac{v L_{characteristic}}{\nu}$
S_L [m/s]	Burning velocity of a premixed flame
t [s]	Time
T [K] or [°C]	Temperature
T_{AF} [K] or [°C]	Adiabatic flame temperature
v [m/s]	Velocity
V [m ³]	Volume
VC	Ventilation-controlled
W [m]	(Compartment) width
W_V [m]	Vent width
x [m]	Geometric dimension in direction of the length of the compartment
x [kmol/kmol]	“Local” molar concentration – concentration of a component within the oxidant or fuel flow
X [kmol/kmol]	Molar concentration (In situations where separate fuel and oxident flows are identified, X denotes the concentration of each component relative to the sum of gas in both flows. Concentrations relative to the amount of gas within one or the other flow are denoted as x)
y [m]	Geometric dimension in direction of the height of the compartment
Y [kg/kg]	Mass fraction
z [m]	Geometric dimension in direction of the width of the compartment

Greek Symbols

α [-]	Absorption coefficient
Δ	Difference
Δh_c [J/kg]	Heat of combustion per mass
Δh_c [J/kmol]	Heat of combustion per mole

η	[-]	Combustion efficiency
H	[J]	Chemical energy
\dot{H}	[W]	Energy flow rate
Θ	[°C or K]	Temperature difference or temperature in celsius scale
K	[$1/m$]	Emission coefficient
ν	[m^2/s]	Kinematic viscosity
ρ	[kg/m^3]	Mass density
τ	[s]	Time constant
ϕ	[-]	Equivalence ratio
		$\frac{m_{fuel,actual}}{m_{O_2,actual}} = \frac{m_{fuel,stoich}}{m_{O_2,stoich}}$
		As the project involves artificial mixtures of inerts and oxygen, the equivalence ratio has been given a different definition from the one used in most literature.
ϕ_{global}	[-]	Global equivalence ratio
ϕ_{in}	[-]	Equivalence ratio defined with the fuel which combusts inside the compartment

Superscripts

•	Rate of change
'	Per unit of length
"	Per unit of surface area
'''	Per unit of volume
~	Values for scaled-down model
^	Estimated value

Subscripts

∞	Values for ambient conditions
A	Air flow
C	Compartment
CP	Values for the Combustion products
$crit$	Critical value
$exit$	Values for exiting mass flow
HC	Hydrocarbon
F	Fuel flow
fl	Flames
in	Occurring inside the compartment
$inert$	Values for the inert gases inside the compartment (mainly N_2 and CO_2 in practice, mainly N_2 , O_2 and He in the experiments during the first stage of the project, mainly N_2 and He for the second stage of experiments)
$initial$	Values immediately on exiting the orifice of the burner
$loss$	[Heat] losses through the walls
out	Occurring outside the compartment
P	Flow within the fire plume
T	A_T : total internal surface area of a compartment

TC
v

Values for the thermocouple
Of the vent

1 Introduction

1.1 Background

Despite advances in the understanding of fire over the past decades [Quintiere 2001] and despite the advances in computing capacity, our ability to predict the behaviour of fires in general and building fires in particular remains very limited.

Fire continues to cause much damage to material property and many deaths and injuries – for example for in the UK in 2002 roughly 100,000 building fires were recorded, causing about 500 deaths and 13,000 non-fatal injuries [Office of the Deputy Prime Minister 2005], and creating material losses of about 1,500 Mio Pounds (2,200 Mio Euro), which is equivalent to 0.14 % of the gross domestic product [Wilmot 2005]. It is not just the biggest fires which need to be addressed if the number of casualties is to be greatly reduced: despite the number of fires over the past years in public buildings causing multiple deaths, the majority of fire deaths occur from incidents in residential properties each involving small numbers of casualties [Gebäudeversicherung des Kantons Bern 1992], [Office of the Deputy Prime Minister 2005].

If active and passive protection measures, and operational procedures and training for firefighters are to be improved, then the available knowledge on the behaviour of fires needs to be increased.

Compartment fires can exhibit a wide range of different behaviours, depending primarily on the type, size and location of the fuel, and on the ventilation.

Most previous research has concentrated on scenarios where the fuel source is located close to the floor. The main mechanisms for such fires have been identified, and to a certain degree predictions of the growth of a fire and the resulting temperatures in the compartment are possible [Karlsson and Quintiere 2000]. The basic scenarios are depicted in schematic fashion in *Fig. 1.1*.

If a fuel source is located in a compartment, then heat, smoke and hot gases will be trapped and the air supply will be restricted. If the compartment is extremely well ventilated, then the effect may be small, and the fire may grow in more or less an identical way to how it would if it were in the open [Drysdale 1998]. This case is depicted in *Fig. 1.1a*. More

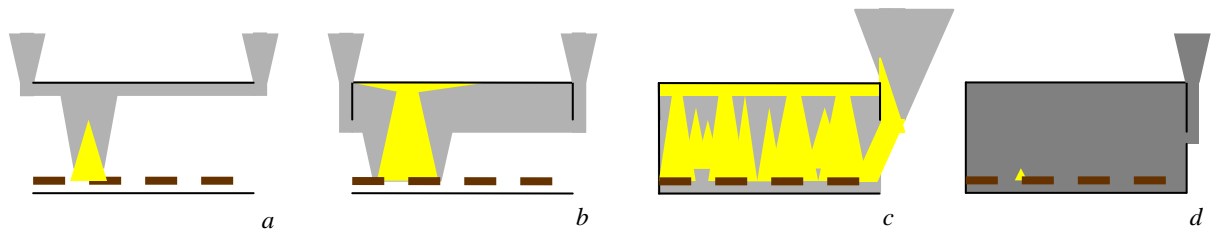


Fig. 1.1: Schematic illustration of the main behaviour types which can be encountered when a fire is in a compartment.

restricted, but still quite large ventilation, will lead to the buildup of a substantial layer of hot smoke and gas underneath the ceiling, as depicted in *Fig. 1.1b* [Drysedale 1998], [Karlsson and Quintiere 2000]. The heat feedback from this layer and from the walls and ceiling to the fuel bed will increase the rate at which the fuel is converted into its gaseous phase and released into the compartment, increasing the size of the fire.

If the ventilation is further restricted, and limited to the order of magnitude of a typical door or window, then the hot layer can grow so large as to fill practically the whole of the compartment [Drysedale 1998], [Karlsson and Quintiere 2000]. At the same time, the heat transfer to the flammable objects will be such that all flammable items in the compartment will ignite. This is shown in *Fig. 1.1c*.

If the vent is very small, the supply of air to the fire may be insufficient to sustain it. Under such conditions, various different patterns of behaviour have been observed, including extinction [Drysedale 1998], [Karlsson and Quintiere 2000], smouldering [Drysedale 1998], [Karlsson and Quintiere 2000], [Gross and Robertson 1965], oscillations of the combustion rate [Takeda and Akita 1981] and spontaneous fireballs [Hayasaka *et al* 1996].

Little research has previously been performed into fires when the fuel source is located close to the ceiling, as may for example occur when electric cables overheat or pipes transporting organic solvents rupture. Consequently, little is known about the behaviour of fire in such cases.

Such scenarios were studied at the Laboratoire de Combustion et de Détonique (LCD) as part of a project looking into questions raised by Electricité de France (EdF) and the Institut pour Radioprotection et Sécurité Nucléaire (IRSN) regarding the risks associated with fires in installations where radioactive materials are processed [Bertin 1998], [Bertin *et al* 2002], [Coutin 2000], [Coutin *et al* 2000], [Coutin and Most 2003]. Such installations pose specific

problems for fire safety engineers, as in many compartments the ventilation rate and pathways are controlled so as to reduce the possibility of radioactive dust escaping to the environment [Audouin *et al* 1997].

This earlier project at the LCD aimed among other things at discovering whether or not sustained combustion is possible when the fuel source is located in a zone filled with fuel and combustion products but to which there is no supply of air, and at describing the behaviour of the flames.

During that project configurations were studied where a gas burner was used to partially simulate the degradation of a solid fuel bed, or the evaporation of a liquid fuel. This allows the fuel flow rate to be set by the person running the experiment rather than it being determined by the heat flux to the fuel bed.

The burner was located inside a compartment fitted with a soffit to trap a layer of hot smoke and combustion products. When the burner is located low in the compartment, a diffusion flame and smoke plume will form above it. When the burner is located close to the interface between the layer of smoke and the air layer below it, flames may appear at the layer interface. These two scenarios are depicted in *Fig. 1.2 a* and *b*. Much of the work concentrated on cases when the burner is located inside the upper layer. Under such circumstances, at low fuel flow rates the flame will extinguish; at higher fuel flow rates, the behaviour depicted in *Fig. 1.2c* will occur: the flame will detach itself from the burner and stabilise itself at the layer interface.

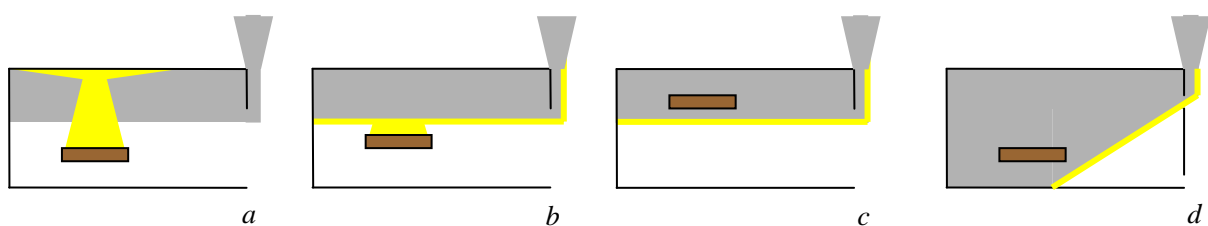


Fig. 1.2: Behaviour patterns observed when a gas burner is placed in a compartment.

The current project was initiated to describe in more detail the phenomena observed by Coutin [Coutin 2000], [Coutin *et al* 2000], [Coutin and Most 2003] during the earlier project. It was performed within the FIRENET research network, an international network funded by the European Union (EU) to study various aspects of compartment fires. A central object of study were blue flames which occur in a configuration as depicted in *Fig. 1.2c* when the fuel

flow rate is just above the minimum necessary to sustain combustion. Furthermore, work was performed to study the behaviour when the size of the vent is reduced, as suggested in *Fig. 1.2d*.

1.2 Literature Review

In order to understand the behaviour of fires with the fuel source close to the ceiling, it is necessary to first understand the combustion process in general and the behaviour of the more usual compartment fires where the fuel source is near the floor. This section therefore starts with an introduction of the combustion process and of the key mechanisms involved in fires when the fuel source is in the open, then presents the behaviour regimes of compartment fires when the fuel source is close to the floor, before exploring the behaviour associated with fires where the fuel source is raised above the floor.

1.2.1 The Combustion Process

There are two basic types of flame: premixed and diffusion [Drysdale 1998]. The flames encountered in compartment fires are mostly diffusion flames, but some of the concepts of premixed burning are required in the discussion of several aspects of fires, notably ignition and extinction.

Flaming combustion is a phenomenon which involves materials in their gaseous phase. Therefore, prior to flaming a condensed fuel (*i.e.* solid or liquid) is converted into vapour and gas through pyrolysis, sublimation and/or evaporation. This conversion is driven by the flux of heat to the surface of the solid or liquid. In simplified terms, the rate of production of vapour per surface area of the solid or liquid pool \dot{m}_F'' (also known as the “**burning rate**”) is determined by the heat flux from the flame and from any external heat source, and a “latent heat of gasification” [Drysdale 1998]

$$\dot{m}_F'' = \frac{\dot{Q}_{fl}'' + \dot{Q}_{ext}'' - \dot{Q}_{loss}''}{q_L} \quad (1.1)$$

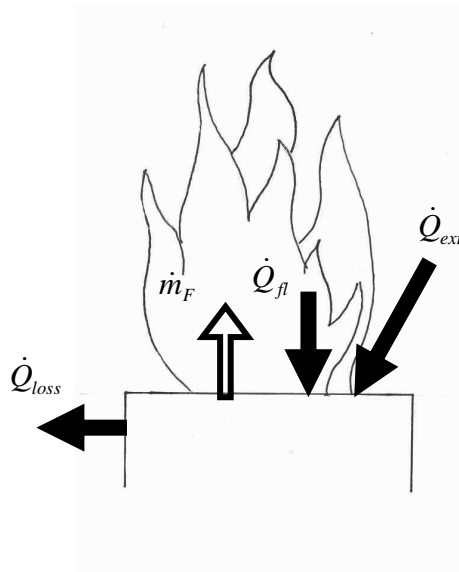


Fig. 1.3: Illustration of the energy flows involved in the degradation of a solid or liquid fuel

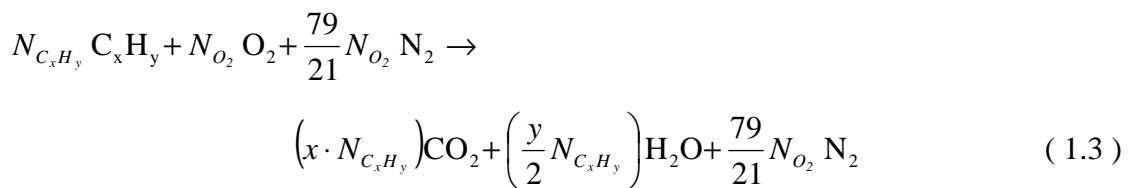
where \dot{Q}_{fl}'' is the heat flux from the flame to the surface, \dot{Q}_{ext}'' the heat flux from external sources to the surface, \dot{Q}_{loss}'' the heat losses and q_L the necessary heat per mass of the fuel for the conversion to the gaseous phase. The fire will grow if the net heat flux to the solid is greater than that required to produce the amount of fuel vapour needed to sustain \dot{Q}_{fl}'' .

The mass flow of gaseous fuel transports a flow of chemical energy \dot{H} which equates to

$$\dot{H} = \dot{m}_F \Delta h_c \quad (1.2)$$

where Δh_c is the heat of combustion per mass of the fuel.

The combustion reaction itself can be described in idealised form with the equation



with the quantities of fuel and oxygen being in stoichiometric proportions

$$\frac{N_{C_xH_y}}{N_{O_2}} = \frac{1}{x + \frac{y}{4}} \quad (1.4)$$

where N_i is the number of moles of each species. The stoichiometric fuel-to-air ratio is more usually expressed in terms of mass rather than moles:

$$\frac{m_{C_xH_y}}{m_{O_2} + m_{N_2}} = r \quad (1.5)$$

or, combined with (1.4)

$$r = \frac{N_{C_xH_y} M_{C_xH_y}}{N_{O_2} M_{O_2} + N_{N_2} M_{N_2}} = \frac{M_{C_2H_2}}{\left(x + \frac{y}{4}\right) \left(M_{O_2} + \frac{79}{21} M_{N_2}\right)} \quad (1.6)$$

where M_i is the molar mass of the species i .

It will not necessarily be the case – indeed particularly with fuels with large molecules it is rarely the case in practice – that all the gaseous fuel is combusted [Drysdale 1998]. Most fires will emit quantities of unburned and partially burned fuel in the form of gases, vapours and aerosols.

The rate of conversion of chemical energy to heat, or “**heat release rate**” (HRR) \dot{Q}_{prod} , can be considered as being equal to the flow rate of chemical energy multiplied by an efficiency factor, the “**combustion efficiency**” η_c

$$\dot{Q}_{prod} = \eta_c \dot{H} \quad (1.7)$$

The HRR depends not only on the material involved and the size of the solid object, but also on its geometry, on the arrangement if the solid comprises several different materials, and on the environment. Prediction based purely on theoretical foundations is therefore in practice almost impossible for anything more than the most simple of configurations, and so normally measurements are required [Drysdale 1998], [Karlsson and Quintiere 2000].

A key factor in any combustion process is the ratio of available oxidant and fuel. This ratio directly affects the chemical reaction in the case of premixed flames, but also in the case of diffusion flames the combustion efficiency is influenced by this ratio.

These ratios are normally expressed in the form of “**equivalence ratios**” [Drysdale 1998], the ratio between the fuel to air ratio and the stoichiometric ratio r :

$$\phi = \frac{\frac{\dot{m}_F}{\dot{m}_A}}{r} \quad (1.8).$$

1.2.2 Fires in the Open

Fire Plumes

Above the solid body of fuel, gaseous fuel will rise upwards, mixing with air to form a plume and burning in a diffusion flame [Karlsson and Quintiere 2000].

The plume comprises three parts as illustrated in *Erreur ! Source du renvoi introuvable.* [Drysdale 1998]: the zone between the height of the fuel bed and the height at which flame is always present, the zone corresponding to the range of heights at which there is an intermittent presence of the flame, and the zone above the height of the furthest reach of the flame tips.

The rate of entrainment of air into the plume will determine the volume and temperature of the resulting smoke and gas.

Several models exist to predict the amount of air entrained into a plume, although none provide a simple, accurate, universal, closed-form formula. Karlsson and Quintiere present a range of models in their textbook [Karlsson and Quintiere 2000].

The rate of entrainment is normally sufficiently high that the amount of air required for combustion of the fuel will have been entrained after only a short distance equating to a fraction of the height of the flames.

Flame Length

If the flames from different fuel sources are to be compared, it is not sufficient for the energy release rates to be compared – also the heights of the flames must be looked at (see Section 2.2.1) [Drysdale 1998], [Karlsson and Quintiere 2000]. In addition, the comparison of heights of flames and of compartment ceilings is of importance if a fire is in an enclosure.

In order to quantify the height, most authors define the height of the flame H_{fl} as the height beyond which the flame tips reach for half the duration of the observation [Drysdale 1998], [Karlsson and Quintiere 2000].

The flame height is primarily determined by the ratio between the initial inertia and the buoyancy of the fuel. This ratio can be expressed through the Froude number Fr or the

“nondimensional energy release rate” Q^*

$$Fr = \frac{v_{initial}^2}{gD} \quad (1.9)$$

where $v_{initial}$ is the velocity of the gaseous fuel when it leaves the orifice of the burner, pool or solid surface, and D is the diameter of the burner/pool/solid [Karlsson and Quintiere, 2000].

An alternative expression used by many authors is the “nondimensional energy release rate”

$$Q^* = \frac{\dot{Q}}{\rho_{\infty} c_p T_{\infty} \sqrt{g} D^{2.5}} \quad (1.10)$$

where \dot{Q} is the heat produced by the combustion and ρ_{∞} , c_p and T_{∞} are the density, specific thermal capacity and temperature of the ambient air. The correlation between the two can be illustrated if the velocity in the Froude number is expressed in terms of the fuel flow rate and burner geometry – see [Karlsson and Quintiere, 2000]. Low values of Fr or Q^* ($Fr < 10^{-5}$ or $Q^* < 1$) correspond to pool fires and fires of solids, where the initial velocity is low. High values ($Fr > 10^7$ or $Q^* > 10^6$) correspond to fires of gas jets.

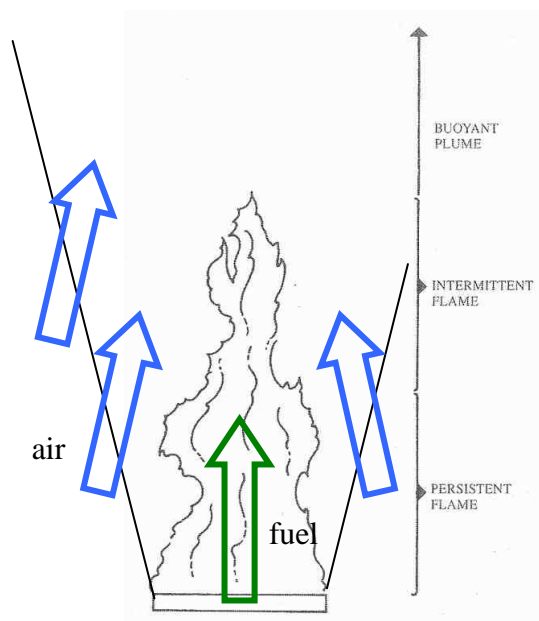


Fig. 1.4: Schematic of a fire plume
adapted from [Drysdale 1998]

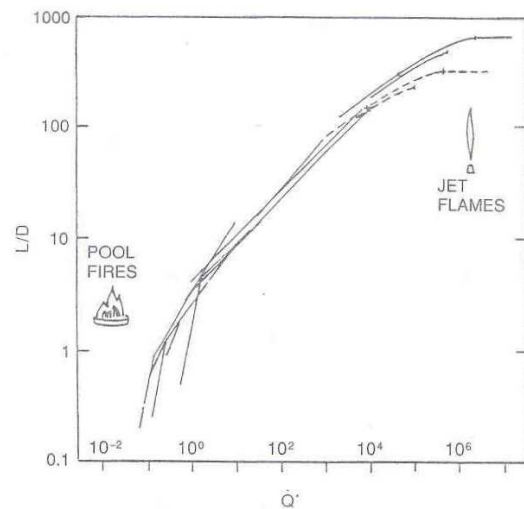


Fig. 1.5: Experimentally determined correlation between the “nondimensional energy release rate” Q^* and the flame length H_f .

Source: [Karlsson and Quintiere 2000]

Fig. 1.5 shows the correlation, determined from several experimental studies, between H_{fl} , and the heat release rate, expressed in terms of Q^* [Karlsson and Quintiere, 2000]. The data are well correlated with Q^* , although to describe the resulting link between the two, separate mathematical formulae are required for different ranges of Q^* – see [Drysdale 1998].

Orloff and De Ris [1982] measured flame heights during tests with burner diameters D ranging from 0.1 m to 0.7 m and energy flow rates \dot{H} ranging between 25 and 250 kW. From their data, they suggested the correlation

$$H_{fl} \approx \frac{\dot{H}}{1.2 \text{ MW/m}^3} \cdot \frac{4}{\pi D^2} \quad (1.11a)$$

or in other words the ratio between the energy flow rate \dot{H} and the volume of flame V_{fl} is constant

$$\frac{\dot{H}}{V_{fl}} \approx 1.2 \text{ MW/m}^3 \quad (1.11b)$$

Within the range of fuel flow rates and burner sizes within that study, this simplified formula would seem to be a reasonable approximation [Drysdale 1998].

1.2.3 Compartment Fires

If a fuel source is placed inside an enclosure, the plume gases and heat will be trapped underneath the ceiling and the air flow to the fire will be restricted. This can lead to the behaviour of the fire being changed substantially, for example through an increase in the amount of heat transferred to the fuel source [Drysdale 1998], [Karlsson and Quintiere 2000]. Often this will increase the rate at which the fire grows and the maximum heat release rate obtained.

1.2.3.1 Fires in Very Well Ventilated Compartments

A compartment fire will usually start with the ignition of a single object in the compartment. The fire will initially grow in a similar fashion to a fire in the open, with the fire

gradually spreading over the object. Smoke, hot gas and flames will rise upwards in a plume and then travel underneath the ceiling and out through the upper part of the vent, while fresh air is entrained in through the lower part of the vent [Drysdale 1998], [Karlsson and Quintiere 2000].

As the passage of hot smoke and gas is at least partially restricted, a hot layer will form underneath the ceiling. The burning object will be subject to heat flux not only from the plume, but also from the layer of smoke and gas and from the ceiling and walls. In accordance with equation (1.1), this extra heat flux will increase the pyrolysis rate, and consequently the rate will normally be greater than if the burning object were in the open.

As the combustion rate is primarily by the type and size of the fuel source, such behaviour is known as “**fuel-control**”.

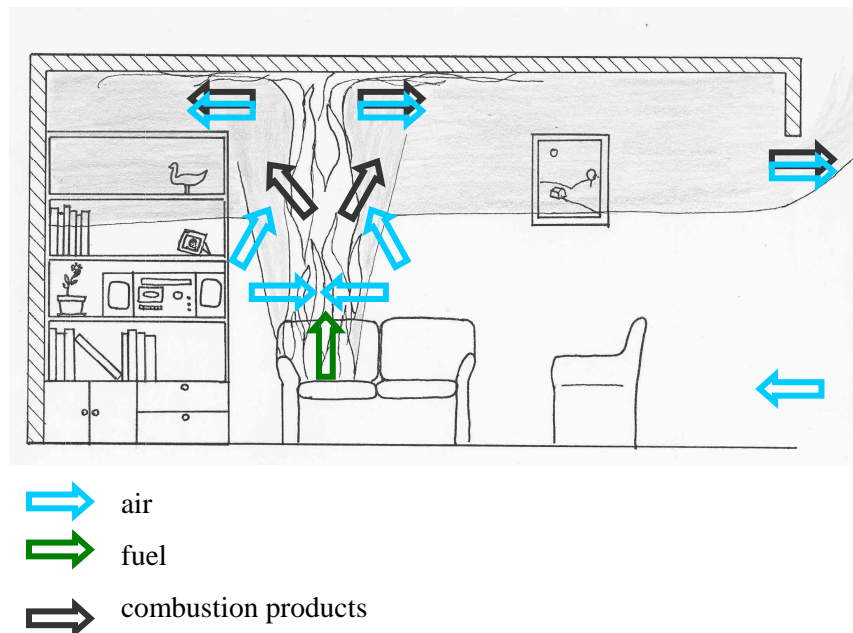


Fig. 1.6: Schematic of the mass flow in a fuel-controlled fire

1.2.3.2 Fires in Compartments with “Normal” Ventilation

If the ventilation to a compartment is limited to one or two doors or windows, then the buildup of smoke and hot gas underneath the ceiling will typically be so great that the behaviour of the fire will be significantly changed.

If left to run its course without any changes to the ventilation or attempts to extinguish it, such a fire will normally pass through a series of phases during its development [Drysedale 1998], [Karlsson and Quintiere 2000].

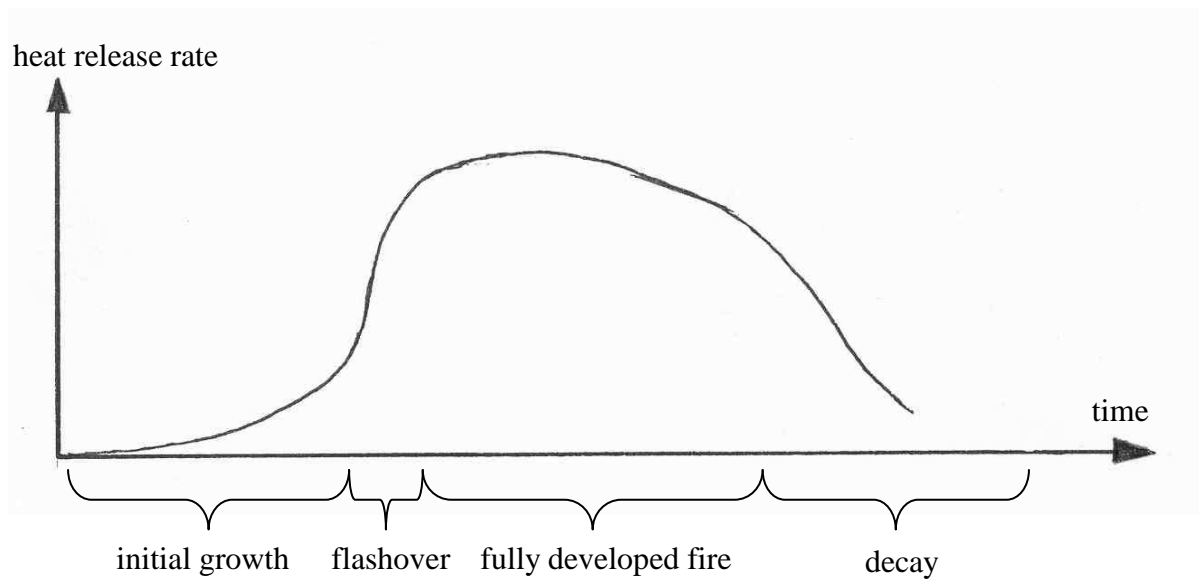


Fig. 1.7: Schematic illustration of the development of the heat release rate over time for a “typical” compartment fire.

1.2.3.2.1 Initial Growth

In most cases, a fire will start with the ignition of a single item of fuel. Initially it will behave much in the same way as described for fires in very well ventilated compartments, and in particular be fuel-controlled [Drysedale 1998], [Karlsson and Quintiere 2000]. The fire will gradually spread over the combustible item and possibly spread to adjacent items, increasing the buildup of the hot layer beneath the ceiling.

1.2.3.2.2 Flashover

After an initial period of gradual fire growth, several mechanisms come into play, including the ignition of other flammable objects throughout the compartment due to heat transfer from the flames, smoke layer, walls and ceiling, and the ignition of smoke and gases at the interface between the upper and lower layers. The various mechanisms tend to reinforce each other, leading to a rapid acceleration in the size of the fire, until all the flammable objects in the compartment are burning – the fire having thus reached its third stage, that of a “fully developed fire” [Drysdale 1998].

Fire growth during the second stage is often very rapid, and it may take less than a minute for the fire to pass from being localised to its original seat to involvement of all flammable objects in the compartment [Fire Experimental Unit 1997]. The rapidity of fire growth during this phase has led to the phase being named “**flashover**”.

Flashover is normally accompanied by an increase in the depth of the upper layer to fill practically the whole of the compartment. Typically it will also be observed that there is a qualitative change in the amount of flames exiting through the vent [Drysdale 1998], [Karlsson and Quintiere 2000]: Before flashover there will typically be no or only limited emergence of flame tips from the vent. After flashover, a large part of the vent will be filled with flame..

Mechanisms

As already mentioned, flashover normally involves a range of mechanisms, each tending to reinforce the others [Drysdale 1998], [Karlsson and Quintiere 2000].

- Due to the transfer of heat downwards from the smoke layer, the other flammable objects will start to pyrolyse. The plumes from the other objects in the compartment will add to the growth in thickness and to the temperature rise of the upper layer. The hot layer will quickly grow so large as to reach almost to the floor.
- The increased production in pyrolysis products will at the same time lead to an increase in the concentration of unburned and partially burned gases and smoke within the upper layer

- The increase in depth of the upper layer reduces the height available for (fresh) air to be entrained into the plume. This will cause further rise in the temperature of the upper layer and the concentration fuel in this layer
- Due to the increase in temperature and the increase in fuel concentration inside the upper layer, combustion may become possible at the interface between the layers
- This adds to the heat transfer to solid objects in the compartment
- Often, these objects will heat up sufficiently to experience non-piloted ignition, which will increase the total heat release rate.

When Flashover Occurs

In order for solid objects at some distance from the original seat of fire to undergo unpiloted ignition, they will typically have to receive a heat flux in excess of 20 kW/m^2 [Drysdale 1998].

In practice, this is typically observed when the upper layer reaches a temperature of around 500 or 600°C [Walton, Thomas 1995].

Both of these observations have been used by various authors as criteria to define when flashover occurs in numerical simulations.

It is not inevitable that the initial burning object will be able to supply enough energy to create the conditions necessary for flashover [Drysdale 1998]. The heat release rate must be sufficient to compensate for conductive losses through the walls and convective losses through the vent, and to raise the temperature in the upper layer sufficiently. An estimate of the minimum necessary heat release rate, and therefore the minimum necessary fuel flow rate, can be obtained from a model for calculating the gas temperature for pre-flashover – i.e. fuel-controlled – fires and extracting the heat release rate that produces a temperature equal to some critical value (most authors recommend 600°C) [Walton, Thomas 1995], [Drysdale 1998].

Combustion in the Upper Layer

Ignition of fuel stored in the upper layer is one of the key phenomena associated with flashover. Studies of the interaction between flames and smoke layers were performed by Hinkley *et al* [1984] and by Beyler [Beyler 1984], [Beyler 1986].

The work by Hinkley and his co-researchers studied the role played by flames in the upper zone to fire spread [Hinkley *et al* 1984]. They ran a series of experiments with wood crib fires and with fires fuelled by gas burners, whereby the crib or burner was located underneath a channel which was open towards the underside. The channel was 7.3 m long and 1.2 m wide and 0.5 m deep

Beyler's work [Beyler 1984] formed part of a study looking at the composition of the atmosphere inside the upper layer. It involved experiments with gas burners and pans of liquid fuels located underneath a circular hood of 1 m diameter and 0.5 m depth.

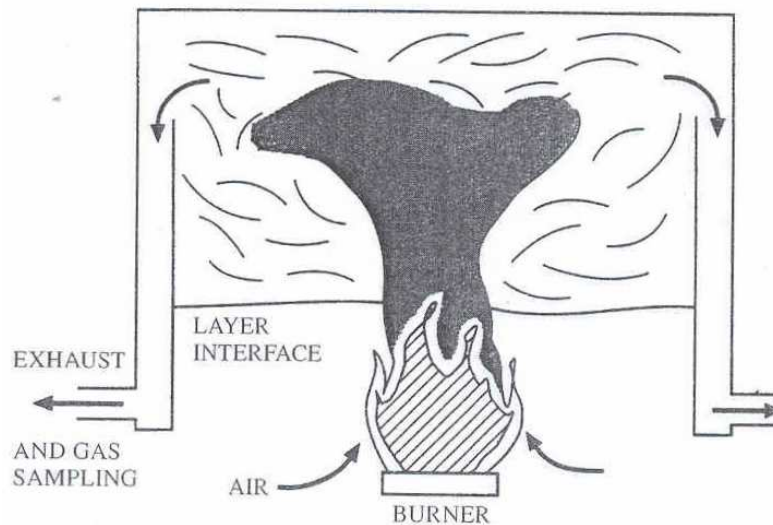


Fig. 1.8: Schematic of the experimental geometry used in Beyler's work.

In a two-layer system, air is entrained into the lower part of the plume. Both Hinkley and Beyler observed that the entrainment of air between the layers other than via the plume is negligible. This is due to the fact that the stratification between the upper and lower layer is thermodynamically stable.

If the lower layer is deep enough for the plume to entrain more than enough air than is needed for complete combustion, then the excess air will be transported to the upper layer. However, this does not mean that the fuel will necessarily have been completely consumed before entering the upper layer.

If the fuel flow rate is sufficiently high or the distance between the base of the plume and the layer interface is sufficiently small, then flames will reach into the upper layer, and possibly impinge on the ceiling and run underneath the ceiling.

As the smoke layer becomes deeper and/or the burning rate increases, there may be insufficient air entrained into the plume to allow complete combustion. In this case, un- and partially combusted fuel will enter the upper layer. This opens the possibility of the fuel concentration inside the upper layer becoming so high so that combustion can occur at the interface between the two layers [Beyler 1984], [Hinkley *et al* 1984].

However, the presence of fuel in the upper layer is not a sufficient criterion to allow combustion at the interface to take place. The inert species in the upper layer act as heat sinks, and if the concentration of inert species is too high, then flammable conditions cannot be obtained [Beyler 1984].

A premixture of fuel and oxidant can only burn if the concentrations of the components are within certain limits, whereby these limits depend on the species involved, the temperature and the pressure.

The lower flammability limit of most hydrocarbons – the most fuel-lean mixture which will burn – corresponds to a mixture which, under adiabatic conditions would produce a flame temperature (“**adiabatic flame temperature**”) of $1550 \text{ K} \pm 50 \text{ K}$ [Drysdale 1998]. This fact allows the lower flammability limit to be estimated from an adiabatic heat balance. If the thermal capacities of the involved species are assumed to be independent of temperature and average values are taken for the range of temperatures encountered, one obtains

$$\Delta h_c = \sum_{products} \left(\frac{\dot{m}_i}{\dot{m}_F} c_{p-i} (T_{AF} - T_\alpha) \right) \quad (1.12).$$

where Δh_c is the heat of combustion per unit mass of the fuel, \dot{m}_i/\dot{m}_F the ratio of the mass of each product to the mass of the fuel, c_{p-i} the specific heat capacity of the product i , T_α the initial temperature of the reactants and T_{AF} the adiabatic flame temperature (*i.e.* 1550 K).

The concept can be adapted to estimate whether or not a stream of fuel and inert gas can sustain a diffusion flame. The minimum necessary fuel concentration in the stream of fuel and inerts equates to the lower flammability limit of a stoichiometric mixture of the fuel/inert stream and the oxidiser stream [Beyler 1984].

Using this concept, Beyler developed a criterion to indicate whether or not combustion at the interface can occur [Beyler 1984]:

$$\underbrace{\left(\dot{m}_F - \underbrace{\dot{m}_p r}_{\text{fuel_consumed_by_plume_air}} \right)}_{\substack{\text{fuel_in_upper_layer} \\ \text{potential_HRR}}} \Delta h_c > \sum_{\text{products}} \dot{m}_i c_{p-i} \Delta T_{\text{adiabatic}} \quad (1.13)$$

where r is the stoichiometric ratio, Δh_c the heat of combustion per mass of fuel, \dot{m}_i is the i -th product species and c_{p-i} the corresponding specific thermal capacity and $\Delta T_{\text{adiabatic}}$ is the difference between the initial temperature and the critical adiabatic flame temperature.

Hinkley noted that the thermal expansion induced by the combustion at the interface generates turbulence, which enables air to be entrained into the upper layer, leading to the occurrence of combustion practically throughout the depth of the upper layer [Hinkley *et al* 1984].

1.2.3.2.3 Fully Developed Fire

By definition, flashover ends when all the combustible objects in the compartment are alight. The fire will thus have entered the third phase – that of “**fully developed fire**”, also often known as “**post-flashover fire**” [Drysdale 1998].

During this stage, the rate at which the solid fuel is converted into vapour will typically be higher than the combustion rate which is possible with the available air. The heat release rate inside the compartment is therefore in a first approximation dependent only on the air supply, which is itself dependent only on the geometry of the vent. Such behaviour is known as “**ventilation-control**” [Drysdale 1998].

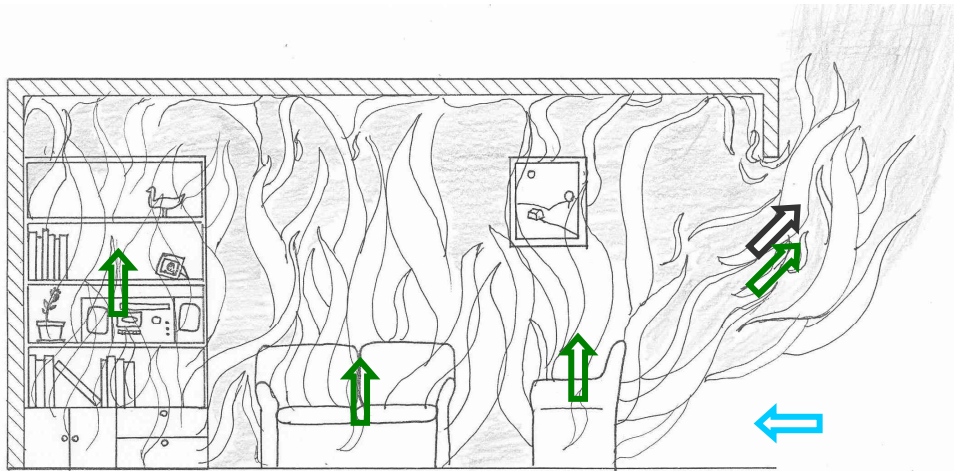


Fig. 1.9: Schematic of the mass flows in a ventilation-controlled compartment fire

Vent Flow Rate and Heat Release Rate

Typically, the atmosphere inside the compartment will no longer show a discernible division into an upper and a lower layer. The atmosphere will be well mixed, with air, combustion products and flame being present throughout the compartment, and the temperature being fairly homogeneous [Drysdale 1998], [Karlsson and Quintiere 2000].

It can be shown that under such conditions [Drysdale 1998], [Karlsson and Quintiere 2000], the flow rate of air entering in through the vent \dot{m}_{in} is roughly equal to

$$\dot{m}_{in} \approx 0.5 \frac{\text{kg}}{\text{m}^{2.5} \text{s}} A_V H_V^{\frac{1}{2}} = 0.5 \frac{\text{kg}}{\text{m}^{2.5} \text{s}} F_V \quad (1.14)$$

Where A_V is the area of the vent, H_V the “effective height” (for a simple door or window, this is equal to the height of the opening) and $F_V = A_V H_V^{\frac{1}{2}}$ is the “**ventilation factor**”, first defined by Kawagoe from experimental observations [Drysdale 1998]. As for most hydrocarbons the amount of heat released per mass unit of air consumed is roughly constant – about 3 MJ per kg of air – the heat release rate can be obtained by multiplying the air flow rate by this factor

$$\dot{Q} \approx \Delta h_a \dot{m}_A \approx 3 \frac{\text{MJ}}{\text{kg}} 0.5 \frac{\text{kg}}{\text{m}^{2.5} \text{s}} F_V = 1.5 \frac{\text{MW}}{\text{m}^{2.5}} F_V \quad (1.15)$$

As complete combustion of the fuel is not possible within the boundaries of the compartment, flames will extend out through the vent. This gives rise to the possibility of the fire spreading to adjacent compartments [Drysdale 1998].

Distinction between Fuel-Control and Ventilation-Control

There is a clear theoretical definition to demarcate between fuel- and ventilation-controlled regimes: Ventilation-control exists in theory when the air flow rate into the compartment is less than that required for complete combustion of the flammable gases and vapours in the compartment.

In practice, as combustion occurs over a finite time and volume, the effects of the limitation of the ventilation can be observed when the ratio between the fuel flow rate and the flow rate of air entering in through the vent is still well below the stoichiometric ratio r . In their description of experiments involving forced ventilation, Backovsky *et al* [1989] spoke of fire behaviour akin to ventilation-control when the air flow rate was up to three times that required for combustion of the fuel.

Definition of Equivalence Ratios

Despite the divergence between the theoretical border between the regimes and the border observed in practice, equivalence ratios – the quantitative comparison of fuel and air flow rates – are nevertheless useful for characterising a fire.

There are three basic cases which can be distinguished:

- the vent flow rate is greater than that required to burn the flammable vapours that are produced in the compartment. In this case, the gas flow exiting the compartment contains more air than necessary to combust any fuel which does not burn in the compartment.
- the vent flow rate is insufficient to combust all the fuel, but greater than that required to combust that part of the fuel which burns inside the compartment. In this case, some air is contained in the exiting gas flow, but for the complete combustion of the fuel, some air from outside the compartment is also required.
- the vent flow rate limits the amount of combustion inside the compartment. In practice, because the reactions take a finite amount of time to complete and because

mixing is not perfect, it is impossible to create conditions where all the oxygen which enters the compartment is consumed inside the compartment. However, the oxygen supply can be low enough to limit the amount of combustion which occurs inside the compartment.

In order to describe mathematically these three cases, two equivalence ratios are necessary.

- the global equivalence ratio, ϕ_{global} , defined using the air flow rate into the compartment and the total fuel flow rate

$$\phi_{global} = \frac{\dot{m}_F}{\dot{m}_{vent} r} \quad (1.16)$$

- the internal equivalence ratio, ϕ_{in} , based on the air flow rate into the compartment and the fuel combusted inside the compartment

$$\phi_{in} = \frac{\dot{m}_{comb-in}}{\dot{m}_{vent} r} \quad (1.17)$$

The internal equivalence ratio cannot be greater than unity, as the amount of fuel combusted inside the compartment cannot be greater than $(r \cdot \dot{m}_{vent})$. As the amount of fuel which is combusted inside the compartment cannot be greater than the total amount of fuel, $\phi_{global} \geq \phi_{in}$.

The first case corresponds to a situation where both of these equivalence ratios are less than unity. In the second case, ϕ_{global} will be greater than unity and ϕ_{in} less than unity. The third case corresponds to conditions where the internal equivalence ratio is practically equal to one.

Experimental Distinction between Fuel-Control and Ventilation-Control

Because in practice the transition between the two regimes is not sharp, the equivalence ratios do not determine exactly at what point the behaviour of a fire changes. Several other criteria have been proposed by various authors to demarcate between the two regimes.

External Flaming: Several authors suggest that a criterion to distinguish between pre- and post-flashover fires can be based on the presence and nature of external flaming. As most real-

life compartment fires are fuel-controlled before flashover and ventilation-controlled after flashover, it should follow that external flaming can be linked with ventilation-control. In post-flashover fires, flames typically fill a large part of the vent and extend out of the compartment. In pre-flashover fires, there may be some flames which extend out through the vent, but they are much smaller [Drysdale 1998].

However, in the experiments described in the later chapters of this report, where the fuel source is just below or inside the smoke layer, the flames always extend out through the vent whenever the fuel flow rate is high enough to sustain combustion. Therefore, the presence or absence of external flaming cannot be taken as an indicator of the combustion regime.

Combustion Products: Ventilation-control is sometimes associated with a lower combustion efficiency than fuel-control, and hence to the emission of greater quantities of smoke relative to the fuel flow rate.

Layer Depths: It is generally observed that the interface between the upper and lower layers remains at an almost constant height throughout the growth of a fire while it is fuel-controlled, and that the interface quickly drops almost to the floor at flashover – i.e. when the fire converts from fuel-control to ventilation-control [Drysdale 1998], [Karlsson and Quintiere 2000]. This observation has been given a theoretical backing by Prah and Emmons [Prah, Emmons 1974].

1.2.3.2.4 Decay Phase

This maximum heat release rate will be maintained until the fuel sources start to become depleted and so the pyrolysis rate drops. The fire enters the “**decay phase**”, which lasts until burnout of the fuel sources [Drysdale 1998], [Karlsson and Quintiere 2000].

1.2.3.3 Underventilated Compartment Fires

If the ventilation is severely restricted, then this may reduce the air flow to a point where the pattern of behaviour described in the last pages cannot establish itself, and in extreme cases combustion may not be sustainable. In this report, such fires will be termed “**underventilated**”, although to prevent possible confusion, the author feels it important to point out that some experts use the term underventilated to describe any compartment fire where the air supply is less than that required for stoichiometric combustion of the fuel; in practical terms, this definition covers all ventilation-controlled fires.

There is a wide range of behaviour patterns which have been observed in cases with severely restricted ventilation [Gross and Robertson 1965], [Takeda and Akita 1981], [Sugawa *et al* 1989], [Hayasaka *et al* 1996], [Audouin *et al* 1997], [Drysedale 1998], [Karlsson and Quintiere 2000]. The currently available knowledge does not allow predictions to be made about what will occur under given circumstances, as it has not been possible to undertake systematic experimental exploration of such fires, because the key parameters can be varied almost infinitely – nature, number, location, size and shape of vents; geometry of the compartment; geometry, makeup and location of fuel sources; insulation of the compartment boundaries. For many of the phenomena, the mechanisms are not well understood.

In the following paragraphs, some of the phenomena that have been observed are described. Many of them bear resemblance to phenomena which can occur when the fuel source is located just underneath the interface between the upper and lower layers or inside the upper layer – as will be explored in Section 1.2.4.

One point which is relevant to all the phenomena presented below is that when and if the flames extinguish, there will often be enough heat stored in the gases in the compartment and in the walls for the fuel source to be the recipient of sufficient heat transfer for pyrolysis or evaporation of fuel to continue [Drysedale 1998].

Extinction

If the compartment is hermetically sealed, then the fire will initially be sustained by the oxygen which is present in the compartment before the fire started [Drysedale 1998], [Karlsson and Quintiere 2000]. Oxygen depletion will however eventually lead to the fire extinguishing.

Extinction of flaming combustion will occur while the oxygen concentration is still well above zero - specifically at about eight to eleven percent, depending on the temperature [D. Drysdale, private communications]. This is very much in contrast to the conditions which exist inside the upper layer in a ventilation-controlled case, where the oxygen concentration has been observed to drop almost to zero. Smouldering combustion on the other hand may continue at oxygen concentrations as low as 3 to 4 % [D. Drysdale, private communications].

A complete absence of ventilation is not required to produce extinction [Gross and Robertson 1965]. If the vents are small enough, the hydrostatic pressure difference between the top and bottom of vent will be too small to overcome the pressure rise inside the compartment due to thermal expansion, and thus hot smoke and gas will flow outwards through the entire surface of the vents, preventing air from reaching the seat of the fire.

Breathing

Scenarios have been observed [Fire Experimental Unit 1997 b], in which smoke and gas initially exit through the whole area of all available vents; the fire then dies down, leading to a cooling of the atmosphere inside the compartment and thermal contraction. Air is thus drawn into the compartment, and reinvigorates the fire, leading to a renewed heating of the atmosphere inside the compartment and reversal of the flow through the vent. This can produce a cyclic behaviour of alternating phases of inflow and outflow of gas through the vent.

Sugawa's Ghosting Flame

Sugawa *et al* [Sugawa *et al* 1989], [Sugawa *et al* 1991] observed unusual flame behaviour which they termed "ghosting flame" during a series of experiments involving a pan of methanol positioned at a range of heights in the centre of a compartment. During these experiments, the fuel was ignited, the ventilation was reduced to two slots located high in one of the short walls measuring in the range of 150 to 160 cm², and then the pool was left to burn itself out.

During the first "6-7 min" after ignition, there would be an orange flame attached to the fuel tray and impinging on the ceiling. The flame would then turn blue. When the tray was located at less than two-thirds of the height to the ceiling, the flame would remain attached to

the pool throughout the test. Different behaviour was observed when the tray was two thirds of the height of the compartment. Sugawa described the flames as follows:

“After about 10 min after the ignition, the flame detached from the fuel surface ... it floated just under the ceiling like a crown shape jellyfish or like an aurora having very thin skin-like flame showing a width of about 5-10cm and a diameter of about 40cm....

“During the burning state, a pulsation frequency of the flame of about 3 Hz was observed and it continued before the ghosting... The pulsation frequency decreased abruptly about 3 sec before the ghosting beginning.” [Sugawa *et al* 1991]

The behaviour of these flames bears some resemblance to the blue observed by Coutin [Coutin 2000], [Coutin *et al* 2000] which are described in Section 1.2.4.

Spontaneous Fireballs

Various authors have noted the possibility of the spontaneous occurrence of explosions originating from an underventilated fire compartment with wood as fuel (e.g. Hayasaka *et al* [Hayasaka *et al* 1996], [Hayasaka *et al* 1998] and by Sutherland [Sutherland 1999]).

To the knowledge of the author, the mechanisms have never been fully explored. It may be that the phenomenon is linked to the “breathing” described above. While the fire is dying down, but before vent flow is reversed and air flows in through the vent, the continuing pyrolysis of wood will lead to an accumulation of unburned fuel in the atmosphere inside the compartment. This mixes with air during the phase of air inflow to create a premix which is ignited when air reaches the seat of the fire and revitalises the fire.

It has been observed that this behaviour pattern can occur several times in a row, as the exiting fireball consumes all the air in the compartment and temporarily prevents fresh air from flowing in, thus reproducing the conditions for the renewed dying down of the fire and buildup of pyrolysis products.

Audouin’s Travelling Flame

During a test with a liquid pool fire in a large-scale compartment with very restricted ventilation, Audouin *et al* [Audouin *et al* 1997] observed a flame that detached itself from the fuel source and moved across the compartment to the vent.

Within about twenty seconds of igniting the fuel, a smoke layer had formed and grown to fill practically the whole of the compartment. The pressure inside the compartment rose so high as to prevent air from entering through the vent. After about three minutes, “As the compartment loses energy through its wall and the intensity of the fire begins to be limited by the lack of oxygen.” The temperatures remained fairly stable for a further five minutes, while the oxygen concentration at low levels inside the compartment continued to sink. Then the “flame detaches itself from the flammable surface and starts migrating through the compartment to the opening”, taking two and a half minutes to cross the eight metres between the pool and the vent. The flame then stabilised itself at the vent, where it continued to burn until the fuel supply ran out.

Bertin and Coutin [Bertin 1998], [Bertin *et al* 2002], [Coutin 2000] produced what seems to be identical behaviour in a compartment with a gas burner integrated into the rear wall.

1.2.3.4 Special Cases

1.2.3.4.1 Compartment Fires with Forced Ventilation

In some instances, particularly in some industrial buildings, the ventilation rate to a compartment is controlled. This will mean that the ventilation rate is independent of the size of the fire. This can produce specific behaviour patterns. However, little research has previously been performed into such scenarios.

In a series of experiments with a gas burner inside a compartment, Backovsky *et al* [1989] observed two types of behaviour, one akin to fuel-control featuring clearly distinguishable upper and lower layers, and the other akin to ventilation-control with the whole compartment being filled with a hot mixture of smoke and gas. The transition between the two occurred when the air flow rate was about twice or three times that required for the combustion of the fuel.

Prétrel *et al* [2003] performed a study with a in a large compartment – 380 m³ – with a comparatively low vent flow rate of 0.3 m³/s, during which pressure oscillations were encountered which might, under other circumstances, create a risk of bursting or implosion of the compartment. The fire would initially grow in size, leading to the creation of an overpressure which was high enough to lead to an outflow of air through the inlet vent, thus

starving the fire of its air supply in much the same way as has been described in Section 1.2.3.3. The oscillations occurred during the subsequent cooling phase, reaching peak values of about ± 1 kPa. It has been suggested that these oscillations are due to repeated extinction and re-ignition of gaseous fuel [J.-M. Most, private communications], although there is not enough data available to allow definitive conclusions.

1.2.3.4.2 Changes in Ventilation

Some phenomena are dependent of changes in the ventilation during the course of events. Most notable are backdraught and the “blowtorch effect”.

Backdraught

There is some incoherence in the literature as to how wide or narrow the definition of the term backdraught should be. Some authors include phenomena such as the spontaneous fireballs described on page 49 (Section 1.2.3.3) within their definition [Hayasaka *et al* 1996]. For the purposes of this report, a narrow definition will be adhered to: a backdraught is an event involving a fireball or explosion exiting from a vent after it has suddenly been opened, allowing mixing between the oxygen-lean, fuel-rich atmosphere from inside the compartment and the ambient air.

The conditions necessary for backdraught are created when a fire burns in a compartment with insufficient air to sustain combustion. Under such circumstances, the combustion rate will drop due to the lack of oxygen, while continuing pyrolysis will enrich the atmosphere inside the compartment with fuel [Fleischmann *et al* 1994]. If a door or window is opened, the difference in density between the hot gases inside the compartment and the cool gases outside will lead to the generation of a gravity current which will transport air into the compartment and fuel out, leading to a mixing of the two. Ignition of the thus created premix most often occurs through the rejuvenation of the original fire.

The Blowtorch Effect

This phenomenon, sometimes referred to as a “high pressure backdraught” occurs when a vent is available in one side of a compartment, and a vent in or near the opposite end is suddenly opened, leading to an increase in the intensity of the fire due to the increased supply of oxygen and pushing flames out through the first vent. Typically, the first vent will be a doorway between the fire compartment and another compartment in the building, and the second will be a window or door to outside the building – thus there will be a difference in temperature and pressure between the air at either side of the fire compartment, which probably influences the directions and rates of airflow.

1.2.4 Fires with Raised Fuel Sources

If a fuel source is located close to the ceiling, then the behaviour of a fire may be substantially different from that in cases where the fuel source is near the floor.

Coutin performed a major study which aimed at describing the types of behaviour that can arise as a function of the location of the fuel source and at understanding the behaviour of the flames [Coutin 2000], [Coutin *et al* 2000].

Experimental work was carried out in a compartment measuring 0.62 m in length, 0.84 m in height and 0.40 m in width. The front of the compartment was open except for a soffit. The presence of the soffit ensured that in all cases a layer of smoke would be trapped under the ceiling. Two soffit depths, measured from the ceiling to the top edge of the vent, were used: 0.19 m and 0.34 m. The compartment is the same as has been used for much of the work of the current project, and is described in detail in Section 3.2.1.

The flames were fuelled with propane, supplied through a horizontal circular porous burner of 60 mm diameter. The location of the burner within the compartment could be varied. Tests were performed with fuel flow rates \dot{m}_F of up to 0.45 g/s, which equates to an energy flow rate \dot{H} of 21 kW (Δh_c of propane: 46.5 MJ/kg), an initial Froude number $Fr = 0.013$ and a nondimensional heat release rate of $Q^* = 21$.

Only steady-state behaviour was studied.

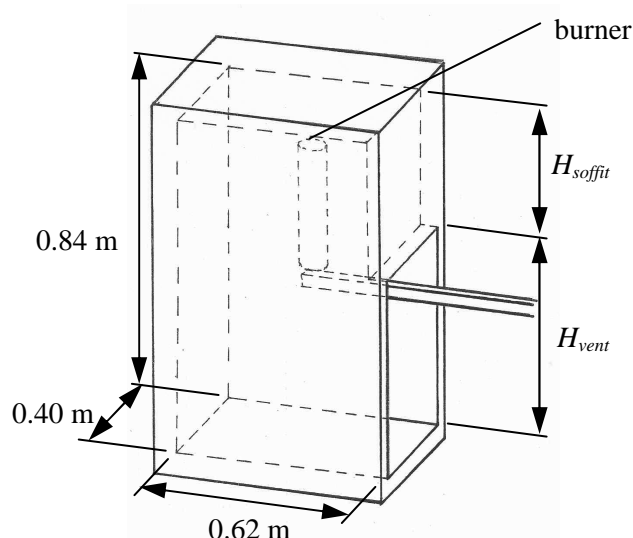


Fig. 1.10: The geometry studied by Coutin.

Many of Coutin's observations can be correlated with those of Hinkley and Beyler described in Section 1.2.3.2.2 [Hinkley *et al* 1984], [Beyler 1984], [Beyler 1986].

If the burner is located low in the compartment, the classical behaviour of a fuel-controlled fire is observed, with a fire plume rising above the burner and flames impinging on the ceiling.

As would be expected, when the burner is positioned close to the upper layer, the behaviour is much the same as that described in section 1.2.3.2.2 (page 40) for a fire when the upper layer increases in depth and approaches the burner: when the distance for air entrainment becomes too short, unburnt fuel will enter the upper layer and ignition may occur at the interface between the two layers [Coutin 2000], [Coutin *et al* 2000].

Hinkley's work showed that the closer the burner is to the upper layer, the thinner this layer. This can be explained by the reduced distance available for air to be entrained into the plume before it enters the upper layer [Hinkley *et al* 1984]. Coutin did not observe this dependence; this is probably due to the small scale of his apparatus.

Both Coutin and Hinkley *et al* observed that the layer became deeper if the fuel flow rate is increased.

Hinkley reported that for the lower values of fuel flow rate studied (up to 360 kW), the air flow beneath interface is in opposition to the flow of the upper layer. For the highest values of

fuel flow rate – above the equivalent of 500 kW – there was a reversal of the flow: A layer of air is formed underneath the smoke layer flowing outwards parallel to the hot gas and smoke [Hinkley *et al* 1984]. Similar behaviour was observed by Coutin, who described a layer of outflowing air beneath the layer of smoke and hot gas [Coutin 2000], [Coutin and Most 2003]. This means that the interface between the zones of hot and cold gas is not located at the same height as the interface between the inflowing and outflowing currents. The consequences for the vent flow rate have not yet been fully explored.

Coutin's work suggested that if the burner is raised into the upper layer, then one of two things can happen, depending on the fuel flow rate: at low fuel flow rates, the flames will extinguish, at higher rates, they will leave the surface of the burner and become stabilised at the interface.

Coutin observed that the minimum fuel flow rate needed for combustion to be sustainable depends on the depth of the soffit and on the position in the lengthwise direction of the burner. A deep soffit and/or a burner position close to the front or rear of the compartment lead to an increase in the necessary flow rate.

At fuel flow rates just above the minimum, the flame covers part of the interface and extends out through the vent. Blue or blue and yellow flames can be observed. At higher fuel flow rates, the flame is yellow and covers the whole of the interface. The purely blue flames particularly occur when the burner is very close to the ceiling and the deeper of the two soffits is in place. These flames fluctuate in size, whereby Coutin determined from an analysis of his temperature data that the fluctuations are aperiodic.

These flames are to some extent reminiscent of flames observed by Sugawa *et al* [Sugawa *et al* 1989], [Sugawa *et al* 1991] (see Section 1.2.3.3, page 48).

Comparisons can also be made to the flames observed by Morehart *et al* [Morehart *et al* 1992a], [Morehart *et al* 1992b] during a study aimed at simulating in a steady-state experiment the conditions which occur during the transient development of a fire, when the oxygen concentration within the plume and the within the upper layer may be different from one another. The work was performed with a gas burner placed under a hood, as shown schematically in *Fig. 1.11*. Air was injected into the upper half of the hood through an array of

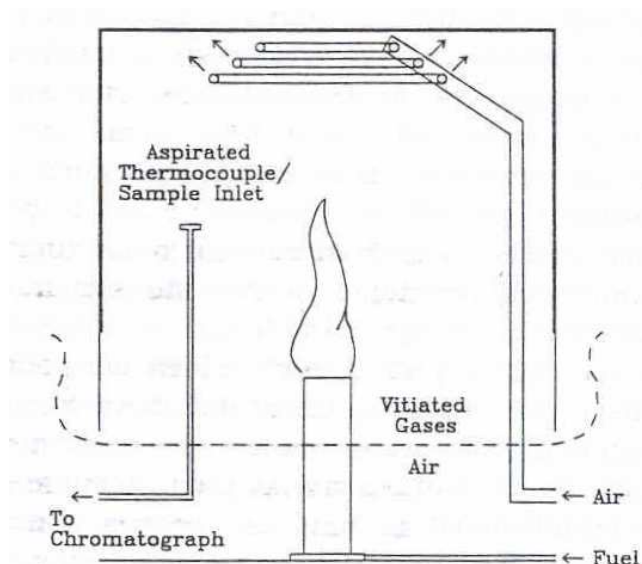


Fig. 1.11: Schematic of the geometry used in the study by Morehart et al.

Source: [Morehart et al 1992b]

1.6 mm holes. “The injected gas is aligned with the mean streamline of the plume induced flow. Excess combustion products mixed with the added air are allowed to spill out beneath the edges of the hood and thus produce a well-defined interface between the recirculating vitiated gases inside the hood and the cool, uncontaminated room air. In these experiments, the burner surface is positioned at least 30 cm above this interface.” Tests were performed using two different fuels: methane and ethylene.

The procedure for each test was as follows:

- the fire was ignited, and the fuel flow rate was adjusted to provide flames which were as large as possible without them reaching the region of the air inlet. Inherent in this was the fact that the air flow rate was larger than that required for stoichiometry.
- The team waited for about half an hour to allow the system to reach a steady state. A gas sample was taken.
- the fuel flow rate was then incrementally increased, with further samples being taken, “until further increases in the fuel flow rate would cause the extinction of the fire.” [Morehart *et al* 1992b]
- The fuel flow rate was kept constant at this maximum value for 20 minutes before a final sample was taken.

Morehart provides the following description of his results [Morehart *et al* 1992a]:

“As the oxygen mole fraction was decreased and conditions approached the limit of flammability ... radiation from soot in the reaction zone became imperceptible, and the regions of combustion were marked only by a weakly luminous blue flame.”

“... the concentration of carbon dioxide and water were present in stoichiometric proportions and no unburnt fuel, carbon monoxide or other products of incomplete combustion could be measured” “Despite significant changes in the characteristics of the flames, the combustion process was complete even under limiting conditions.”

“Near the limit condition, the flames lifted from the burner surface and were typically attached to only a small portion of the burner rim; flame geometry and attachment fluctuated strongly.”

When ethylene was used, “it was possible to adjust the fuel flow rate so that the non-luminous ... flames were balanced 10 to 15 cm above the burner surface. With no alteration to the fuel or air addition rates, it was possible to maintain this limiting condition much longer than the residence time of the gas within the hood”

“... when natural gas fires at limiting conditions detach from the burner surface, the flames travel slowly upward away from the burner by as much as 3 to 4 burner diameters ... before complete extinction”.

In all three cases discussed – Coutin, Sugawa and Morehart – the temperatures were low compared to those which are typically observed in fuel-controlled or ventilation-controlled fires with the fuel source near the floor. For the blue partial interface flames, Coutin measured temperatures in the upper layer ranging from 350°C to 550°C. The flame was determined to be in the region of 800°C. Morehart *et al* measured temperatures in the smoke layer in the range of 100 to 160°C.

Both Morehart and Coutin concluded that the blue colour was due to absence of soot, which itself was due to low combustion temperature due to dilution of the fuel in combustion products.

Coutin performed Laser Doppler Anemometry measurements of the velocity field in the vent. He showed that the rate of air inflow was greater than that needed for complete combustion. The margin of error of these measurements was however too great to allow quantitative correlations to be made between the vent flow rate and the fuel flow rate. The observations suggest that the height above the floor of the burner did not influence the vent flow rate.

Coutin suggested that the blue flame which partially covers the interface is of triple flame structure. This is supported by his observation that the edge of the flame is brighter than the rest of it.

To some extent, the combustion is comparable with the conditions inside industrial furnaces with recirculation of a part of the combustion products (“flameless combustion” or “MILD combustion” – Moderate or Intense Low oxygen Dilution), whereby in those cases the aim is to reduce the flame temperature in order to reduce the formation of oxides of nitrogen.

1.3 Aims

The current work was performed to provide new knowledge on the behaviour of fires when the fuel source is close to the ceiling. In particular, it had the following aims:

- identify the mechanisms which allow the flame to stabilise itself at the interface between the upper and lower layers and the structure of the blue flame partially covering the interface
- explore the effect of changes in fuel type, fuel flow rate (and with it the thermal output power), the vent depth and the geometry of the vent on the stability of the flame
- ascertain whether a transition from the fuel-controlled behaviour observed by Coutin [Coutin *et al* 2003] to ventilation-controlled behaviour can be produced, and if so, describe the behaviour under the ventilation-controlled regime.

1.4 Contents of this Report

In the following chapter, the equipment used during this project and the measurements performed are presented. The first section – 2.1 – describes the two installations. Section 2.2 presents the burners. In Section 2.3, the diagnostics are listed: visualisation of the light emitted by the flame, particle imaging velocimetry (PIV), recording of the temperatures, analysis of the chemical composition of the upper layer and determination of the area covered by the flame. The chapter finishes with a section – 2.4 – describing the operating procedures which were followed during the experiments together with the results of preliminary tests which were needed to gain the necessary experience to allow the procedures to be defined.

In Chapter 3 the experimental results are presented and discussed. The chapter starts with a description, in Section 3.1, of the behaviour of the flames. Section 3.2 explores the case with a blue flame partially covering the interface between the layers, discussing the flow patterns, flame structure and stability of the flame. Section 3.3 describes the area covered by the flame and discusses the question of whether the area is suitable as an indicator of the heat release rate \dot{Q} . Section 3.4 finally looks at the changes in behaviour which occur if the ventilation is reduced, and describes the study of the transition from fuel-control to ventilation-control.

The thesis finishes with a short summary of the conclusions on Chapter 4

2 Experimental Apparatus

This chapter describes the equipment used during the project.

Section 2.1 provides a description of the two experimental compartments – the “Bertin” compartment in which the majority of the work was performed and a larger apparatus referred to as the “Telephone Box” which was constructed to allow a study of the effects of scale.

Section 2.2 presents the fuel sources used, namely the two burners used in the Bertin compartment and the burner used in the “Telephone Box”, and also the wooden pellets used as secondary fuel in the tests to study the potential of the interface flames to produce flashover.

Section 2.3 lists the diagnostic tools and the configurations for the different measurements. Simple visual observations were made to determine the conditions under which extinction occurs, to estimate the size of the air and smoke layers, and to record the time to ignition of the secondary fuel. Video photography was used to determine the area covered by the flame. Particle Imaging Velocimetry (PIV) was used to record the velocity field around the edge of the flame, the flow rate of air in through the vent and the flow field around the orifice of the burner. Thermocouples were used to measure the gas temperatures inside the compartment and the surface temperatures of the wooden secondary fuel. Gas chromatographs and online gas analysers were available to determine the composition of the gases in the upper layer.

Section 2.4 describes the operating procedures which were followed during the experimental work. In order for these procedures to be defined, some preliminary measurements were necessary to provide initial experience with the installation. These results also contributed to the insight gained into the mechanisms involved in the studied phenomena.

2.1 Compartments

2.1.1 Bertin Compartment

Most of the experimental work was carried out in the compartment used by Coutin in his study, although some modifications were made to the geometry [Coutin 2000], [Coutin *et al* 2000]. The construction and geometry are described in detail in [Bertin 1998].

Geometry

The compartment was of modular construction to allow variations of the configuration of the windows, insulation and ventilation.

An inverted channel was constructed to be attached to the compartment at the level of the soffit so that the flames and gas which exit through the vent are forced to flow horizontally (see *Fig. 2.1* and *Fig. 2.2*).

The compartment had inside measurements of 0.62 m in length, 0.84 m in height and 0.40 m in width. The front side was open except for a soffit of 0.19 m depth. A panel was available which could be used to increase the soffit depth to 0.34 m. The external channel was 1.5 m long, and 0.075 m deep. It had to be slightly narrower than the width of the compartment – specifically 0.36 m, due to the presence of brackets at the sides of the vent on which the upper part of the compartment rested.

A horizontal panel could be inserted to act as a raised floor, 0.15 m above the normal floor level, so that when it was installed together with the 0.19 m soffit, the same vent height was obtained as with the 0.34 m soffit and the original floor.

Construction

The upper sections of the wall, the ceiling and the extension to the soffit were constructed from 2 mm thick plate steel welded to a steel frame and insulated with a 50 mm thick layer of Kerlane[®] ceramic fibreboard.

A window of 420 mm long by 140 mm high was cut through the left-hand one of the side walls and covered with fire resistant glass. It was however found that this window fogs up too

quickly with soot to be of much practical use – even when sootless flames are studied, soot is produced at the start of the experiment before the system reaches its steady state.

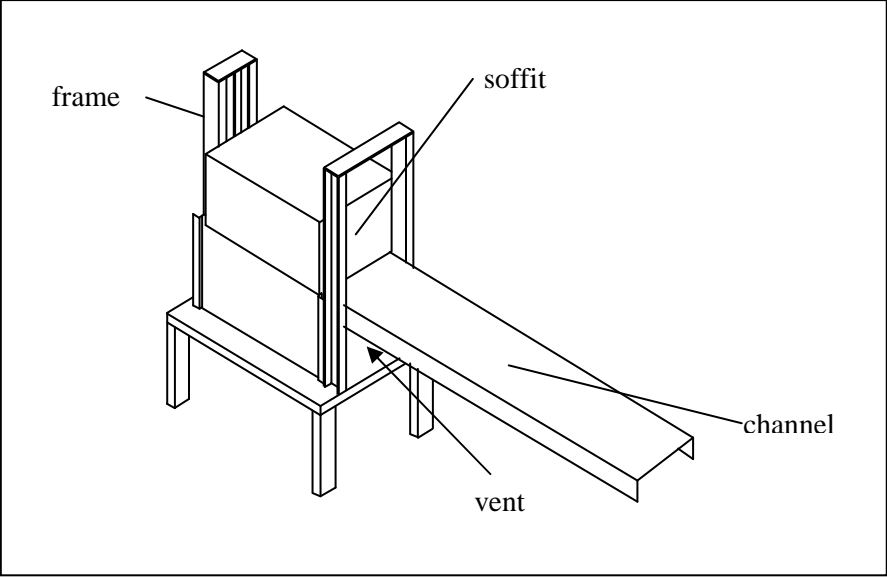


Fig. 2.1: The Bertin Compartment with the external channel and wheeled frame

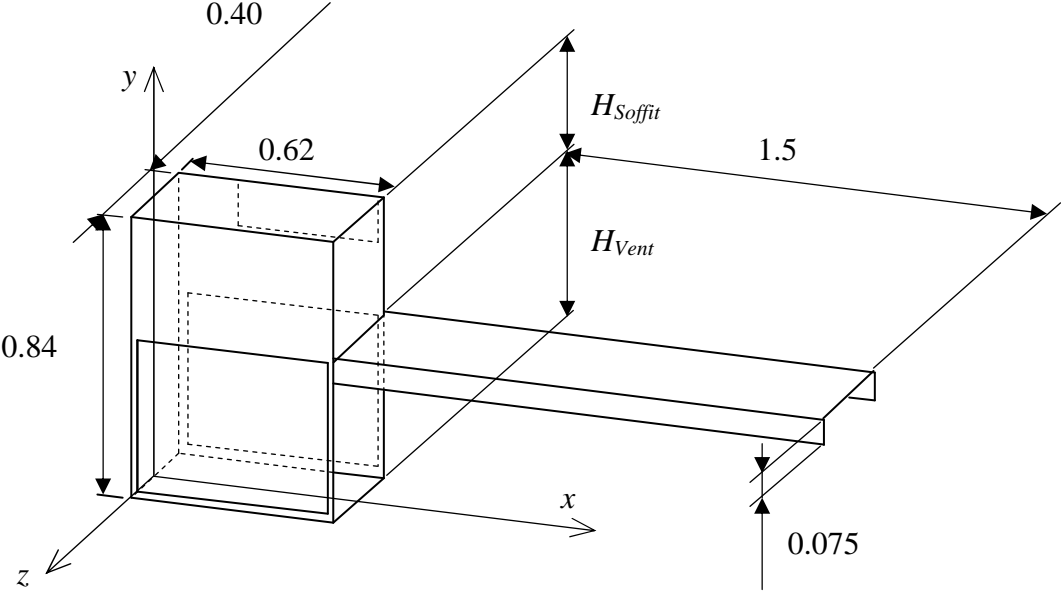


Fig. 2.2: Schematic of the Bertin Compartment showing the dimensions

Two different types of module were available for the lower sections of the side walls:

- metal panels containing tubes for cooling water. The cooling system had been used during Coutin's work, but during the current project these panels served only as insulated walls.
- windows of ceramic glass.

The lower section of the rear wall was formed by a vertical porous burner. This had been used during previous research, but in the current study it only served as a wall.

The floor was made of a 50 mm thick layer of fibre insulation board into which a ceramic glass window of 0.24 m × 0.19 m was incorporated.

The whole compartment was bolted onto a steel frame and mounted on wheels.

The external channel was made of sheet steel, 2 mm thick

Ventilation

A series of fibreboard panels of 6 mm thickness was produced to partially block the vent to produce a range of vent sizes. These are listed in *Table 2.1*.






description	configuration	height H_V	width W_V	ventilation factor F_V
full opening		0.5 m	0.4 m	0.141 m ^{2.5}
vertical slot – half		0.5 m	0.2 m	0.0707 m ^{2.5}
vertical slot - quarter		0.5 m	0.1 m	0.0354 m ^{2.5}
vertical slot – one eighth		0.5 m	0.05 m	0.0177 m ^{2.5}
vertical slot – one sixteenth		0.5 m	0.025 m	0.0088 m ^{2.5}

Table 2.1: Sizes of vent used

2.1.2 “Telephone Box”

The second experimental compartment comprised a square double-walled hood. It was designed so that smoke which spills out from underneath the inner hood is captured in the outer hood and led to a chimney, allowing measurements of the composition of the gases. Due to its square shape, symmetrical flow fields were produced with the air entrainment from all four sides being equal.

Heat loss from the inner hood was limited not just by the insulation, but by the presence of hot gases and smoke in the space between the two hoods.

Inner Hood

The external measurements of the inner hood were: length and width 0.80 m, depth 0.30 m. It was made from 2 mm thick steel sheets, with lining of ceramic fibre-board – 25 mm thick on the ceiling, 20 mm on the walls. This produced internal measurements of 0.76 m in length and width and 0.27 m in depth

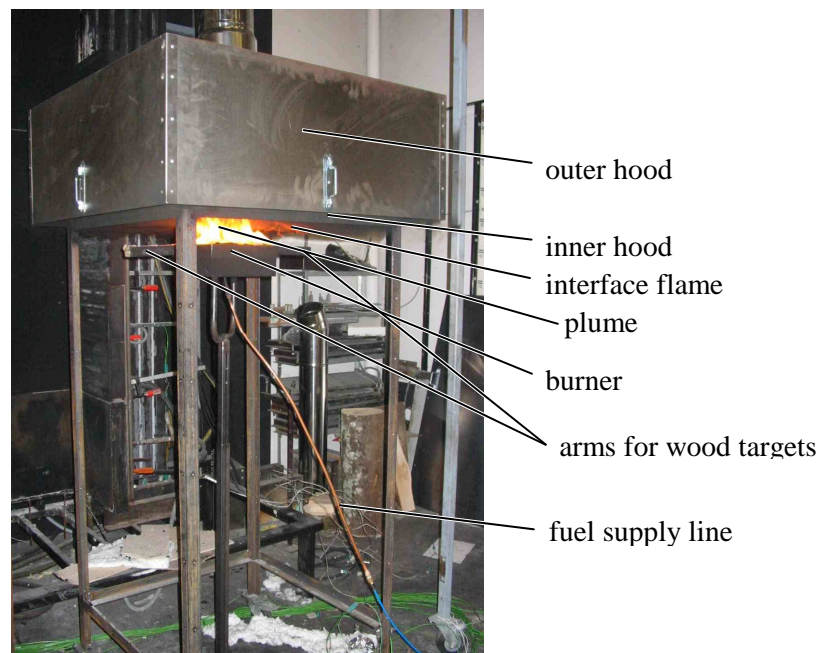


Fig. 2.3: Photograph of the installation during one of the tests

Outer Hood

The outer hood measured 1 m square, by 0.4 m deep and was made from thick steel sheets of 2 mm thickness. It was fitted with a chimney of Ø 0.2 m in the centre of the ceiling through which the smoke and gases could exit.

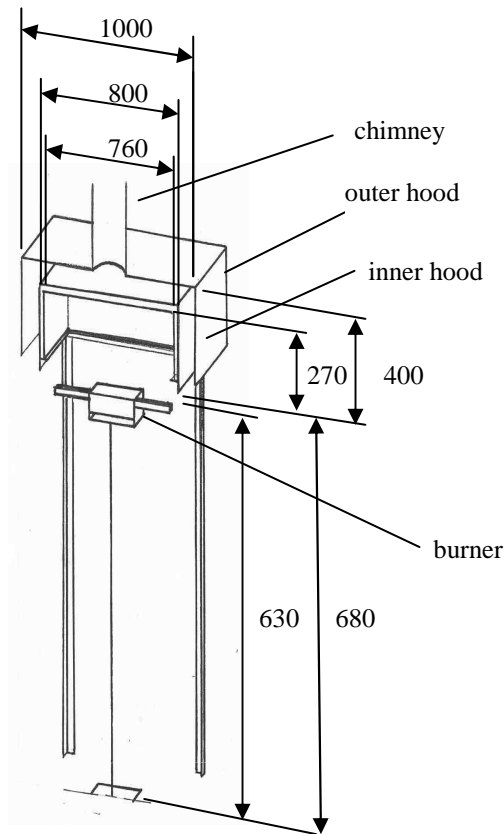


Fig. 2.4: Cutaway of the “Phone Box”

2.2 Fuel Sources

2.2.1 Use of Gas Burners to Simulate Solid or Liquid Fuels

The key difference between gas burners on the one hand and liquid pools and solids on the other is that for gas burners the fuel flow rate is determined by the pressure in the fuel supply line, whereas with liquids and solids the fuel supply rate is dictated by the heat flux to the surface of the pool or solid. The decoupling of received heat flux and fuel flow rate means

that gas burners do not reproduce the increase in gas supply rate associated with the increase in heat flux to solids or liquids from ceilings, walls and smoke layers, nor the drop in supply rate associated with a reduction in heat transfer following extinction or a reduction in combustion rate. For an experimenting scientist, this may be an advantage or a disadvantage depending on his objectives.

When in the open, a fire from a gas burner will otherwise behave in the same way as a fire from a liquid or solid and have the same ratio of (H_{fl}/D) if the Froude number Fr is the same.

Gas burners have been used by many researchers to simulate the flames from a solid while allowing the fuel flow rate to be decoupled from incident heat flux. Both configurations with a burner in the open (for example [Orloff, De Ris 1982]) or in a compartment (e.g. [Thomas, Heselden 1962], [Quintiere *et al* 1984], [Backovsky *et al* 1989], [Bertin 1998], [Coutin 2000], [Coutin *et al* 2000], [Bertin *et al* 2002] [Ohmiya *et al* 2003]) have been studied.

As well as the fundamental difference regarding the regulation of the fuel flow rate, there are several other differences between a fire fuelled by a gas burner and one fuelled by a solid object or pool of liquid. When solids or liquids burn, a part of the energy released by the combustion process is “absorbed” by the process of pyrolysis or evaporation; this is not the case when the fuel is in its gas phase from the outset. The gases and vapours which arise from pyrolysis or evaporation will be at their pyrolysis/evaporation temperature, whereas gaseous fuel issuing from a burner will normally be at a much lower temperature – depending on the configuration it may be below room temperature due to the expansion which accompanies the drop in pressure as the gas passes from a bottle to the burner, or it may be higher if the pipeline through which the fuel flows is subject to heat transfer from the flame. When solid objects burn, the fuel flow rate can increase both via an increase in the surface area of effected fuel, and an increase in the flow rate per surface area. In the case of a gas burner, only the second of these two is possible.

There are further differences between the behaviour of compartment fires supplied by gas burners and ones supplied by solid or liquid fuels. If there is no other fuel source inside a compartment, then flashover is not properly definable. Solids which form char can continue to smoulder after flaming combustion has ceased. Equivalent behaviour does not exist for gas

burners. If the vent to a compartment is very small, a gas burner may fill the compartment with fuel, flushing out the air, so that a flame will end up being stabilised at the vent; in essence, the compartment ends up acting like an extension to the fuel supply line and the vent like the orifice of a burner.

For all these reasons, gas burners have most often been used in studies of steady-state conditions, rather than of the growth of fire.

2.2.2 Burners used in the Study

2.2.2.1 Porous Burner

The porous burner was used in the smaller compartment. The porous burner acts in effect as a point source of fuel. It was designed to produce a low initial velocity of the fuel as it exits the burner, so as to simulate as well as possible the flow of pyrolysis products from a solid fuel.

The burner comprised a disk of sintered bronze beads set at the top of a steel cylinder (see *Fig. 2.5* and *Fig. 2.6*). The cylinder mantel incorporated a circuit of tubes for cooling water. The diameter of the disk was 62 mm, that of the cylinder 88 mm. Beneath the disk was a void to allow the fuel flow to settle (“chamber de tranquillisation des gaz” in *Fig. 2.6*).

This burner was used with flow rates of propane \dot{m}_F of up to 0.71 g/s, which equates to an energy flow rate \dot{H} of 33 kW, giving an initial velocity $v_{initial}$ of 0.14 m/s, a Froude number Fr of 0.03 and a nondimensional heat release rate Q^* of 30 (see Section 1.2.2). At this fuel flow rate, a flame height H_{fl} of 0.7 m is produced, which equates to a ratio of flame height to burner diameter of 11.

The lower end of the cylinder was attached to an arm which in turn was attached to a motorised 3-axis displacement table.

One disadvantage of this burner is that the 88 mm diameter tube acts as a non-negligible obstacle to the air flow in the compartment.

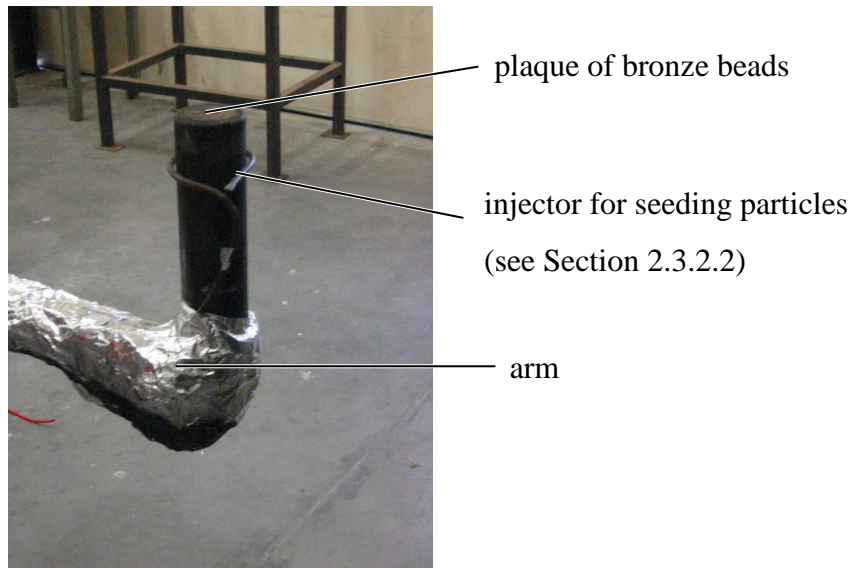


Fig. 2.5: The porous burner

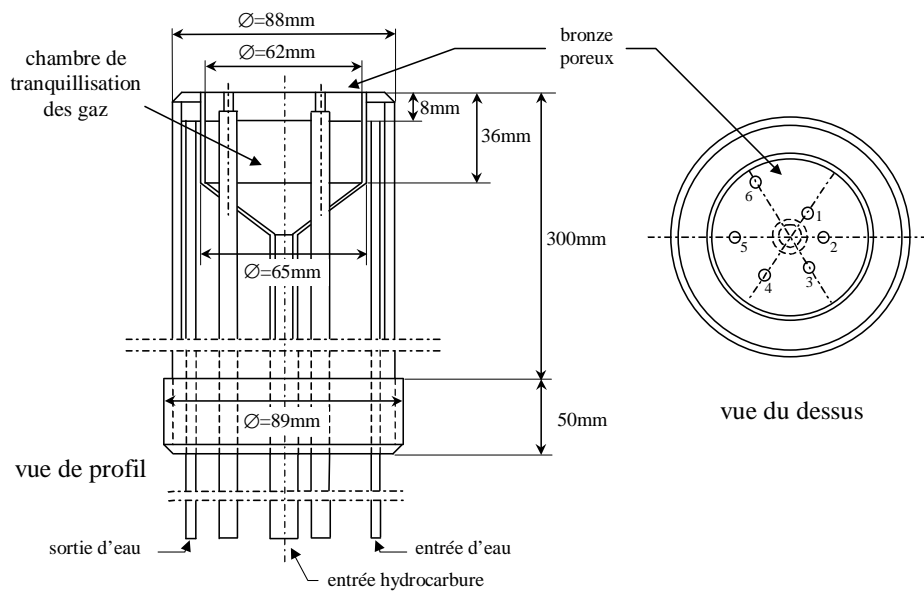


Fig. 2.6: Cross section of the porous burner.

2.2.2.2 Line Burner

The line burner was used in the smaller compartment. It was designed to act as a line source of fuel spread out across the width of the compartment. This enabled the creation of a flow field which was close to two-dimensional.

It was constructed from a copper tube of 8 mm external diameter with 18 holes of 2 mm diameter acting as upward-facing nozzles.

A fuel flow rate \dot{m}_F of 0.71 g/s ($\dot{H} = 33 \text{ kW}$) will produce an initial velocity $v_{initial}$ of 7.0 m/s , a Froude number Fr of 80, a nondimensional heat release rate Q^* of 9000 and a flame height of 0.3 m. This is rather far removed from the flow typically encountered when a solid or liquid fuel burns. However, when the burner is placed close to the ceiling, the jets are broken up, and so the behaviour is not that different from that which occurs when the porous burner is used, as could be observed during the experiments.

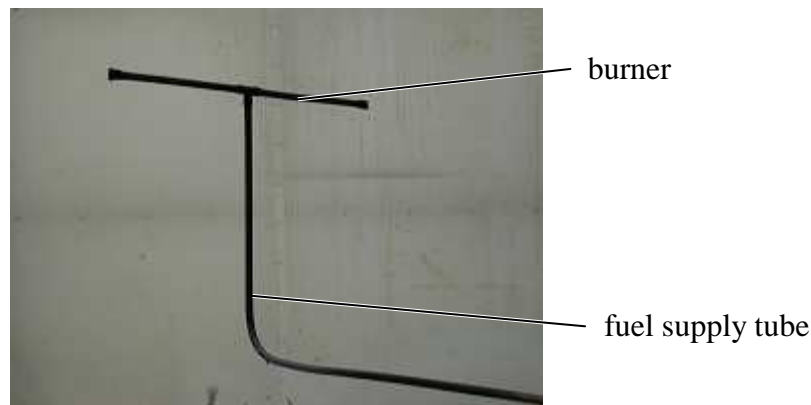


Fig. 2.7: The line burner

2.2.2.3 Sand-Bed Burner

The sand-bed burner was used in the “Telephone Box”. As with the porous burner, it was designed to produce a low initial velocity. As larger fuel flow rates were used in the Telephone Box than in the Bertin compartment, it was appropriate to use a burner with a larger surface area.

The sand absorbs a part of the heat released by the fire. As a consequence, the fuel is heated as it passes through the sand-bed, so when it exits the burner, it is hotter than in the case with the porous burner. The fuel does not reach the temperature of the vapours and gases emitted by a pyrolysing solid, but in comparison with a porous burner, a sand-bed burner more closely reproduces the conditions found when a solid object is pyrolysed. In particular, the comparatively high initial temperature of the fuel produces a very sooty flame.

The sand-bed burner used in the experiments comprised a rectangular steel box, open at the top. A sheet of perforated steel was placed horizontally inside to divide the box into two chambers: a lower gas tranquilisation chamber, and the sand-bed. The burner had a square surface area of 0.25 m by 0.25 m. It was 0.10 m deep.

It had two arms attached on opposite sides, each 0.34 m long, made of a U-profile of steel filled with ceramic fibreboard. These were designed to hold heat flux meters and blocks of wood to act as secondary fuel.

The burner was used with fuel flow rates of up to 1.2 g/s, or, expressed in terms of energy flow rates, up to 55 kW. This corresponds to an initial Froude number of 4×10^{-5} or a dimensionless heat release rate Q^* of 1.2. With this maximum flow rate, flames of about 1.1 m are produced, giving a ratio of the flame height to the hydraulic diameter of the burner of 4.2.

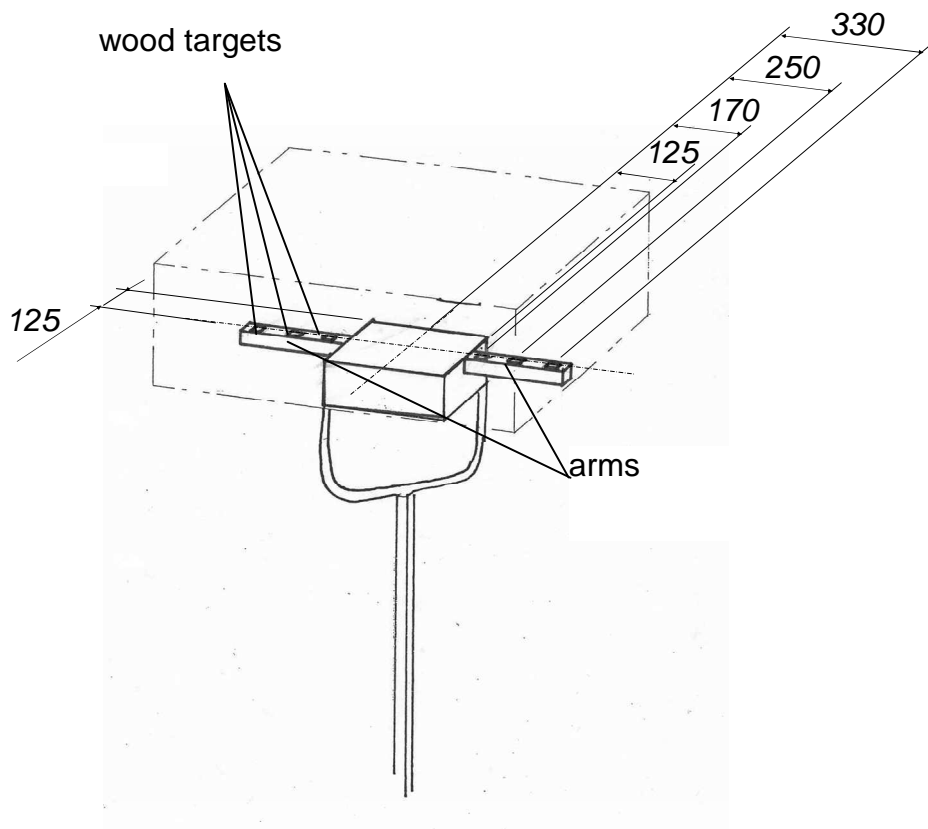


Fig. 2.8: Geometry of the gas burner and secondary fuel sources

2.2.3 Gas Supply

Experiments were performed both using methane and propane. The gas was supplied from bottles through a pressure governor and a mass flow regulator.

The flow regulator was calibrated for air, rather than for the fuel gases used. The conversion factor used to calculate the fuel flow rate from the controller display values was only known within 10 % accuracy. This meant that there was the potential for the introduction of a systematic error, although the ratio between any two given flow rates and the reproducibility were accurate to within 2 %.

2.3 Measurements performed and Diagnostics used

2.3.1 Imaging of Flame

Much information can be gained from simple visual observation of the spontaneous emission from the flame of light in the visible spectrum.

A digital camera and digital video camera-recorder were available. Observations were possible through the windows in the sides and floor of the compartment, and through the vent.

Shape and Colour of the Flame

The shape, size, colour and movement of the flame provide clues to the aerodynamics and chemistry of the system.

The yellow colour normally associated with flames stems from the incandescence of soot particles. The hydrocarbon radicals present in a flame emit blue light, but the intensity is normally so weak that it is not visible with the naked eye above the yellow from the soot, and so is only perceived when there is no soot present in the flame [Drysdale 1998].

The shape, size, colour and movement were directly recorded with the video camera.

Area Covered by the Flame

The area covered by the flame was determined to study the correlation between the area and the heat release rate (see Section 2.3.5) and as part of the exploration of the behaviour regimes and the stability of the combustion.

Zone Size

As mentioned in Section 1.2.3.2.2, the depths of the upper and lower layers vary depending on the conditions and indicate the combustion regime.

The size of the upper and lower layers was determined by measuring with a ruler and the naked eye the distance between the floor and the flames at both the rear wall and at the vent. It was assumed that the interface is a flat plane between these two positions.

Extinction

The question of what conditions are necessary for sustainable combustion to be possible and what conditions will lead to the flame extinguishing is fundamental to the ability to predict the behaviour of a fire.

In order to explore the interface between those conditions which allow sustained combustion and those conditions which do not, the limits must be approached from the side where combustion is possible. Observations can be made that the flame extinguishes if the fuel flow rate or the ventilation is reduced from a value at which sustained combustion is possible, whereas obviously self-ignition is not to be expected if the fuel flow rate or the ventilation is initially set below the minimum value necessary to sustain combustion and then raised above this minimum.

Within this project, conditions are defined as permitting sustained combustion if extinction is not witnessed within ten minutes of those conditions being implemented. It should however be borne in mind that, because the extinction limits are approached from conditions of higher fuel flow rates, and hence higher temperatures, this procedure may lead to the limits being recorded at slightly lower fuel flow rates than is actually the case, i.e. that unsustainable cases are likely to be recorded as sustainable, while sustainable ones are not likely to be recorded as unsustainable.

2.3.2 Velocity Measurements

Particle Imaging Velocimetry (PIV) is an optical technique to determine velocity fields in fluids. It involves “seeding” the flow, that is dispersing visible particles, vapour droplets or – an option with liquid flows – gas bubbles in the fluid flow field, shining a sheet of light through the region of interest, and taking two photographs in quick succession of the light from the sheet scattered by the particles (Mie scattering) [Dantec 2002]. The displacement is then calculated between the image of the particles on the first photograph and the image on the second. The calculation is performed by dividing the image into “interrogation windows” of a set number of pixels and performing a correlation calculation between the corresponding windows in each photograph.

This technique was used during the current project to determine the velocity of the gas at the edge of the flame v_e , the flow rate of air in through the vent, and the flow pattern around the orifice of the burner.

2.3.2.1 Equipment

The PIV system used was built by LaVision.

Laser

The laser used was a Quantel CFR 200 dual-cavity Nd:YAG pulsed laser. It gives a maximum output of 125 mJ per pulse, with a pulse duration of 6 ns. The time delay between pulses can be varied between 1 μ s and 0.1 s – the appropriate value being dependent on the gas velocities which are to be resolved. The beam has a width of 0.6 mm at half intensity.

The light emitted by such lasers is in the infrared range (the wave length is 1064 nm). To obtain light within the visible spectrum, the beam is passed through a potassium dihydrogen phosphate crystal (KH_2PO_4 , also known as KDP) – this material has the property of changing the frequency of light that passes through it [Cleveland Crystals 2006]. As the light passes through the crystal, its wavelength is halved to 532 nm, which equates to a green colour.

The beam is then passed through a prismatic lens to generate a light sheet with an opening angle of roughly 60° , while retaining the beam width of 0.6 mm.

Camera

The camera used was a LaVision Flowmaster 3 CCD (charged couple device) digital camera specifically designed for the use with PIV systems. It can store the information from one exposure directly on the CCD chip, allowing a second image to be taken after a delay which is shorter than that necessary to transfer the information from the camera to the control unit. The first frame is taken with an exposure time of 10 μ s, the second with 125 ms. The time delay between the two frames must be synchronised with the delay between laser pulses.

The camera has a resolution of 1240×1048 pixels. Its lens has a focal depth of about 5 mm.

Filter & Shutter

Under normal operating conditions, a filter is fixed to the camera lens to block light from sources other than particles scattering the light from the laser. The filter used had a 10 nm bandwidth centred around the wavelength of the laser, 532 nm.

In order to be able to correlate the velocity field with the position of the flame, the measurements around the flame edge were performed without this filter. Under these conditions, a liquid-crystal shutter was installed to reduce the exposure time for the second image of each pair, as the light from the flame was strong enough to risk damaging the CCD chip if the full 125 ms exposure time were allowed. The light scattered by the particles was brighter than the flame, but lasted only for the duration of the laser pulse. Therefore, by setting an appropriate exposure time, it was possible to capture both the light scattered by the particles and enough light from the flame to allow it to be visible on the image without the light from the particles being drowned out. The appropriate exposure time depended on the luminosity of the flames: for orange flames, a 15 ms exposure time was chosen; for blue flames, the time was 50 ms.

Seeding

The seeding needed to be adapted to the individual measurements.

For the measurements made in the upper layer and in the vicinity of the flame, the seeding must be heat-resistant. Because of this, solid particles were used. Specifically zirconium oxide was chosen as it had less of a tendency to cake together in lumps as did the other types of particle which were available.

Solid particles need to be injected into the system with a gas flow. Injection with the fuel flow through the burner was not possible because the flow rates were too low for sufficient particles to be entrained, and for safety reasons because the seeder was not gastight. In addition to this, seeding is not possible through the porous burner, as the particles would get trapped in the pores. It was therefore necessary to inject the particles into the compartment with a separate gas flow. It was found that if the particles are injected into the upper zone, enough would filter down to the layer of fresh air to allow measurements at the interface between the upper and lower layers. Nitrogen was used, as air would have substantially influenced the combustion. The flow rate was set at the minimum necessary to provide

enough particles, but so as not to disturb the flow patterns more than could be avoided; specifically a value of $0.23 \times 10^{-3} \text{ m/s}$ was set.

The injection systems are presented on the following pages with the presentation of the configurations.

The measurements in the lower layer were performed with paraffin fog (“disco smoke”), as it is cheap, can be administered with a low initial velocity so as not to perturb the flow, and follows the air flow well. However, at high temperatures, the paraffin droplets evaporate, and so the fog cannot be used in proximity of the flame.

The fog was produced with a Z 1500 model generator by Antari from Eurofluid fog fluid. The droplets have a characteristic diameter of $0.3 \mu\text{m}$.

The fog is led from the generator to a box which acted as a tranquilisation chamber. The box had a slit on the top side, parallel to the vent (or in other words at right angles to the laser sheet). The fog flowed out through this slit and was entrained into the compartment with air flow.

Control Unit

The laser, camera and shutter were controlled and synchronised, and the data were collected with a PC-based control unit.

The system allowed an acquisition frequency of 2 Hz.

Treatment parameters

The vectors were calculated from interrogation windows of 64×64 pixels. The quality of the seeding did not allow smaller windows. To increase the number of vectors obtained, the windows were defined with 50 % overlap of neighbours.

The vectors were calculated via two iterations of the cross-correlation calculation, whereby the interrogation windows for the second iteration were shifted by the equivalent of the displacement calculated in the first iteration.

Two algorithms were used to remove unwanted vectors [LAVISION 2002]. Vectors were removed if

$$\frac{C_1 - C_{base}}{C_2 - C_{base}} < 2.6 \quad (2.1)$$

where C_1 and C_2 are the values of the highest two peaks of the correlation function and C_{base} the baseline value of the correlation function. Vectors were also removed if they fell outside the range of the value of the median of surrounding vectors plus or minus the root mean square of the six surrounding vectors which are closest to each other in value; if a vector is rejected by this algorithm, then the three vectors corresponding to the next-highest peak values of the correlation function for the interrogation window are compared to the median of the surrounding vectors, and if one of them falls within the range of median plus or minus root mean square, it is considered as the valid vector.

2.3.2.2 Velocity Field around the Burner

Concept

As part of the study of the aerodynamics in the upper layer, measurements were made of the velocity field around the burner.

These measurements were only performed with the porous burner.

Configuration

The measurements were made in the central plane ($z = 0$ m, $z/w = 0$).

The laser light was projected into the compartment through the window in the floor.

As this window was to the rear of the burner and the light cannot pass through the burner, measurements were restricted to an area behind the burner – see *Fig. 2.9*.

The camera was positioned to look through the window incorporated in the upper half of the left-hand wall. The field of view measured 0.175 m in length and 0.100 m in height and was located between $x = 0.102$ m (0.16 L) and 0.277 m (0.44 L), and $y = 0.70$ m (0.83 H) and 0.84 m (1.0 H). This equates to a pixel for every 0.14 mm; the interrogation windows (64 pixel \times 64 pixel) equated to an area of 8.8 mm \times 8.8 mm (see *Fig. 2.9*).

Seeding

Zirconium oxide particles were injected via a copper coil surrounding the burner, with eight holes producing upward jets parallel to the fuel flow.

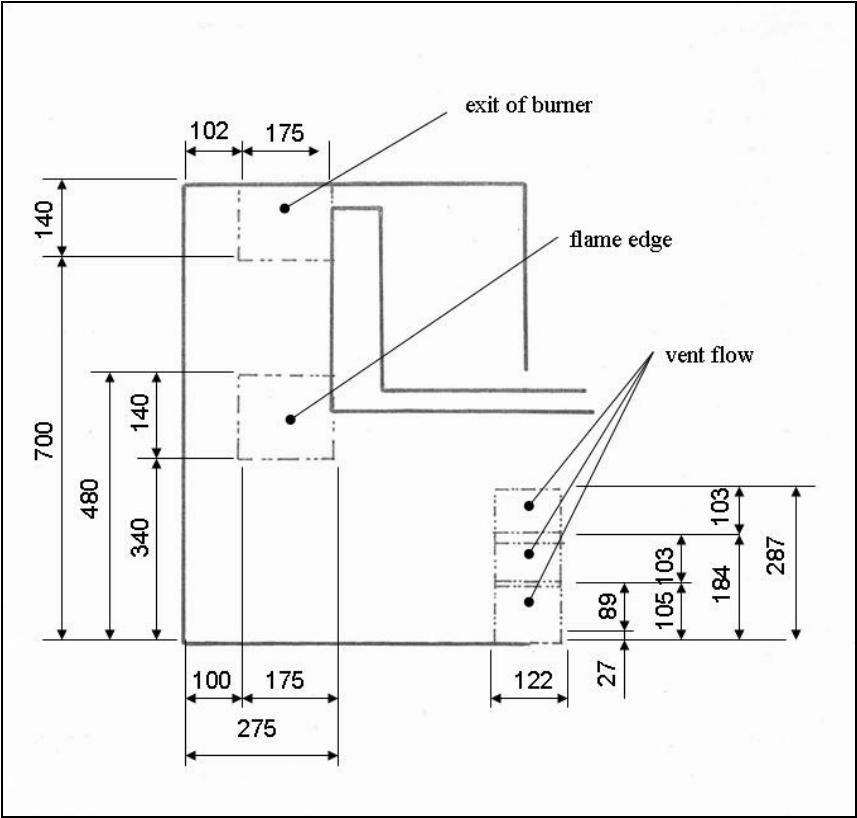


Fig. 2.9: Fields of view for the PIV measurements

Accuracy

These measurements were primarily performed to gain a qualitative insight into the flow patterns. Therefore, detailed questions as to the quantitative accuracy of these measurements were not posed.

2.3.2.3 Velocity Field around the Edge of the Flame

Concept

A combined recording of the laserlight scattered by the seeding particles and the light from the flame allowed the velocity field to be determined relative to the flame.

Due to the low acquisition frequency of 2 Hz, it was not possible to resolve the movement of the flame edge relative to the experimental apparatus. However, as the location of the edge of the flame fluctuates around a mean position, the average velocity of the air and upper layer gases at the flame edge relative to the compartment is equal to the average velocity at the flame edge relative to the flame. Therefore, by submitting the individual fields of velocity vector to a coordinate transfer relative to the edge of the flame, an average vector field can be calculated, showing the movement of the gas around the flame edge relative to the flame.

Configuration

The laser was positioned to project the light in through the vent.

The measurements had to be performed with the external channel removed, so as to create space for the laser heads.

The camera was positioned looking in through the windows in the lower section of one of the walls. The field of view was located in the central plane ($z = 0$ m) in a field of view measuring 174 mm in length by 100 mm in height, located between $x = 0.24$ m (0.41 L) and $x = 0.44$ m (0.72 L), and between $y = 0.43$ m (0.52 H) and $y = 0.50$ m (0.60 H) (see *Fig. 2.9*). This equates to a pixel for every 0.14 mm. The interrogation windows (64 pixel \times 64 pixel) equated to an area of 8.8 mm squared.

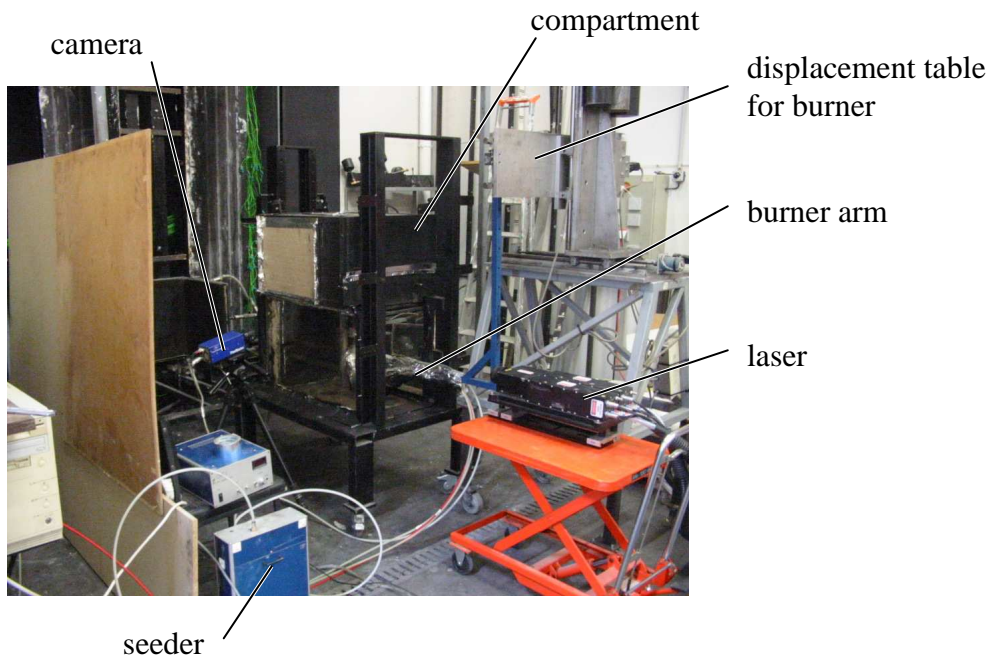


Fig. 2.10: Compartment and PIV system for the measurement of the velocity at the flame edge.

Seeding

Zirconium oxide particles were injected into the upper layer through a copper tube inserted through the ceiling and containing eight holes to produce a horizontal fan of jets. It was shown that sufficient particles flow from the upper layer to the lower layer to allow the velocity field immediately below the smoke layer to be recorded.

Accuracy

The gas velocities fluctuate significantly – values were recorded varying from 0.1 m/s to 0.8 m/s . The analysis of the data was restricted to average values. A comparison of data from several series of measurements suggest that an error margin of $\pm 10 \%$ should be attached to the averages.

2.3.2.4 Vent Flow Rate

Concept

The velocity field was determined in the central plane of the vent. From this, the velocity field through the vent was extrapolated. The air flow rate is estimated by a numerical integration of the velocity data over the surface of the vent.

Configuration

The available equipment did not allow accurate measurements to be made if the whole height of the vent was included in the field of view of the camera. Therefore, the plane was divided into three fields of view, and the velocity field was determined for each individually. These fields of view are illustrated in *Fig. 2.9*. They each measured 122 mm in length by 103 mm in height, giving a resolution of 0.098 mm per pixel or 6.3 mm per interrogation window of 64×64 pixels.

The laser was positioned to project its light in through the vent. The camera was placed beside the compartment, looking in through the window in the lower half of one of the walls. The measurements had to be performed with the external channel removed, so as to create space for the laser heads.

Seeding

Seeding was performed with paraffin fog (“disco smoke”), as described on page 74. As mentioned, the fog evaporates when it gets near the flames, and so seeding is not available for the region immediately below the flames. However, the air in this region flows outwards, not inwards; the whole of the inflowing stream was seeded.

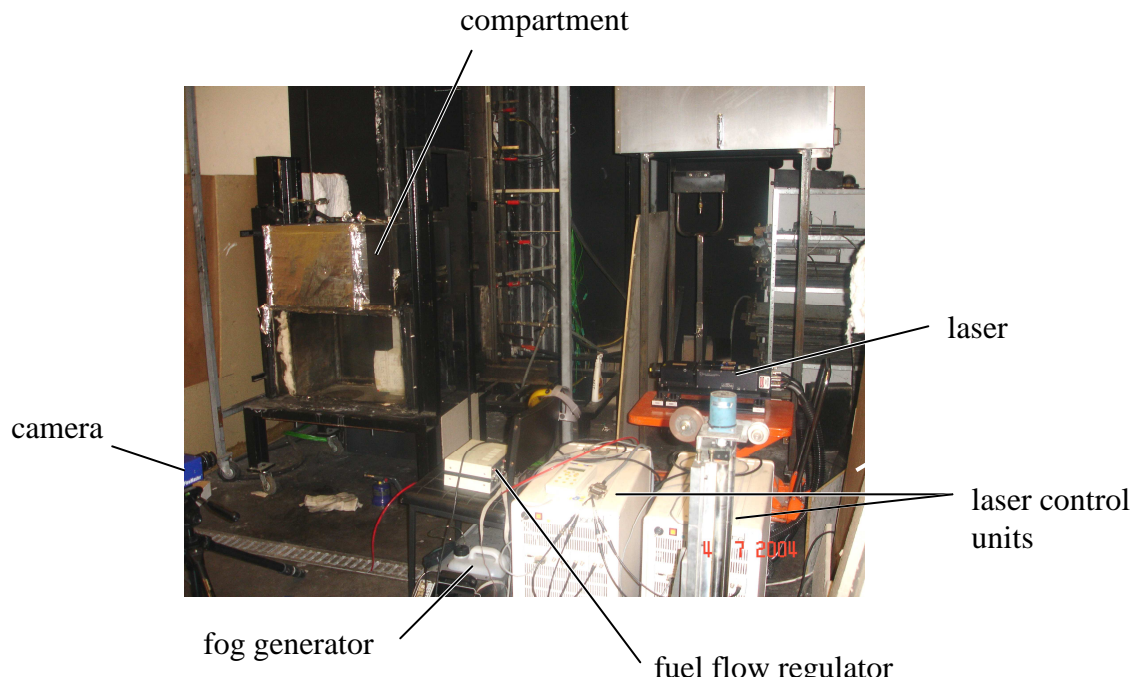


Fig. 2.11: Installation with the PIV configuration for measuring the vent flow

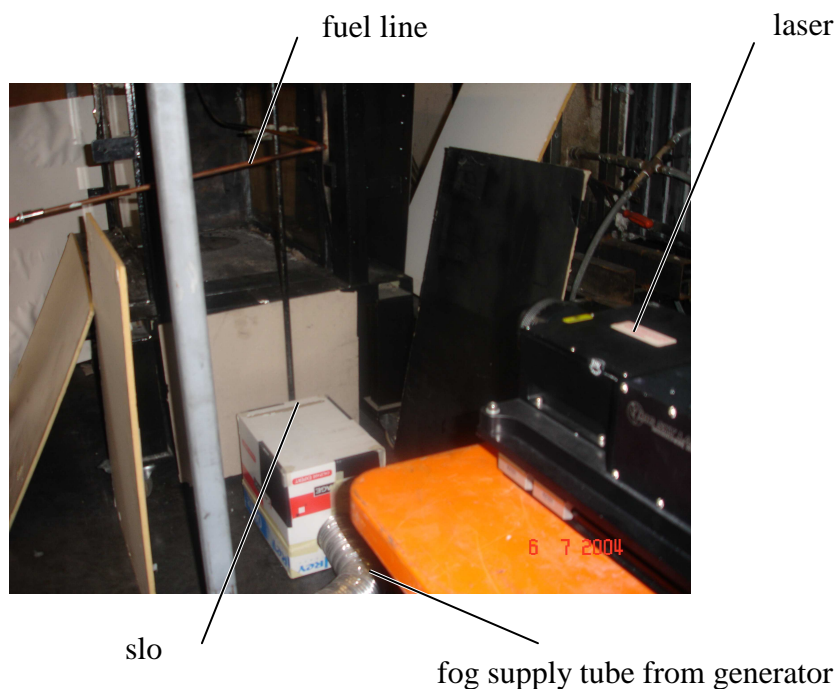


Fig. 2.12: View from in front of the compartment showing the box used as a tranquilisation chamber for the seeding flow.

2.3.3 Temperature Measurement

Temperature measurements were performed with type K (chromium-nickel/aluminium-nickel) thermocouples.

Thermocouples

Bertin Compartment

For the Bertin compartment, one thermocouple tree with twelve thermocouples was available. Due to technical problems, the tree was modified several times throughout the tests, so the heights of the thermocouples are not the same in each test.

The thermocouples made from wire of 50 μm diameter, welded end to end, so there was practically no “bead” of larger diameter at the joint. For the method of fabrication, see [Poireault 1997]. Using Neveu’s model (see [Poireault 1997]), the time constant was calculated as

$$\tau_{TC} = \frac{\rho_{Gas} c_{p-Gas} d_{Wire}^2}{4Nu\lambda_{Gas}} = 60\mu\text{s} \quad (2.2)$$

with ρ_{Gas} , c_{p-Gas} and λ_{Gas} being the density, thermal capacity and thermal conductivity of the atmosphere in which the thermocouple is located, d_{Wire} the diameter of the wire of the thermocouple, and $Nu = (0.24 + 0.56 Re^{0.45})$ the Nusselt number for a Reynolds number $Re < 44$ calculated with the thermal properties of the gas and the diameter of the wire.

Measurements of the surface temperature of the walls, floor and ceiling were performed with sheathed thermocouples. These were made of wires of 0.15 mm diameter, with a bead of 0.4 to 0.5 mm. The outer diameter of the sheath was 1 mm. According to the manufacturer, the time constant is 0.15 s.

The radiative losses were considered to be low enough to be neglected as there is only a fairly minor difference in temperature between the thermocouple and the walls of the compartment and as the absolute temperatures are not very high.

Telephone Box

Measurements were made of the surface temperature of the wood targets using sheathed thermocouples.

The measurements are expected to reliably reproduce the temperature up to the time of ignition, but after ignition, the pyrolysis of the wood may lead to the thermocouple losing contact with the wood. Also, the flame will tend to increase the temperature of the thermocouple.

Datalogging

The thermocouples were plugged into a multichannel datalogger with a maximum acquisition frequency of 2 Hz. This meant that the time lapse between measurements was much larger – in the case of the fine-wire thermocouples, several orders of magnitude larger – than the time constant of the thermocouples, and so thermal inertia of the couples did not significantly affect the results. However, this low acquisition frequency did not allow the rise and fall in temperature caused by the passage of the flame over a thermocouple to be properly logged.

2.3.4 Chemical Analysis

It was not possible to obtain instantaneous measurements throughout the upper and lower zones. Equally, the technology available did not allow a probe to be installed to follow the flame so as to take samples from a position defined relative to the flame.

Instead, samples were taken from a few locations in the upper zone. Online analysis allowed the development over time of the concentrations of the major species to be determined. Gas chromatography was used to obtain average values of the concentrations of most of the stable species present.

The atmosphere inside the upper layer is constantly in movement and is not homogeneous. Therefore, variations in the concentrations of species between samples are greater than the inaccuracy of the analysis techniques.

Sampling

Samples were drawn through a steel tube inserted through the ceiling. Its thermal inertia led to a quenching of the chemical reactions, so only the stable species were analysed.

Online Analysers

A bank of on-line gas analysers is available in the laboratory. However, only the analysers for carbon monoxide, carbon dioxide, methane and ethylene are working reliably.

Because of the difficulties filtering the smoke from the gas samples, the use of the analysers is restricted.

The tube transporting the sampled gas from the experimental installation to the bank of analysers is thermostated at 60°C to prevent the water vapour from condensing and thus prevent the other gases being dissolved in the liquid water. Any water vapour in the sample is extracted immediately prior to analysis, so this species is always missing from the total.

The reaction time of the analysers is too slow for it to follow the instantaneous changes in local concentration, although it can follow the trend after ignition of the burner as the originally fresh air in the top part of the compartment is replaced with fuel and combustion products.

Gas Chromatography

Samples were collected in steel syringes with a volume of 0.9 l.

The water vapour was removed from the samples prior to analysis, but the concentration of water vapour can be deduced from the amount of carbon present in the samples.

The samples were passed through two chromatographs.

The hydrogen concentration was determined with an apparatus by Girdel. Argon was used as a carrier gas, flowing at $0.33 \times 10^{-3} \text{ m}^3/\text{s}$ (20 ml/min). A Tamis 13 X column was used, heated to 42°C. The detector was of the thermal conductivity type (TCD), thermostatted at 70°C.

For the analysis of the content of hydrocarbons in the samples, a Perichrom 2100 was used. The carrier gas was helium. The samples were passed through three columns, all heated to 80°C. One line passed $0.5 \times 10^{-3} \text{ m}^3/\text{s}$ (30 ml/min) of carrier gas through a column with an aluminium matrix in a $1/8$ -inch stainless steel tube and through a flame ionisation detector

(FID) at 250°C. A second line passed $0.33 \times 10^{-3} \text{ m}^3/\text{s}$ ($20 \text{ ml}/\text{min}$) of carrier through a Tamis 5A and a Poropack Q, and then through a TCD at 140°C.

The technicians operating this equipment estimated the errors to be about plus or minus 5 % of the output values.



Fig. 2.13: A sample being taken for analysis the with the gas chromatograph

2.3.5 Area Covered by the Flame

2.3.5.1 Aims and Concept

Aims

As mentioned in Section 1.2.2, Orloff and De Ris [1982] observed during tests with horizontal gas burners that for a wide range of fuel flow rates and burner sizes, the volume of the reaction zone was roughly proportional to the heat release rate. If a similar correlation between the amount of energy released and the size of the flame could be found for the interface flames, this would for example allow a distinction to be drawn between the amount of heat released by the part of the flame which is inside the compartment, and the part which is outside. It was not expected that a link would be determined with sufficient accuracy to allow the combustion efficiency to be determined – i.e. to determine the ratio between the amount of fuel injected into the compartment and the amount of fuel which is in fact

combusted. However, information gained may be useful towards the study of to what degree the vent flow rate is determined by the total heat release rate and to what degree it is determined by the heat released inside the compartment.

The search for a correlation involved answering questions such as whether the combustion efficiency remains constant or whether the ventilation has an influence on the size of the flame – does the decreased oxygen supply into the compartment lead to an increase in the size of the internal part of the flame and/or does the reduced oxygen supply increase the time it takes for the fuel to combust (which would lead to an increase in the length of the flame).

The area covered by the flame – or more precisely the area covered by the part of the flame which is inside the compartment – was also used as an indicator of the stability of the flame. The concept of stability is important particularly for numerical modelling. Three cases can be distinguished, according to the surface covered by the internal part of the flame A_{fl-in} :

- stable flames: $\frac{A_{fl-in}}{A_c} = 1$
- unstable flames: $0 < \frac{A_{fl-in}}{A_c} < 1$
- extinction: $\frac{A_{fl-in}}{A_c} = 0$

where A_c is the floor area of the compartment.

Definition of Quantity to be Measured

In the most commonly studied compartment fire scenarios, the part of the flame outside the compartment is vertical, whereas any flames inside the compartment at the interface between the upper and lower layers will be predominantly horizontal. Due to this, the buoyancy effects on the two parts of the flame are not equal, in particular with regard to the entrainment of air, making any comparison between the two difficult to interpret. Therefore, the external channel was conceived so that the gas and flames would continue to move horizontally after they exit the compartment.

In order for measurements to be performed, the practical question needs answering as to how to define the “size” of the flame. Engineering judgement suggests that as a first

approximation one can allow oneself to assume that the thickness of the flame is constant, but as the flame is not flat, it is not possible with the available technology to measure its surface area.

As the flame runs horizontally, it lends itself to a study of the projection of the area of the flame onto a horizontal plane. It should however be borne in mind that the internal part of the flame is of cellular nature, with tips reaching up into the upper layer, and is therefore “more three-dimensional” – or in the vocabulary of fractal geometry, is of a higher dimensionality – than the external part. A comparison of the projections of the two areas can therefore not be an accurate depiction of the ratio between the volumes of the internal and external parts of the reaction zone. One of the questions which were studied is whether or not this distorts the resulting ratios so much as to make them irrelevant.

2.3.5.2 Technology used to measure the area covered by the flame

The measurements were made by taking a series of images with a digital camera, comparing the area within the image that is covered by the flame with the area of the compartment and channel, and then averaging over the series of images.

The camera was placed on the floor of the laboratory underneath the experimental compartment, looking upwards. Images of the part of the flame which was inside the compartment could be recorded through the window in the floor of the compartment.

The channel was too long to fit inside the field of view of the camera, so the external part of the flame had to be divided into three separate sections and the size of each section recorded individually. The four fields of view (one internal, three external) are illustrated in *Fig. 2.14*. The field of view inside the compartment runs from $x = 0$ m to 0.58 m (0 L to 0.95 L), the first external field of view from 0.62 m to 1.21 m (L to 1.95 L), the second external from 1.21 m to 1.69 m (1.95 L to 2.73 L) and the third external from 1.69 m to 2.16 m (2.73 L to 3.48 L). There is a small part of the flame immediately inside the vent which was not contained in any of the fields of view. The camera viewing angle was too small – or the distance between the camera and the compartment too small – to fit the entire length of the compartment inside the camera. The same section of the interface in question was not visible

by a camera placed outside the compartment as the front edge of the floor of the installation blocked the view. It was decided that the inaccuracy that this produces was tolerable.

In the field of view inside the compartment, the fuel line blocked the line of sight to about 2 % of the studied area. In the first of the three external fields of view, the fuel supply line and the stand holding the burner and fuel supply line block the line of sight to 6 % of the area of this particular field of view or 2 % of the area of the channel. In most of the images where there was flame above the fuel flow pipe, enough light was reflected from the flame to the camera for the pipe to register as “light” – i.e. flame – rather than “dark”/background. Therefore the error caused by this obstruction can be considered to be marginal.

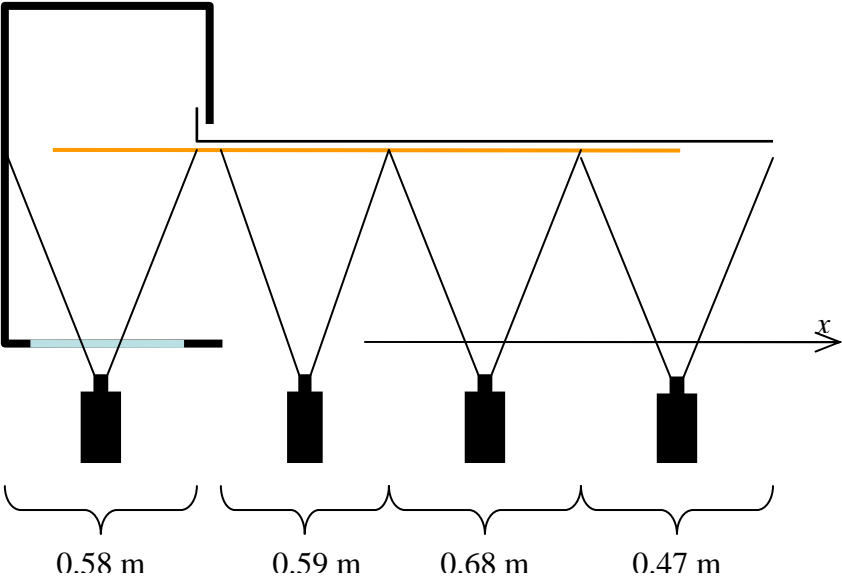


Fig. 2.14: Configuration for the determination of the area covered by the flame

As only one camera was available, recordings could not be made simultaneously from the four fields of view, but instead a series of images was taken first for one field of view, then for the next etc. This makes it impossible to recreate the instantaneous size of the flame. However, providing the average area within each set of images is sufficiently close to the average area within the field of view over time, then the average values for the whole of the area of the flame can be correctly created by adding the average from each set of images because of the mathematical rule

$$\overline{\sum_i x_i} = \sum \bar{x}_i \text{ if } x_i \geq 0 \forall i \quad (2.3).$$

The images not only contain the “useful” field of view, but also show a part of the surrounding walls. The DaVis[®] image treatment software developed by LaVision which formed part of the PIV system was used to determine which part of the image was relevant for the measurements.

The area covered by the flame in each image was calculated by converting the image into greyscale, calculating a histogram of the number of pixels at each level of grey and then counting how many pixels are above and below a threshold grey value which represents the luminosity of the background. The threshold between the “dark grey” of the background and the light grey of the flames was determined using the image treatment software for the PIV system.

Average areas can then be calculated by averaging the number of “light” and “dark” pixels in each series of images. A sensitivity study showed that the number of images from which the average was calculated could be limited to 64.

Accuracy

A study of the images showed that the largest source of errors stemmed from the fact that the transition between light and dark is not clear, and so in many cases there is a number of pixels which show part of the background which have the same intensity value as a number of pixels which show flame. This is particularly the case when the flame is of low luminosity. Further inaccuracies are incurred due to the effects of perspective and the relatively short distance between the camera and the height at which flame was located, which meant that it would have demanded more effort than could be afforded to exactly draw the line around where the flame touches the wall.

A comparison of data collected under identical circumstances suggested that the spread corresponds to up to 7 % of the average value.

2.4 Operating Procedure

2.4.1 Ignition Procedure

Most of the measurements, particularly those in the Bertin compartment, were performed with the burner located in the vitiated zone above the level of the soffit.

It was found that it is very difficult to obtain sustainable combustion if the burner is located in this zone from the very beginning of the test when the burner is ignited. Therefore, the burner was positioned in the lower half of the compartment before ignition.

When the burner was ignited, the fuel flow rate was raised to at least 3.5 g/s (equating to 16 kW).

Initially, jet flames exist above the burner. Over the course of the next two minutes or so, distinct upper and lower layers establish themselves, the upper one reaching from the ceiling to just below the level of the soffit. After about another minute, the combustion spreads from the plume across the interface between the smoke and air layers; the part of the fire plume below the interface remains essentially unaltered, but the part of the flame in the plume above the interface disappears. The system is left for roughly another half a minute to stabilise and heat up further, and the burner is then raised to its final position.

It was found that if the fuel flow rate was lower than the 3.5 g/s or if the burner was immediately raised into position, the flames would quickly extinguish – even though steady-state burning is possible with a lower fuel flow rate. Fuel flow rates much higher than 3.5 g/s were avoided for safety reasons.

When the burner is in its final position, the fuel flow rate can be adjusted to the desired value. If measurements are to be made at a lower fuel flow rate than 3.5 g/s , the rate was not usually reduced for at least half a minute after the burner reached its final position, although extinction rarely occurred once the burner was in position.

2.4.2 Time to Steady State

The flame stabilises and takes on the pattern of behaviour of steady state within about three minutes of the burner being raised into the upper layer. However, this should not be taken to mean that the system has reached steady state.

In the following, the results are shown from a series of measurements performed in the Bertin compartment to see how long it took each measured quantity to reach its steady-state value. Some of the tests were performed for a range of parameter values. Results shown here are for a case where the most substantial changes might be expected: a flame partially covering the interface between the hot and cold layers, of which parts are blue, parts orange and parts amber in colour. The tests were all performed with the burner located at $x = 0.31 \text{ m} = 0.5 L$ and $y = 0.80 \text{ m} = 0.95 H$. The compartment was configured with a full-size vent.

Area Covered by Flame

Fig. 2.15 shows the measurements of the area covered by the internal part of the flame made during a period of 1 h 40 min after ignition. The line burner was used during this series of measurements, with a fuel flow rate of 0.24 g/s , which equates to an energy flow rate of 11 kW.

During the period of observation, there is no significant change in the area covered by the flame.

It can therefore be concluded that the area reaches its steady-state value within the first quarter of an hour after ignition.

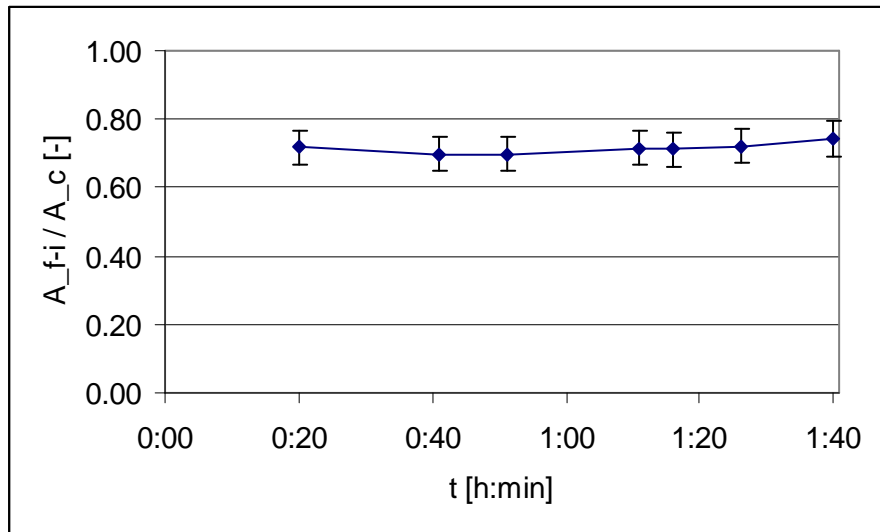


Fig. 2.15: Average area covered by the flame during warmup phase after ignition. Data is from a configuration with the shallow soffit and raised floor; the line burner was used, located at $x = 0.32$ m (0.5 L), $y = 0.80$ m (0.94 H); fuel flow rate 0.24 $\frac{\text{g}}{\text{s}}$ (equating to 11 kW)

Flame Colour

While the measurements show that the area covered by the flame does not alter significantly after about the first quarter of an hour from ignition, the images used to determine the area covered by the flame show that there occurs a change of colour over a much longer timeframe.

Fig. 2.16 shows a representative example of the set of images used to create the value of the first datapoint shown in *Fig. 2.15*, and a representative example of an image from the set used to create the last datapoint.

Initially, a large part of the flame is blue, and those parts which are orange are of relatively low luminosity. Over the period of about an hour from ignition, the flame becomes more yellow and more luminous.

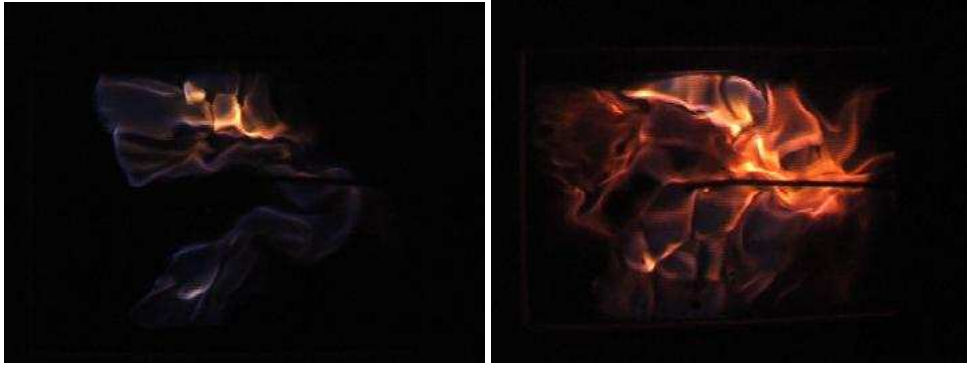


Fig. 2.16: Two still images extracted from the video footage used to calculate the graph depicted above. Left: 20 min after ignition; right: 100 min after ignition

This shows that the system has not reached steady state after twenty minutes. However, the available equipment did not allow a quantitative analysis of the colour and luminosity of the flame, so it is difficult to define an objective criterion as a threshold to steady state.

Temperatures

Several measurements were made of the transient temperatures during heating after ignition of the burner. Only one example is presented here. It involved use of the line burner, and the deeper soffit. The fuel flow rate was 0.30 g/s , which equates to 14 kW .

A thermocouple tree was placed at $x = 0.54 \text{ m} = 0.87 L$, $z = 0.03 \text{ m} = 0.08 W$. Data are shown in *Fig. 2.17* from thermocouples placed 0.12 m , 0.25 m , 0.37 m , 0.42 m , 0.48 m , 0.51 m , 0.56 m , 0.62 m , 0.66 m and 0.77 m above the floor of the compartment; these distances equate to $0.15 H$, $0.30 H$, $0.44 H$, $0.53 H$, $0.57 H$, $0.60 H$, $0.67 H$, $0.74 H$, $0.79 H$ and $0.91 H$. The fluctuations in the temperature values have been smoothed by calculating a running average of the data over two minutes (equating to twelve individual measurements).

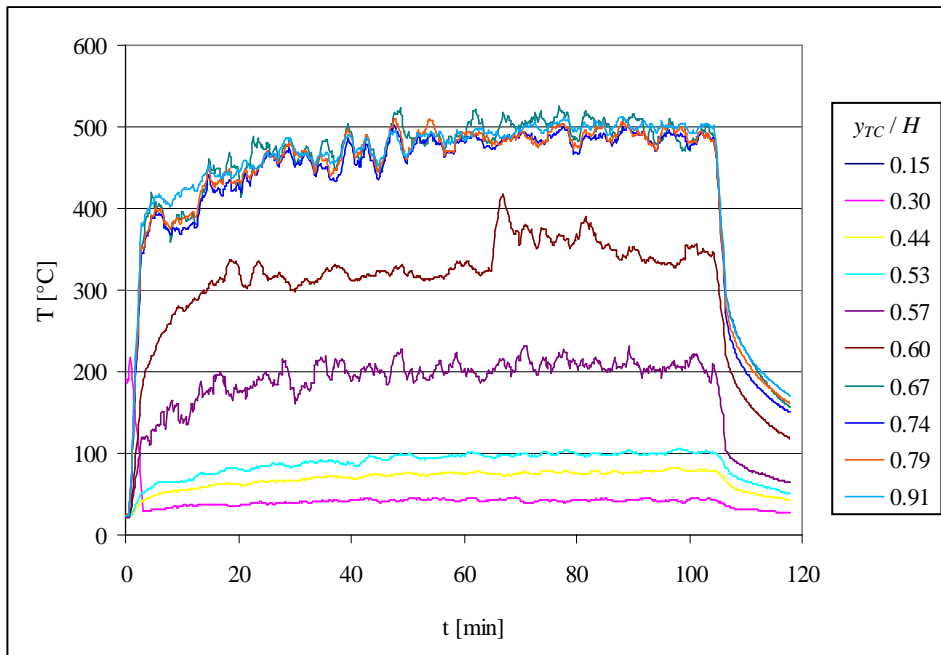


Fig. 2.17: Gas temperatures during a period of 120 minutes after ignition. The fuel supply was cut off after 107 minutes, which caused the drop in temperatures from that point on. The values shown are averages calculated over two minutes to smooth the fluctuations caused by the passing of the flame

The lowest four thermocouples lie in the lower zone. The fifth and sixth thermocouples ($y/H = 0.57$ and 0.60) lie close to the flame. For most of the time, they are below the flame, but occasionally the flame passes over them, so the average temperature they indicate is higher than that of the lower layer. The four thermocouples between $y/H = 0.67$ and the ceiling lie within the upper layer.

During the first five minutes of the test, the thermocouples in the upper zone indicate low temperatures – this is the phase before the flame detaches itself from the burner and stabilises itself along the interface. After this initial phase, the asymptotic rise that one would expect is observed, with the temperatures levelling off after about an hour.

107 minutes after ignition of the flame, the fuel supply was cut, and consequently the flame extinguished and the temperatures started to drop.

The plot suggests that the gas temperatures take about 60 minutes to reach a plateau.

Gas Species

Fig. 2.18 shows the output from the methane and ethylene analysers from gas taken from the upper layer during the first minutes after ignition for a test run with a fuel flow rate of $0.30 \frac{g}{s}$ (14 kW). The samples were taken from the point $x = 0.16 \text{ m}$ (0.25 L), $y = 0.63 \text{ m}$ (0.75 H), $z = 0.0 \text{ m}$ (0.0 W) – i.e. in the central plane, about half way between the layer interface and the ceiling and half way between the rear wall and the burner.

The curves show a time lag of about six minutes from ignition of the burner before apparatus starts to respond. It is a reasonable assumption that there remains a constant response lag throughout the duration of the measurement.

After the analysers start to register a change, the output takes about a quarter of an hour to stabilise.

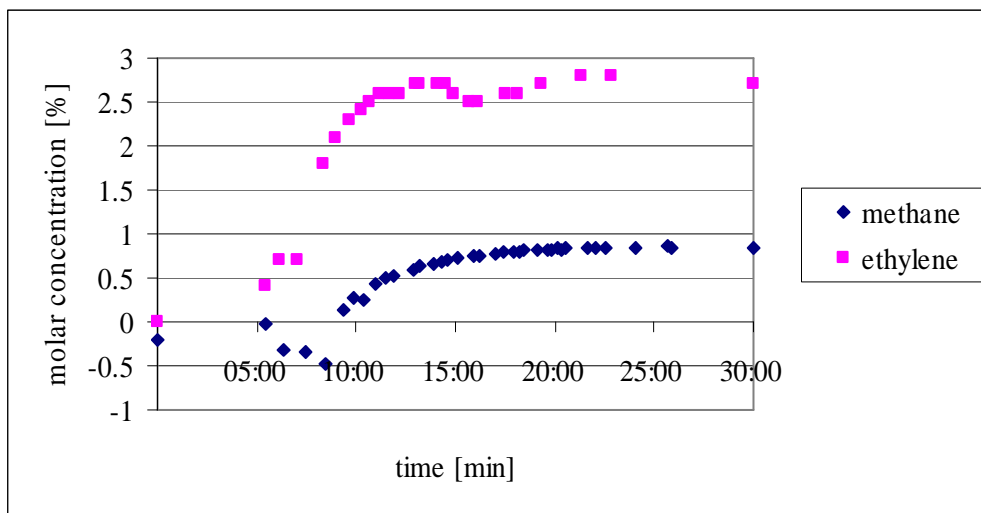


Fig. 2.18: Histories of concentrations of methane and ethylene measured in the upper layer during the first 30 minutes of a test.

Summary and Conclusions for Subsequent Experimental Work

The observed times to steady state are summarised in *Table 2.2*.

quantity	time to stability
behaviour pattern	3 min
area covered by flame	< 15 min
colour of flame	> 30 min; quantitative analysis not possible with available equipment
temperature	60 min
gas concentrations	15 min
edge velocity	60 min

Table 2.2: Summary of the observations described on the previous pages

In light of these results it was decided that the system should be left at least an hour to warm up after ignition before the measurements are made.

3 Results and Discussion

This chapter presents the data collected during the various experiments.

Section 3.1 provides a description of the shape, size, colour and behaviour of the flames for various fuel flow rates.

Section 3.2 presents the results from the tests performed to illuminate the aerodynamic structures and the structure of the flame: PIV, temperature fields and chemical composition of the upper layer. The question of flame stability is also discussed.

In Section 3.3, the data on the surface covered by the flame are presented and the correlation between the area and the heat release rate is discussed.

Section 3.4 explores the influence of the vent on the measured quantities. After a brief qualitative description of the changes in behaviour when the ventilation is reduced, data on the size of the layers, the minimum fuel flow rate needed to sustain combustion, the temperatures and the air flow rate entering in through the vent are presented. The section ends with a discussion of the transition from fuel-control to ventilation-control and of the conditions under which sustained combustion is or is not possible.

3.1 Observation of Shape and Behaviour of the Flame

The first step in the exploration of the phenomena was the description of the range of behaviour patterns which can occur. Direct observation of the shape, colour and behaviour of the flame was used to identify and demarcate the different patterns of behaviour and the ranges of conditions under which they occur.

Following on from this, more detailed observations of the flame provided first indicators to the chemistry of the flames and to the mechanisms involved in their stabilisation. Of particular interest was the behaviour of the flame near extinction, as the observations provided clues to the influence of the parameters which determine under what conditions the flame is sustainable.

3.1.1 Overview

Table 3.1 gives an overview of the types of behaviour encountered during runs in the Bertin compartment when the line burner was used, located at $x = 0.31$ m ($0.5 L$), $y = 0.80$ m ($0.95 H$) and supplied with propane; the deep soffit was in place and the vent was otherwise unrestricted. Most of the measurements described in the following sections were made with this configuration.

Inside the compartment distinct upper and lower layers are visible, whereby the upper layer reaches from the ceiling to just below the level of the soffit. The flame is located at the interface between the two. Depending on the fuel flow rate, it will cover part of the whole of the interface. It extends out through the vent.

3.1.2 Flame Shape and Behaviour

3.1.2.1 Generalities

In the following is a more detailed description of the shape and behaviour of the flame for the two most extreme cases: the yellow/amber flame covering the whole of the interface which occurs at high fuel flow rates and the blue flame covering part of the interface which can be found if the fuel flow rate is close to the minimum necessary to sustain combustion.

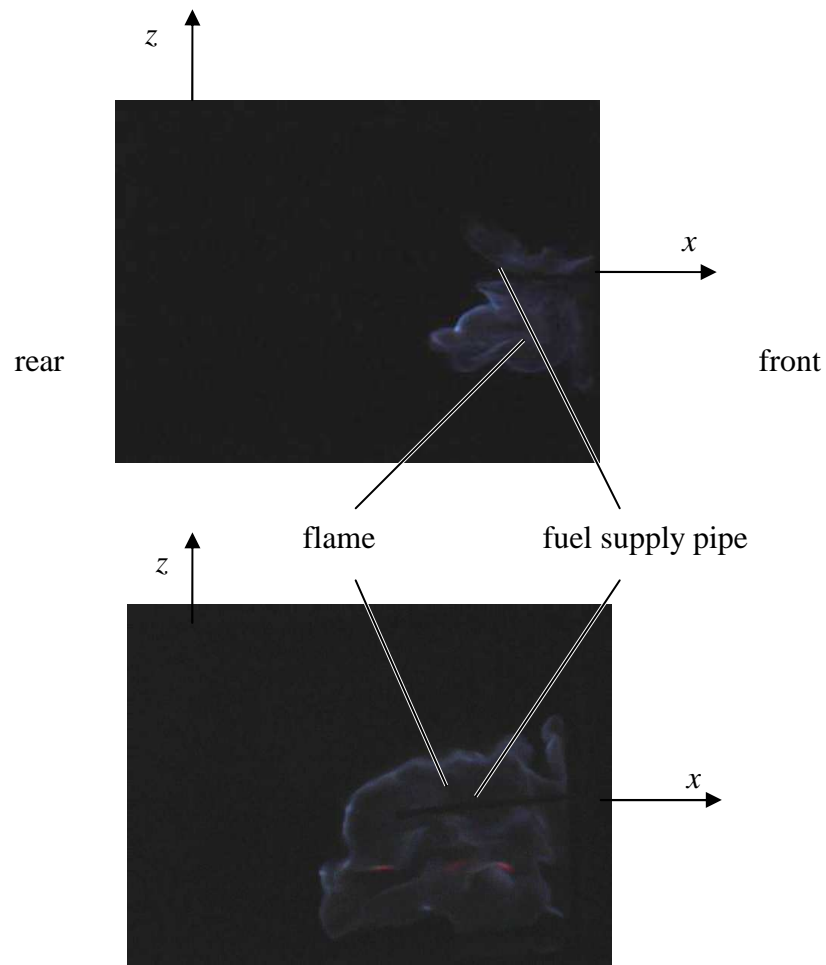
The former case is taken as a baseline for the study of the behaviour as a function of the size of the vent – see Section 3.4. The latter is the regime for which the search for better understanding of the mechanisms was a main focus of the project.

In both cases, two regions can be distinguished inside the compartment: a zone reaching from the floor to just below the level of the soffit which contains air, and above it a zone containing a mixture of smoke and hot gases, including combustion products, fuel and nitrogen.

The flame is located at the interface where these two zones meet.

Fuel flow rate	Energy flow rate	Flame size	Flame shape	Flame colour
$< 0.21 \frac{\text{g}}{\text{s}}$	$< 9.8 \text{ kW}$	no flame		
$0.21 \frac{\text{g}}{\text{s}}$ to $0.27 \frac{\text{g}}{\text{s}}$	9.8 kW to 13 kW	size fluctuates greatly; sometimes grows to attach itself to part of the length of the side walls, occasionally reaches back to the rear wall	"ridge"	blue
$0.27 \frac{\text{g}}{\text{s}}$ to $0.33 \frac{\text{g}}{\text{s}}$	13 kW to 15 kW	size fluctuates greatly; flame usually reaches to the rear half of the compartment, sometimes reaching to the rear wall	cellular	blue with occasional localised flashes of orange
$0.33 \frac{\text{g}}{\text{s}}$ to $0.38 \frac{\text{g}}{\text{s}}$	15 kW to 18 kW	flame spends a lot of the time reaching to the rear wall, but is rarely attached to this wall across the whole of its width	cellular	blue with occasional localised flashes of orange
$0.38 \frac{\text{g}}{\text{s}}$ to $0.43 \frac{\text{g}}{\text{s}}$	18 kW to 20 kW	flame sometimes covers the whole of the interface; it usually reaches to the rear of the compartment and is usually attached to at least part of the rear wall	cellular	“valleys” are blue; with increasing fuel flow rate, the peaks pass from blue to purple and then orange; frequent flashes of orange and amber
$0.43 \frac{\text{g}}{\text{s}}$ to $0.60 \frac{\text{g}}{\text{s}}$	20 kW to 28 kW	flame sometimes covers the whole of the interface; it usually reaches to the rear of the compartment and is usually attached to at least part of the rear wall	cellular	“valleys” are blue, peaks orange
$0.60 \frac{\text{g}}{\text{s}}$ to $0.65 \frac{\text{g}}{\text{s}}$	28 kW to 30 kW	covers the whole of the interface for most of the time	cellular	“valleys” are blue, peaks amber
$0.65 \frac{\text{g}}{\text{s}}$ to $0.71 \frac{\text{g}}{\text{s}}$	30 kW to 33 kW	almost constantly covers the whole of the interface	cellular	amber

Table 3.1: Overview of the various regimes encountered in the Bertin compartment when the fuel source is located immediately below the ceiling, the deep soffit is in place and the vent is otherwise unrestricted. The fuel flow rates indicated are from tests where the line burner was used, located at $x = 0.31 \text{ m} = 0.5 L$, $y = 0.80 \text{ m} = 0.95 H$; propane was used as a fuel.



Above: Fig. 3.1: View from underneath of the flame: line burner, large soffit, 0.24 s/s fuel flow rate ($\dot{H} = 11 \text{ kW}$), unrestricted vent

Below: Fig. 3.2: View from underneath of the flame: line burner, large soffit, 0.30 s/s fuel flow rate ($\dot{H} = 14 \text{ kW}$), unrestricted vent



Fig. 3.3: View of the flame from underneath taken through the window in the floor of the compartment: line burner, large soffit, 0.36 s/s fuel flow rate ($\dot{H} = 17 \text{ kW}$), unrestricted vent

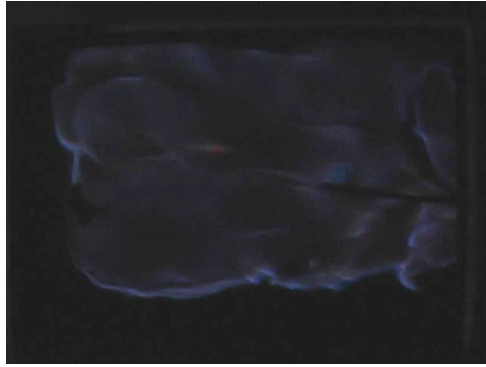


Fig. 3.4: View of the flame from underneath taken through the window in the floor of the compartment: line burner, large soffit, 0.40 $\frac{s}{s}$ fuel flow rate ($\dot{H} = 19$ kW), unrestricted vent

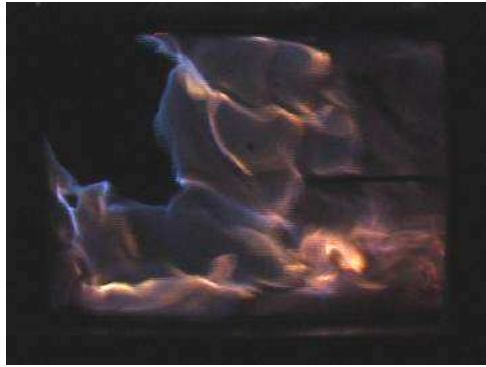


Fig. 3.5: View of the flame from underneath taken through the window in the floor of the compartment: line burner, large soffit, 0.52 $\frac{s}{s}$ fuel flow rate ($\dot{H} = 24$ kW), unrestricted vent



Fig. 3.6: View of the flame from underneath taken through the window in the floor of the compartment: line burner, large soffit, 0.63 $\frac{s}{s}$ fuel flow rate ($\dot{H} = 29$ kW), unrestricted vent



Fig. 3.7: View of the flame from underneath taken through the window in the floor of the compartment: line burner, large soffit, 0.71 $\frac{\text{g}}{\text{s}}$ fuel flow rate ($\dot{H} = 33 \text{ kW}$), unrestricted vent

3.1.2.2 Blue Partial Interface Flames

When the fuel flow rate is between 0.21 $\frac{\text{g}}{\text{s}}$ and 0.27 $\frac{\text{g}}{\text{s}}$, a flame can be observed which comprises a bright blue edge and a blue sheet which is much less bright and is inclined upwards at an angle of between 15 and 20° covering the whole region between the edge and the vent. There is a flame tip reaching well into the upper layer and often impinging on the ceiling.

The size of the flame fluctuates greatly in size, whereby the fluctuations are aperiodic: the flame edge sometimes remains almost steady for several seconds, sometimes advances towards the rear of the compartment or recedes towards the vent with a velocity high enough for it to be difficult to follow with the naked eye.

Within the range of fuel flow rates where this flame type prevails, the inclination of the flames decreases if the fuel flow rate is increased.

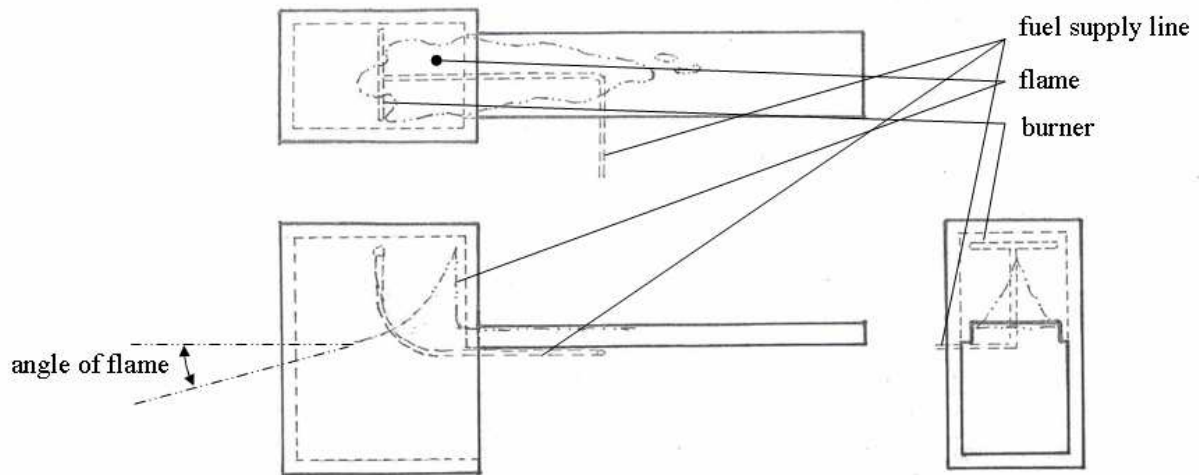


Fig. 3.8: Illustration of the typical shape of the flame as seen from above, the side and the front

3.1.2.3 Yellow Full Interface Flames

At a fuel flow rate of 0.71 g/s , the flame is a highly luminous amber colour (see *Fig. 3.7*). For most of the time it extends across the whole width and length of the compartment. For brief periods it detaches from the wall at two corners in the rear of the compartment. The flame extends beyond the soffit and flows upwards parallel to the outside surface of the soffit. The external part of the flame reaches roughly 0.65 m up from the level of the soffit.

There is no discernable smoke given off by the fire.

The flame is of cellular nature: on average about twelve peaks reach into the upper section of the compartment, with troughs between each. The size and shape of the peaks and troughs constantly change. Several of them, particularly towards the front and around the edges of the compartment, reach up to the ceiling

The glass of the windows above the level of the flame sheet quickly becomes covered in soot. This shows that soot is produced inside the compartment. It is probably stems from quenched tips of the peaks of that part of the flame which is inside the compartment.

3.1.3 Extinction

One of the key questions which are relevant for engineers is the determination of the conditions under which the flame can and cannot be sustained. An exploration of the range of parameter values at which sustained combustion is not possible is presented later in this chapter, in Section 3.4.3. However, observation of the behaviour of the flame close to and at extinction also contributed to the discussion of the controlling parameters.

As just mentioned in the description of the blue flames, when the fuel flow rate is close to the critical value, the area of the flame fluctuates greatly. If the fuel flow rate is reduced to below 0.21 $\frac{\text{g}}{\text{s}}$, the flame will continue to burn for a while – possibly several minutes – but then at some point a waning phase of the fluctuation of the flame is not followed by a waxing phase, but instead the flame reduces its size to zero and extinguishes.

3.2 Aerodynamics, Flame Structure and Stability

This section presents the data from measurements performed as part of the effort to better understand the behaviour and structure of the blue flames partially covering the interface between the upper and lower layers. PIV measurements of the velocity field around the burner provided insight into flow pattern inside the compartment and in particular helped to answer the question as to whether there exists a recirculatory motion inside the upper layer. PIV measurements were also performed around the edge of the flame to provide further information on the flow patterns and to help test the hypothesis that the flame is of a triple-flame structure (see Section 1.2.4 and [Coutin 2000]). Temperature measurements and an analysis of the chemical composition of the upper layer provided further information on the conditions inside the compartment.

3.2.1 Velocity Field at the Exit of the Burner

As part of the efforts to explore the path taken by the fuel between the exit of the burner and the reaction zone, PIV measurements were made immediately underneath the ceiling around the burner.

These measurements were only made for cases in which the original burner was used. As already described in Section 2.3.2.2, seeding was provided in the form of zirconium oxide particles, injected into the upper layer in an upwards direction parallel to the burner.

As only qualitative information was extracted from these measurements, only one representative example is shown here. *Fig. 3.9* shows the average flow field from 50 measurements taken from a run with the porous burner installed at $x = 0.31 \text{ m} = 0.5 L$, $y = 0.80 \text{ m} = 0.95 H$, $z = 0.0 \text{ m} = 0 W$, with a fuel flow rate $\dot{m}_F = 0.24 \text{ g/s}$ ($\dot{H} = 11 \text{ kW}$). The time delay between the two images of this series was set at a value to well resolve the relatively low velocity of the gases in the upper layer, rather than the faster velocity of the fuel immediately having exited the burner. The blank zone to the right of the vector field is the burner.

The fuel exits the burner near the top right hand corner of the image with an initial velocity that is vertical. The image shows that fuel travels along the ceiling towards the back wall, while smoke and combustion products are drawn upwards parallel to the burner, and then flow towards the rear of the compartment underneath the layer of fuel. It can be assumed that at the interface between the fresh fuel and the upper layer gases, mixing between the two streams occurs, thereby diluting the fuel in combustion products.

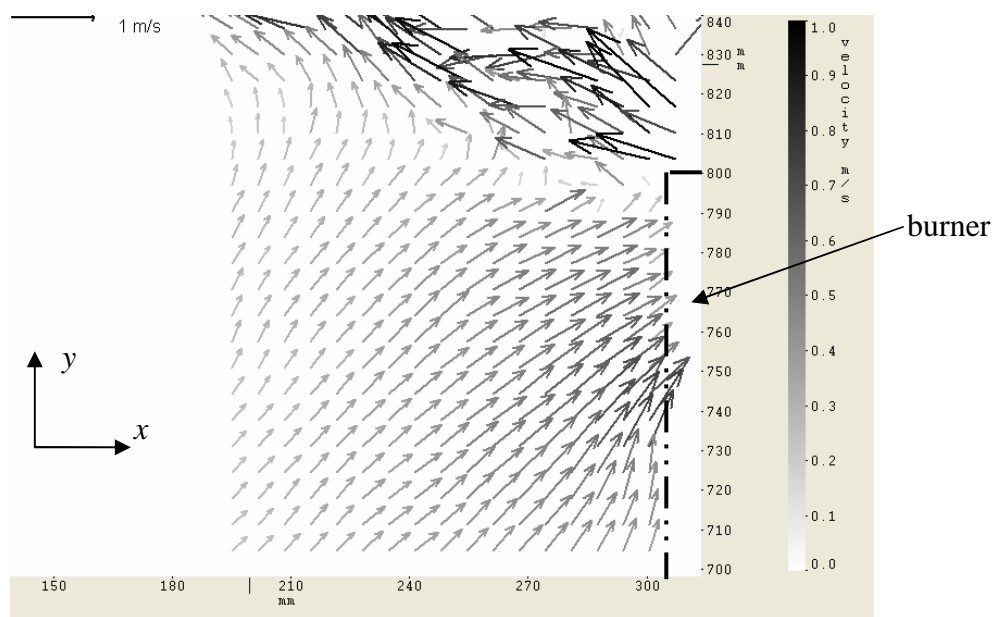


Fig. 3.9: Average velocity field at the exit of the burner. The values are taken from a configuration with the large soffit installed and an otherwise unrestricted vent; the porous burner was used, positioned at $x = 0.32 \text{ m} = 0.5 L$, $y = 0.80 \text{ m} = 0.95 H$; fuel flow rate 0.24 g/s (equating to 11 kW)

3.2.2 Velocity Field around the Edge of the Flame

Measurements of the velocity field around the edge of the flame were performed to assist in identifying the structure of the flame in those cases where the flame does not cover the whole of the interface.

Fig. 3.10 shows an instantaneous velocity field determined from a pair of PIV images overlaid onto the 2nd image of the pair to illustrate the location of the flame. The image is from a case where the line burner was used, with a fuel flow rate of 0.30 g/s , which equates to an energy flow rate of 14 kW. The zirconium oxide seeding particles were introduced through the set of horizontal jets just below the ceiling.

Only seeding particles which are in the plane of the laser sheet are visible. However, the light from the flame which reaches the camera is from the whole width of focal depth of the camera, a distance of several millimetres. Because of this, the sheet of the flame covers an area in the picture, rather than appearing as a line.

Despite the fact that seeding is only introduced into the upper layer, there is a good density of seeding throughout the field of view.

The flow approaches the flame edge in a roughly horizontal trajectory. When reaching the level of the flame edge, the gases are accelerated upwards, so both the velocity and the inclination of the trajectory are increased.

Gas velocities within the field of view were found to range between about 0.1 and 1.1 m/s. The average Reynolds number is in the order of 10^5 . This fact, plus the wavy shape of the flame, show that the flame is in the transition between laminar and turbulent.

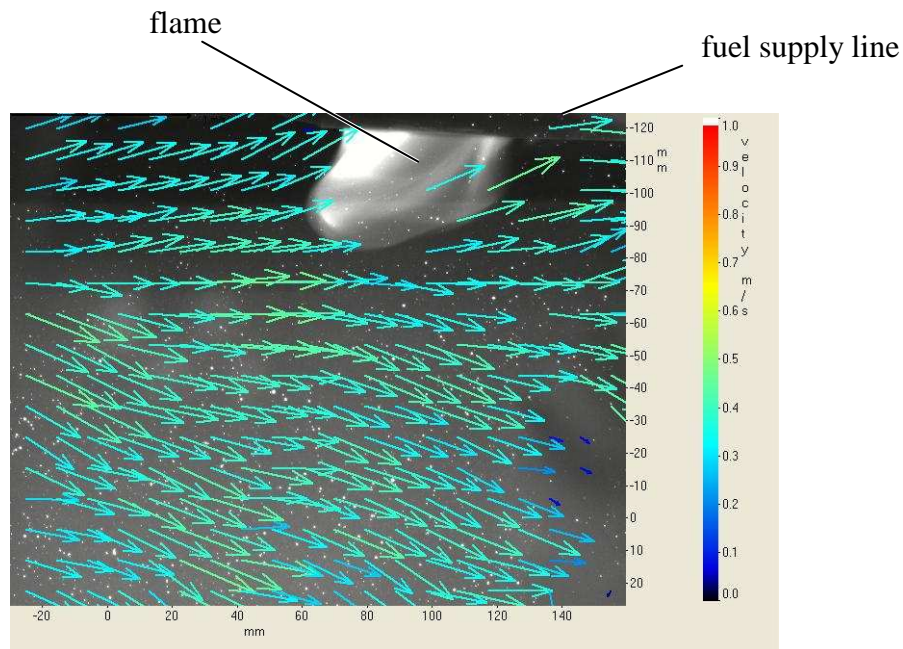


Fig. 3.10: Example of a velocity field calculated from a pair of PIV images overlaid onto the 2nd image of the pair showing the location of the flame.

Configuration: large soffit, fuel flow rate 0.30 g/s (equating to 14 kW)

Motion of the Flame Edge

As mentioned above in Section 3.1.2.2, the edge of the flame moves back and forth within the compartment. However, as there is not steady displacement in one direction or another, the movement of the edge can be considered as an oscillation around an average location – albeit that the average location is a function of the fuel flow rate, geometry and other parameters. This concept is important for the determination of the average velocity of the gas relative to the edge of the flame (see immediately below).

Because of the relatively long time delay of 0.5 seconds between the recording of each pair of images, the PIV only allowed an estimate rather than a measurement of the velocity of the displacement of the flame edge. Observation of video recordings were also used to estimate the velocity of the edge. Both methods provide an estimate that the velocity of the edge relative to the compartment ranges from 0 to 0.5 m/s.

The fluctuations in the velocity of the edge are due to local fluctuations in the gas velocity and to inhomogeneities in the temperature and composition of the gas ahead of the flame.

3.2.2.1 Velocity Field relative to the Flame

The velocity of the flame edge relative to the gas in which it is located (v_{edge}) is equal to the velocity of the flame edge relative to the compartment (v_{flame}) minus the velocity of the gas relative to the compartment (v_{gas}).

$$v_{edge} = v_{flame} - v_{gas} \quad (3.1)$$

If the position of the edge of the flame fluctuates around an average location, then this means that the average velocity of the flame relative to the compartment $\overline{v_{flame}}$ is zero. Therefore, the average velocity of the gas at the flame edge relative to the compartment $\overline{v_{gas}}$ is equal to the negative of the average velocity of the gas at the flame edge relative to the flame $\overline{v_{edge}}$.

$$\overline{v_{edge}} = \overline{(v_{flame} - v_{gas})} = -\overline{v_{gas}} \quad (3.2)$$

A measurement of the time average of the velocity of the gas relative to the flame edge can be obtained by averaging the PIV data in a coordinate system fixed to the flame.

$$\hat{x} = x - x_{flame}; \hat{y} = y - y_{flame} \quad (3.3)$$

Fig. 3.11 shows an average flow field calculated from 50 individual PIV vector fields which have been submitted to the coordinate transfer defined in equation (3.3). The location of the flame is indicated on the image. The vector fields stem from a case where the deep soffit was installed and the line burner was used, located at $x = 0.31 \text{ m}$ ($0.5 L$), $y = 0.80 \text{ m}$ ($0.95 H$), with a fuel flow rate of 0.30 g/s ($\dot{H}=14 \text{ kW}$)

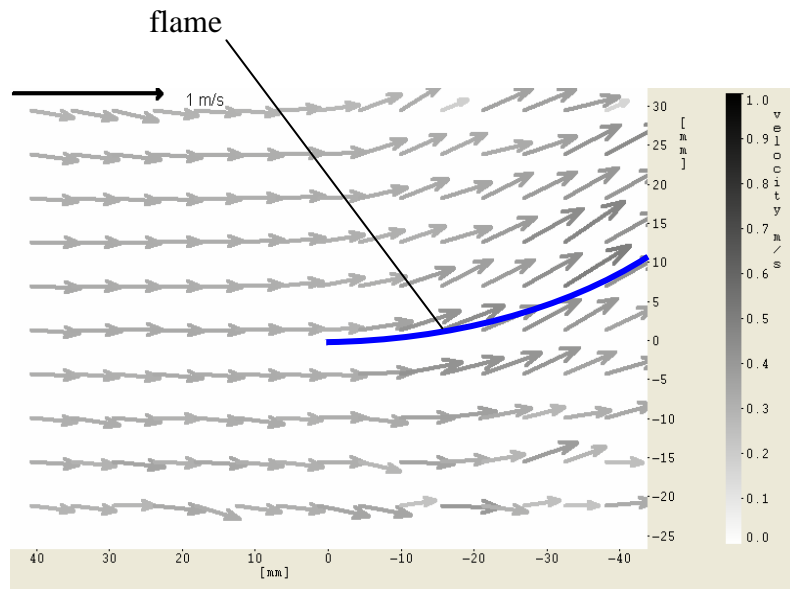


Fig. 3.11: Average vector field calculated after coordination shift of 21 PIV measurements to bring the flame edge into the origin of the coordinate system.

As can be seen, the gas enters the flame edge in a nearly horizontal trajectory from the rear of the compartment.

The average value of the velocity is $0.31 \text{ m/s} \pm 0.05 \text{ m/s}$. The velocity shows a slight tendency to increase if the fuel flow rate is increased, as is shown in Fig. 3.12 in which a plot of the measured values of the edge velocity against the energy flow rate $\dot{H} = \dot{m}_F \Delta h_c$ is shown. The increase in gas velocity with the fuel flow rate can be attributed to the increased heat release driving the natural convection of air into the compartment and hot gases out.

Behind the edge the flow remains parallel to the sheet of flame. It is accelerated and deflected upwards, reaching a velocity of 0.6 m/s . This acceleration can be attributed to thermal expansion of the gas due to the heat released in the flame.

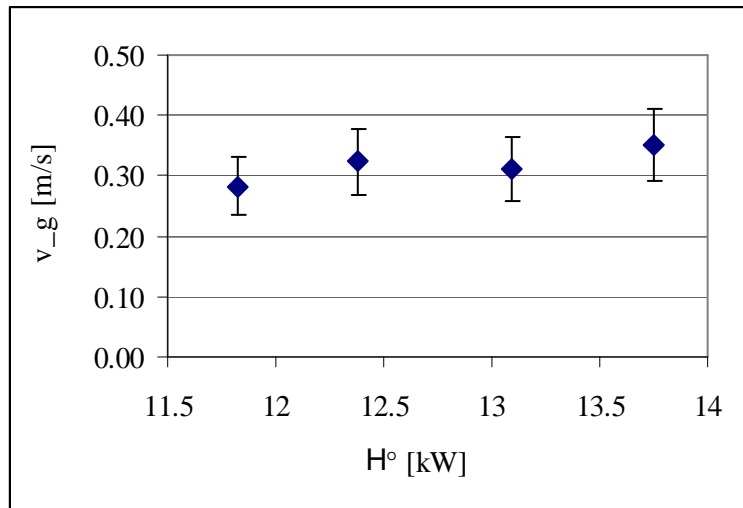


Fig. 3.12: Plot of the measured average edge velocity as a function of the fuel flow rate.

3.2.3 Temperature Field

Temperature measurements were made for several configurations and at several locations. The results contributed to the discussion of the flame stability and the energy balance.

3.2.3.1 Temperature Histories

A typical history is shown in Fig. 3.14 from twelve thermocouples on a tree located at $x = 0.39$ m (0.63 L), $z = -0.04$ m (-0.1 W) (see Fig. 3.13). It is from a test with a fuel flow rate of 0.30 $\frac{g}{s}$ – equating to $\dot{H} = 14$ kW – when the deep soffit was in place, and the line burner used, located at $x = 0.32$ m (0.5 L), $y = 0.80$ m (0.95 H). The thermocouple tree was located at $x = 0.39$ m (0.63 L), $z = -0.04$ m (-0.1 W).

The acquisition frequency of the datalogger of 1 Hz was too low to follow the rise and fall of the temperature of each thermocouple as the flame passed over it, and so the plot can only show the range of temperatures produced.

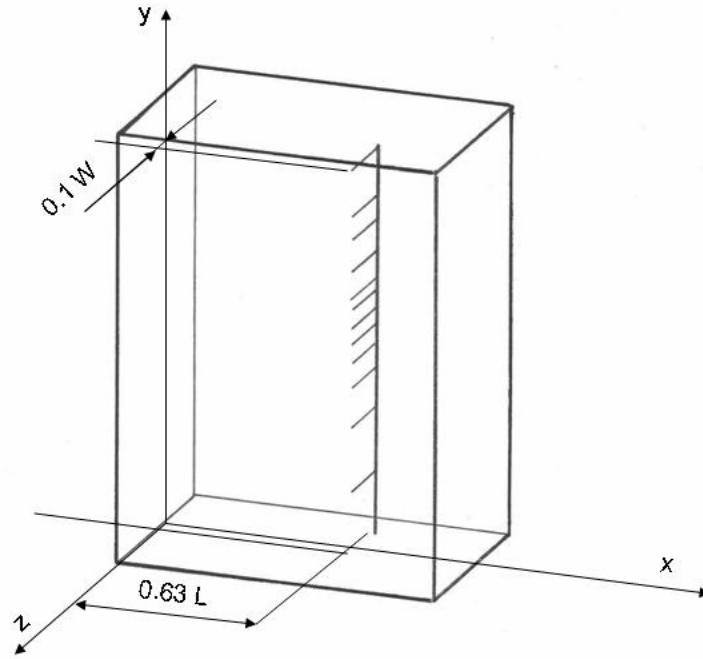


Fig. 3.13: Location of the thermocouples from which the plot in Fig. 3.14 was produced.

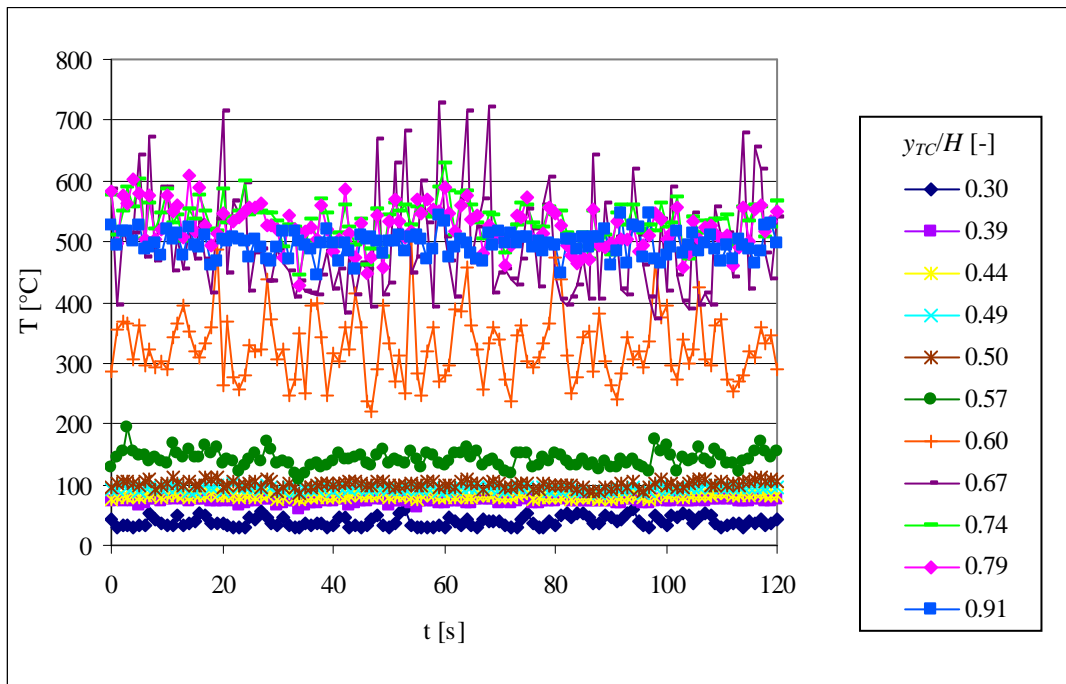


Fig. 3.14: Temperature history for a run with the large soffit and unrestricted vent, 14 kW energy flow rate, line burner; location of the tree: $x = 0.39$ m, $z = -0.35$ m.

The lowest thermocouples – those located between $y/H = 0.30$ and $y/H = 0.50$ – were in the lower layer. They show fairly stable values in the region of 30°C to 100°C. The next thermocouple ($y/H = 0.57$) was close to the flame and registered a higher temperature of around 140°C. The thermocouple at $y/H = 0.60$ lies just below the flames for most of the time, registering temperatures in the region of 300°C; the peaks indicate occasional exposure to the flame, but because of the low acquisition frequency the temperature recorded is not the flame temperature. The thermocouple at $y/H = 0.67$ is above the flame for most of the time, and so delivers a value for the temperature of that layer, in the region of 500°C; occasional peaks of up to 730°C indicate the passage of the flame past this thermocouple. The top three thermocouples (y/H between 0.74 and 0.91) lie in the upper layer. Their temperature fluctuates slightly, but remains in the region of 500°C.

The acquisition frequency of 1 Hz, limited by the datalogger, did not allow the temperature rise to be followed as the flame passed over the thermocouple. The temperature range of 700°C to 730°C is therefore probably below the temperature of the flame. In some cases temperatures of up to 1000°C were measured, which is probably nearer the temperature of the flame.

3.2.3.2 Maps of Average Temperatures

Fig. 3.15 and *Fig. 3.16* show maps of the time averaged temperatures in a vertical plane parallel to the side walls at $z = 0.04$ m (0.1 W); in the former case, the fuel flow rate was 0.30 g/s ($\dot{H} = 14$ kW), producing a flame which partially covers the interface between the upper and lower zones. In the latter case, the flow rate was 0.71 g/s (33 kW), giving a flame which covers the whole of the interface. In both cases the deep soffit was installed; the line burner was used, located at $x = 0.31$ m (0.5 W), $y = 0.80$ m (0.95 H). The external channel was not installed

Both temperature maps clearly show the presence of a cold zone in the lower part of the compartment and a hot zone in the upper part.

Because the external channel was absent, the hot gases which leave the compartment flow upwards parallel to the external surface of the soffit. The influence of the upwards acceleration is visible in the plot for the 33 kW case (*Fig. 3.16*): the temperature interface

between the two layers turns upwards towards the front of the compartment, as the acceleration upwards of the gases starts before they leave the compartment. The effect is obviously less strong in the 14 kW case.

In the 33 kW case, a region of high temperature can be seen at the interface between the two layers. This is consistent with the presence of the flame. Within each layer there is practically no temperature gradient in horizontal direction.

A slightly different picture is produced for the lower fuel flow rate (*Fig. 3.15*). There is no band of high temperature visible at the interface. This is probably partly due to the fact that the flame radiates less heat and partly to the movement of the location of the flame: the flame is sometimes above, sometimes below each thermocouple in this region, spending only very short periods of time touching each; the averaging process delivers values of well below that of the hot gas for locations towards the bottom of the upper layer, and values much closer to that of the upper layer gases higher up. The fact that the flame does not cover the whole of the interface all of the time influences the temperature in the upper zone: towards the front of the compartment, where the flame is constantly present, the temperature is the same as in the 33 kW case; towards the rear of the compartment, it is lower. The temperatures in the lower layer are slightly less than those in the 33 kW case.

The temperature maps indicate that the temperature in the upper layer is only weakly dependent on the fuel flow rate. This is more clearly illustrated if the temperature of the layer is plotted as a function of the fuel flow rate, as is provided in *Fig. 3.17* for cases with the deep soffit. At fuel flow rates above about $0.45 \frac{\text{g}}{\text{s}}$ ($\dot{H} = 21 \text{ kW}$), when the flame covers the whole of the interface most of the time, there is little difference between the temperature in the front half of the compartment and that in the rear, and no discernible increase in temperature if the fuel flow rate is increased. At lower fuel flow rates, the temperature increases with increasing fuel flow rate and the front part of the upper layer is 30 or 35°C warmer than the rear. The latter observation is probably due to the fact that the flame is not always present in the rear part of the compartment.

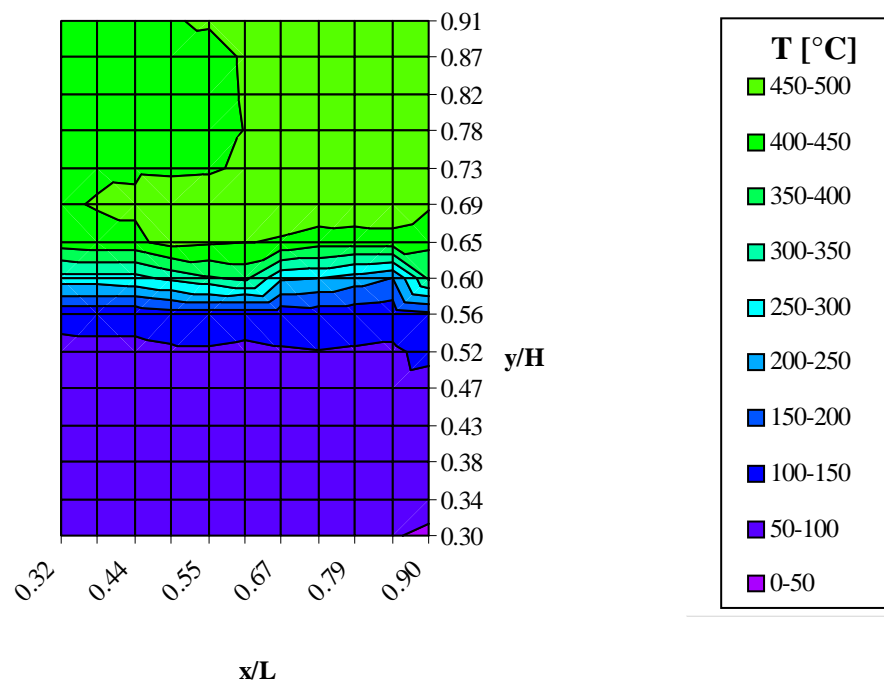


Fig. 3.15: Map of temperatures in the plane $z = 0.04 \text{ m} = 0.1 \text{ W}$. Large soffit and otherwise unrestricted vent; burner located at $x = 0.31 \text{ m} = 0.5 \text{ L}$, $y = 0.8 \text{ m} = 0.95 \text{ H}$, fuel flow rate $0.30 \text{ }^{\circ}/_s$ (equating to 14 kW).

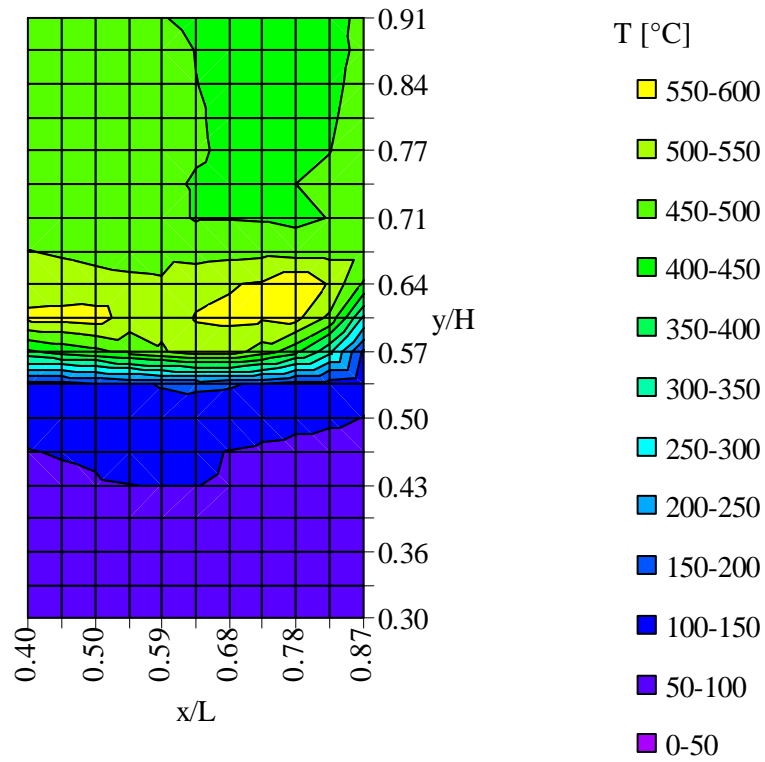


Fig. 3.16: Map of temperatures in the plane $z = 0.04 \text{ m} = 0.1 W$. Large soffit and otherwise unrestricted vent; burner located at $x = 0.31 \text{ m} (0.5 L)$, $y = 0.8 \text{ m} (0.95 H)$, fuel flow rate $0.71 \text{ }^8/s$ (equating to 33 kW).

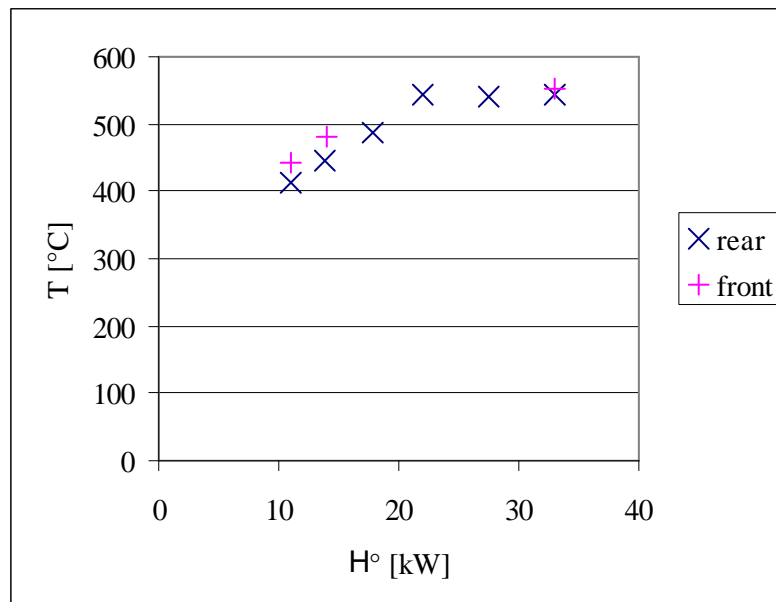


Fig. 3.17: Temperature in the front and rear of the upper layer plotted against the fuel flow rate

3.2.4 Chemical Makeup of the Upper Layer

Knowledge of the chemical species present in the compartment and their concentrations can be linked with several other aspects of the fire:

- The chemistry determines the combustion regime and flame behaviour
- The chemical makeup of the gas is one of the factors which determines the size of the flames and whether sustainable combustion is possible.
- The composition of the gases in upper and lower layers is needed to calculate the thermal capacities of the atmosphere and thus the heat stored within each layer.

Table 3.2 shows average values determined by gas chromatography of samples taken from several locations in the upper layer during test runs with the deep soffit installed and the porous burner located at $x = 0.31$ m ($0.5 L$), $y = 0.80$ m ($0.95 H$), $z = 0.0$ m ($0.0 W$), and a fuel flow rate of $\dot{m}_F = 0.30$ g/s ($\dot{H} = 14$ kW).

The concentration of H_2O was calculated from a carbon balance, as water vapour has to be removed from the sample prior to analysis to prevent corrosion of the apparatus and the solution of any of the species in water.

6.4 % by volume of the upper layer gases are combustible species, diluted with combustion products (CO_2 8.9 %, H_2O 14 %) and nitrogen (68 %). Some residual oxygen – 2.4 % – was also detected.

Because of the low oxygen concentration, this mixture is above the upper flammability limit, which is why combustion is only possible at the interface with the lower layer. However, the oxygen concentration is higher than that typically found in the exiting gas flow from a ventilation-controlled fire, when values of less than one percent are often encountered [Drysdale 1998].

species	molar concentration [-]	
O ₂		0.023 ± 0.011
Ar	0.008 ± 0.0001	
N ₂	0.678 ± 0.006	
inert gases from air		0.686 ± 0.006
H ₂ O	0.137 ± 0.013	
CO ₂	0.089 ± 0.006	
total combustion products		0.226 ± 0.015
CO	0.015 ± 0.002	
H ₂	0.003 ± 0.004	
CH ₄	0.006 ± 0.001	
C ₂ H ₆	0.001 ± 0.0003	
C ₂ H ₄	0.007 ± 0.001	
C ₃ H ₈	0.025 ± 0.008	
C ₃ H ₆	0.003 ± 0.001	
i-C ₄ H ₁₀	0.001 ± 0.001	
n-C ₄ H ₁₀	0.000 ± 0.0002	
C ₂ H ₂	0.002 ± 0.0004	
C ₄ H ₈	0.000 ± 0.0001	
total combustible		0.064 ± 0.008

Table 3.2: Average values provided by the gas chromatograph for locations inside the upper layer.

3.2.5 Tests with Methane as Fuel

All the tests described so far involved propane, which is heavier than air. Tests using methane instead of propane were carried out to see if the partial interface flames could be produced with a lighter-than-air fuel. These tests were performed with the original burner located at $x = 0.32$ m (0.5 L), $y = 0.8$ m (0.95 H) and $z = 0.0$ m (0 W). The large soffit was installed.

These experiments resulted in the same qualitative behaviour as those using propane.

No quantitative exploration was performed of the effect of the change in fuel on the minimum fuel flow rate to sustain combustion, the range of fuel flow rates which produce purely blue flames or of the flow rate above which the flame covers the whole of the interface.

3.2.6 Discussion

3.2.6.1 Flow Pattern

The flame is hotter than the layer of smoke and gases above it, and thus, as Coutin observed [Coutin 2000], a thermally unstable stratification exists. This instability creates a convective movement in the upper layer, which in turn promotes the mixing of fuel with combustion products from the upper layer.

The PIV data from just under the ceiling suggest that the gas in the upper layer undergoes a recirculatory motion. This is supported by two other observations.

Firstly the inclination of the flame sheet, coupled with the fact that the gas flow is parallel to the sheet, suggests that some gas from the combustion zone is drawn upwards close to the burner by natural convection induced by the buoyant flow.

Secondly the gas concentrations at the layer interface stabilise before the concentrations in the heart of the upper layer, as can be seen from the difference between the time it takes from ignition to stabilise the behaviour of the flames on the one hand, and the gas concentrations half way between the ceiling and the flame on the other (see Section 2.4.2).

These three points suggest that the gas flows follow the pattern schematised in *Fig. 3.18*. Fuel from the burner does not flow or diffuse downwards across the whole length and breadth

of the upper layer, but travels along the ceiling, then downwards close to the walls and finally turns to move towards the vent.

Along this path it mixes with gas from the upper layer, and thus the fuel is diluted in combustion products.

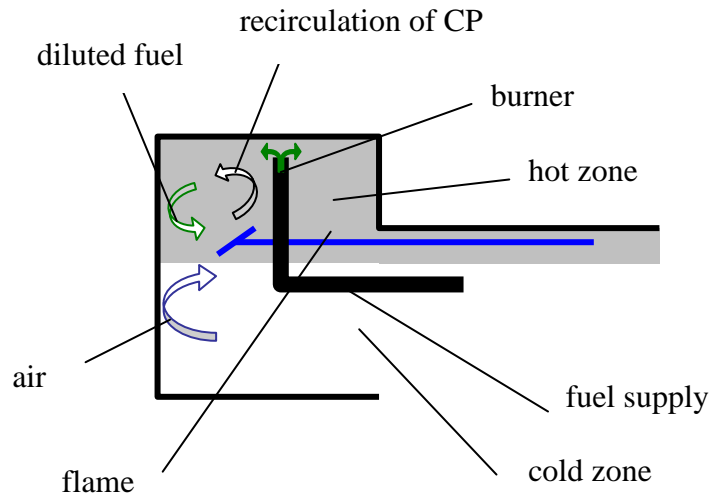


Fig. 3.18. The proposed aerodynamic system

In the combustion zone, some of the gas is drawn upwards into the upper layer due to buoyancy induced by thermal expansion. Some oxygen may enter the upper layer via this path from quenched flame tips.

The air supply to the flame is drawn in through the vent by natural convection induced by the heat released from the flame.

The observations during the warmup (Section 2.4.2) provide clues as to which parameters control each aspect of the behaviour of the flame.

Combustion products are produced at a rate sufficient to fill the upper zone within a few seconds. The time it takes to fill this zone is therefore not a determining factor.

The area covered by the flame reaches its steady state value in the same timeframe as the chemical composition of the upper layer, rather than the much longer timeframe it takes the temperature to reach its steady-state value. This seems to suggest that the area covered by the flame is determined primarily by the chemistry, not the temperature.

In contrast to this, the observed change in colour of the flame indicates an increasing production of soot, which must be linked to the gradually increasing temperature.

The observed fluctuations in the size of the flame and the gas velocity stem from the fact that each mechanism depends on the others, but there are time lapses between causes and effects: the flow is driven by the instantaneous temperature field, but the air, fuel and combustion products take time to pass along their respective circuits; the temperature field is driven by the instantaneous heat production and is therefore a function of the instantaneous flame size, but follows the heat release with a time lag; the flame size is a function of the instantaneous flow velocities and species concentrations.

3.2.6.2 Flame Structure

The observations support Coutin's hypothesis [Coutin 2000], [Coutin *et al* 2002] that the flame edge is a triple-flame structure [Phillips 1965]: As the gas mixture from the upper layer (fuel and inert gases) travels at the interface horizontally towards the vent, there is some mixing with air from below the interface, producing a stratified premixture. The mixture of fuel and combustion products and the air enter the edge of the flame with an almost horizontal trajectory. This edge is made up of two premixed wings – a fuel-rich upper one and a fuel-lean/oxygen-rich lower one. These two wings leave behind them not only combustion products, but also unreacted gas – the excess fuel on the rich side and the excess oxygen on the lean side. Between these two flows of combustion products and leftover reactants, a diffusion flame is established see *Fig. 3.19*.

This hypothesis is supported both by the fact that the relative velocity of the gas to the flame edge $\bar{v}_e = 0.31 \text{ m/s}$ is – within the accuracy of the measurements – equal to the laminar premixed burning velocity S_L of propane: For propane at stoichiometry under standard conditions S_L is 0.4 m/s ; as the temperature, dilution and equivalence ratio in the present case are not sufficiently well known, the relevant value of S_L cannot be determined.

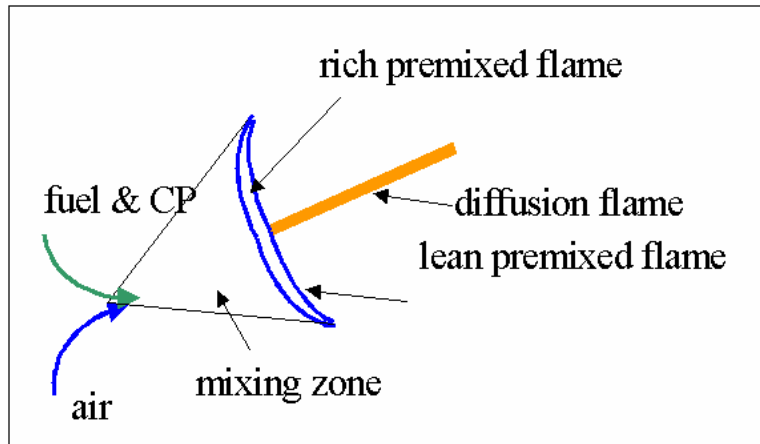


Fig. 3.19. Illustration of the triple flame structure

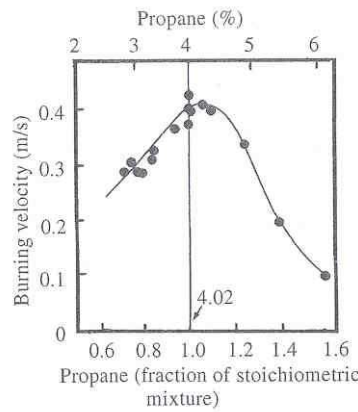


Fig. 3.20: Burning velocity of premixed propane and air as a function of the equivalence ratio

Source: [Drysdale 1998]

3.2.6.3 Flame Stability

The experiments show that when the flame covers part of the interface, its size and location are not steady – the flame is unstable. In contrast, when the flame covers the whole of the interface, it is stable.

Three cases can therefore be distinguished, according to the surface covered by the internal part of the flame A_{fl-in} :

- stable flames: $\frac{A_{fl-in}}{A_c} = 1$
- unstable flames: $0 < \frac{A_{fl-in}}{A_c} < 1$
- extinction: $\frac{A_{fl-in}}{A_c} = 0$

where A_c is the floor area of the compartment.

In Section 3.2.2, the edge velocity of the triple flame is compared with the flow velocity of the gas ahead of the flame. If the fuel flow rate is increased, both the laminar burning velocity – and with it the edge velocity – and the flow velocity will increase. However, these two increases are due to different mechanisms, and therefore do not occur at the same rate.

The gas flow velocity is linked to the vent flow rate. This is driven by the temperature difference between the atmosphere inside and the atmosphere outside the compartment. The temperature is determined by the reaction rate within the compartment $\dot{H}_{react-in} = \dot{Q}_{prod-in}$. The relationship is not linear, as the heat losses do not increase linearly with the heat release rate: The vent flow measurements (see Section 3.4.5) show that the velocity of the gas increases in less than linear proportion to the fuel flow rate.

The edge velocity of the triple flame is a function of the stratification of the gas/air mixture ahead of the flame, the dilution of the fuel and the temperature ahead of the flame [Phillips 1965]. As the gas velocity increases in less than linear proportion to the fuel flow rate, it can be expected that increases in the fuel flow rate lead to increases in the concentration of the fuel ahead of the flame. This will tend to increase the laminar burning velocity. The correlation between the temperature and the laminar burning velocity is positive – in a first approximation [Glassman 1977], the laminar burning velocity S_L is a function of $(T_{ign} - T_0)^{-0.5}$, where T_{ign} is the ignition temperature of the gas and T_0 the initial temperature. As increases in the fuel flow rate will lead to increases in the temperature, this will tend to increase the edge velocity. The effect is however weak, as not only is the relationship between the temperature and the edge velocity less than linear, but the influence of the fuel flow rate on the temperature is weak.

As long as a detached flame exists, these two velocities balance each other out, whereby the movement of the flame is due to local variations of the two velocities. The observation that at high fuel flow rates the flame increases in size and becomes attached to the rear and side walls can be interpreted as being due to the edge velocity increasing by more than the gas flow velocity, and therefore the premixed wings of the flame propagating against the gas flow. It can therefore be concluded that:

- stable combustion – $\frac{A_{fl-in}}{A_c} = 1$ is linked to $v_{edge} > v_{gas}$
- unstable combustion – $\frac{A_{fl-in}}{A_c} = 1$ is linked to $v_{edge} \approx v_{gas}$

3.2.6.4 Presence of External Flaming

Large external flames are often associated with ventilation-controlled conditions. In the scenario described here, the flow rate of air entering in through the vent is several times that required for combustion of the fuel; despite this, burnout of the fuel does not occur rapidly enough for all the fuel to be consumed before flowing out through the vent.

The slow reaction rate is probably due to the stable thermal stratification between the lower layer and the reaction zone; due to this stratification, there is little mixing between the air from below the reaction zone and the gas mixture above the reaction zone. This low rate of mixing limits the combustion rate.

3.2.6.5 Influence of Fuel and Comparison with Morehart's Configuration

As mentioned in Section 1.4, Morehart *et al* produced sustainable lifted flames in tests with a heavier-than-air fuel, but not with a fuel that was lighter than air [Morehart *et al* 1992a]. The experiments described in Section 3.2.5 show that in the configuration described here, the relative density of the fuel to air makes no significant difference to the behaviour of the flame.

The difference probably lies in the different makeup of the upper layers in Morehart's configuration and in the configuration used in the current project. In Morehart's configuration,

the introduction of air into the upper half of the compartment probably produces a stratification of the chemical makeup which is the inverse of that produced in Coutin's experiments: a layer of oxygen-containing gases above a layer predominantly containing combustion products and fuel. Morehart's lifted propane flame must have stabilised between these two layers. When methane was used, due to the buoyancy of the fuel, no equilibrium could be produced between the downward forces of the cold air and the upward forces of the fuel and heated combustion products, producing the observed behaviour with the flame continuing to rise.

3.3 Analysis of the Area Covered by the Flame

Measurements were made of the area covered by the flame as a function of the fuel flow rate and of the width of the vent. The results presented in the following are from tests performed with the line burner located at $x = 0.31$ m ($0.5 L$), $y = 0.80$ m ($0.95 H$). The deep soffit was in place.

The data were studied to see whether the area can be used as an indicator of the heat release rate, or at least whether the ratio between the area covered by the internal part of the flame (A_{fl-in}) and the area covered by the external part (A_{fl-out}) can be taken as an indicator of the ratio between the amount of heat released inside the compartment $\dot{Q}_{prod-in}$ and the amount of heat released outside $\dot{Q}_{prod-out}$. This section presents the reflections made during this study.

Area Plotted against the Fuel Flow Rate

Fig. 3.21 shows the areas calculated for a range of fuel flow rates up to 0.71 g/s ($\dot{H} = 33$ kW) while the vent was unrestricted except for the soffit.

At fuel flow rates below 0.21 g/s ($\dot{H} = 9.8$ kW), combustion is not sustainable, and hence a flame area of zero is observed. At fuel flow rates above this minimum, there is both internal and external flaming. If the fuel flow rate is increased, the average area covered by the internal

part of the flame increases until, at flow rates of about $0.6 \frac{\text{g}}{\text{s}}$ (28 kW) it almost constantly fills the whole of the area circumscribed by the walls of the compartment.

At fuel flow rates just above the minimum, the external part of the flame is about the same size as the internal part. Its size remains almost constant until flow rates of about $0.47 \frac{\text{g}}{\text{s}}$ (22 kW). Further increases in the fuel flow rate lead to rapid increases in the area covered by the external part of the flame.

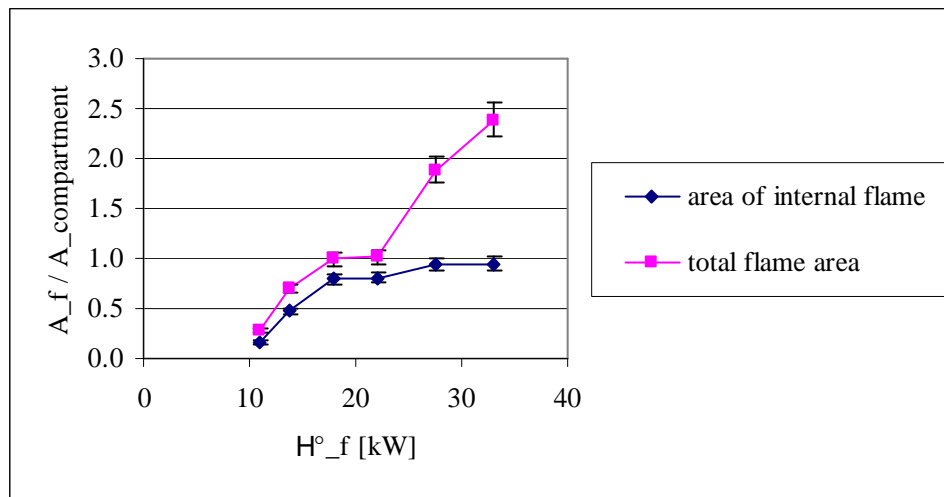


Fig. 3.21: Dimensionless area covered by the internal part of the flame and by the whole of the flame as a function of the energy flow rate.

Data from the Bertin compartment with the large soffit installed and an otherwise unrestricted vent; the line burner was used.

Discussion of the Inflection in the Relationship between Area and Fuel Flow

The curves defined by the datapoints in *Fig. 3.21* rise monotonically with increasing fuel flow rate, but their gradients do not vary monotonically: the curves describe a “double S-bend”, first rising steeply, then levelling off, then increasing in steepness and finally the area covered by the internal part of the flame plateaus as it reaches the extent of the space between the four walls while the external part continues to increase but with a lower rate of growth.

One hypothesis to explain this is that the area is influenced by the colour of the flame, or rather by the rate of radiative heat loss from the flame. The range of fuel flow rates which

corresponds to the centre of this inflection ($\dot{m}_F = 0.4 \text{ g/s}$ to 0.5 g/s ; $\dot{H} = 19$ to 23 kW) corresponds to the range where the change in the colour of the flame from blue to orange occurs. As discussed by both Morehart [Morehart *et al* 1992] and Coutin [2000], the orange/yellow colour is the result of incandescence of the soot particles which are only formed at higher temperatures. The soot emits more thermal radiation than the hot gases. It can be postulated that the increase in heat losses which accompany the change in colour will tend to decrease the chemical reaction rate, and so subsequently it will take longer for the gases to burn out, and they will travel further before they have been completely reacted.

However, the measurements of the area and observations of the flame colour during the warmup phase (see *Fig 2.15* and *Fig 2.16*) do not support this hypothesis: during the warmup phase there is a change in colour of the flame which is not accompanied by a change in the area covered by the flame.

It may be that other factors such as the temperature have an influence on the area, but the work performed during the current project has not led to any conclusions.

Area Covered by the Flame as a Function of the Vent Size

If the area covered by the flame is determined by the heat release rate, then one would expect the size of the vent not to influence the area. In *Fig. 3.22*, the area is plotted for a range of vent widths between fully open (0.4 m, equating to a ventilation factor F_V of $0.14 \text{ m}^{2.5}$) and one-eighth of the width of the compartment (0.05 m, equating to an F_V of $0.035 \text{ m}^{2.5}$) and for a fixed fuel flow rate of 0.71 g/s ($\dot{H} = 33 \text{ kW}$).

At this fuel flow rate and for this range of vent sizes, the flame nearly constantly covers the whole of the area between the four walls of the compartment; this is not altered by variations of the width of the vent.

The measurements suggest that if the width of the vent is reduced from 0.4 m to 0.1 m, the area covered by the external part of the flame drops slightly, although this drop is by less than the error margin of the measurements. However, a further reduction in the ventilation leads to a sudden large drop in the area covered by the external part of the flame.

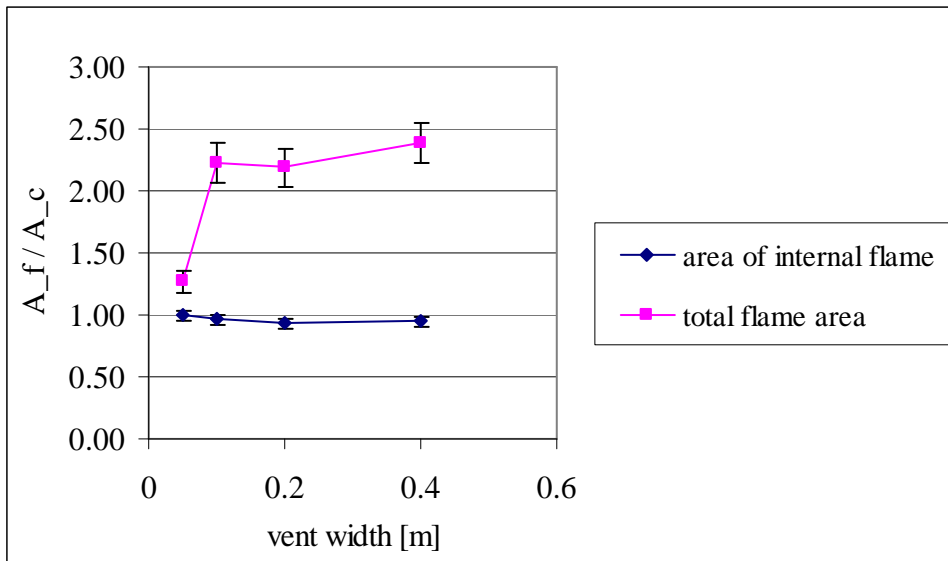


Fig. 3.22: Area covered by the flame as a function of the width of the vent for a vent height of 0.49 m. Data from the Bertin compartment with the large soffit installed; the line burner was used; fuel flow rate 0.71 g/s ($\dot{H} = 33 \text{ kW}$)

Discussion of the Reduction in the Area at Small Vent Sizes

The sudden drop in the area covered by the external part of the flame can be attributed to the fact that the flow passes from laminar to turbulent, as can be seen by the change in the shape and nature of the flame. The reduction in vent area leads to a reduction in vent flow rate, however the drop in flow rate is less than proportional to the vent area; this translates into an increase in the flow velocity. The shape and movement of the flame indicate that at large vent sizes, the flow is slow enough to be practically laminar, whereas for the smallest vent width, it is turbulent. The turbulence leads to efficient mixing of fuel and air, and hence to a rapid consumption of the fuel and therefore a short flame.

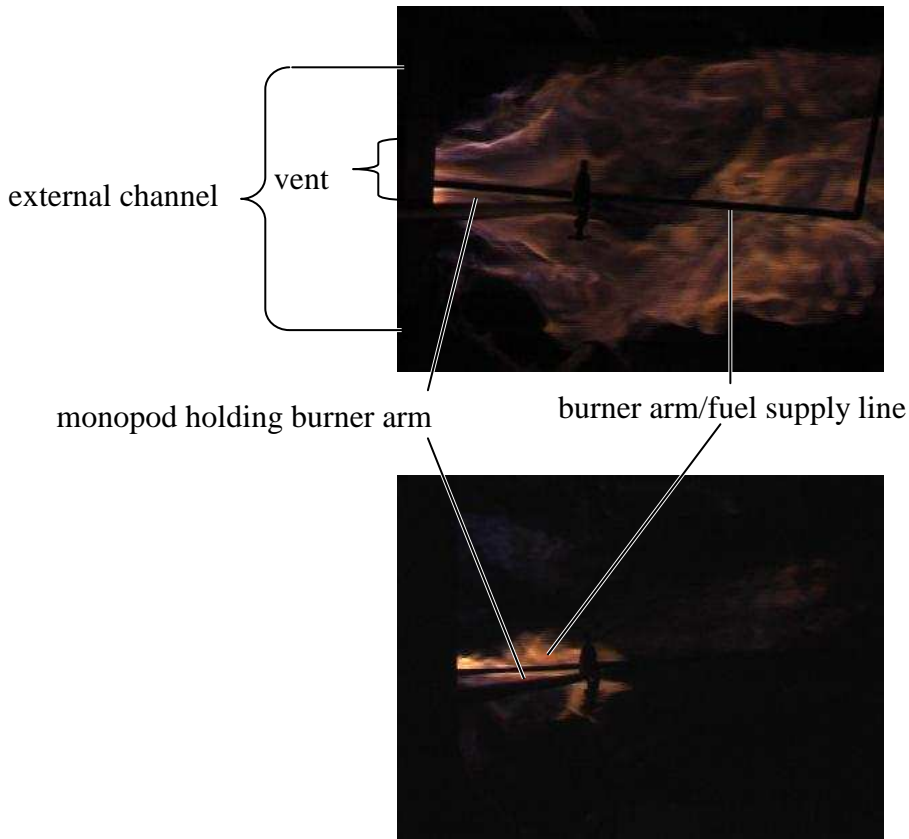


Fig. 3.23: Comparison of the external part of the flame for a 0.71 % fuel flow rate and two different vent widths: Top: vent 0.1 m (0.25 W); Bottom: vent 0.05 m (0.125 W)

Combustion Efficiency

It is obvious from Fig. 3.21 that the area covered by the flame is not directly proportional to the fuel flow rate.

If the hypothesis is correct that the area is proportional to the heat release rate, then the deviations from linearity in the relationship between the area and the fuel flow rate will be due to variations in the ratio between $(\dot{m}_F \Delta h_c)$ and the heat release rate, *i.e.* in the combustion efficiency

$$\eta_c = \frac{\dot{Q}}{\dot{H}} \quad (3.4).$$

A first question that can be asked if one is setting out to judge whether there are significant variations of the combustion efficiency over the range of fuel flow rates studies, is whether the smoke emission from the flame can be used as an indicator of the combustion

efficiency. Visual observations suggest that there is very little smoke given off by the system independent of the fuel flow rate for vent sizes from the full width (0.4 m) down to 0.1 m. This does not prove that the combustion efficiency is high or constant, but is compatible with a high combustion efficiency. (As described in Section 3.4.1, if the vent is restricted more severely then the behaviour of the fire changes significantly, and more smoke is produced, but in that case the shape of the flame is so different, that a discussion in the context of the link between the area of the flame and the heat release rate is not sensible.)

The question as to whether the inflection in the relationship between A_{flame} and \dot{m}_F is due to a variation in the combustion efficiency can be explored by comparing the measured area of the flame with the area which one would expect if the link between the area and the heat release rate were linear and the combustion efficiency were constant. In the latter case, the area would be linearly dependent on the fuel flow rate. *Fig. 3.24* compares such a linear relationship with the relationship between the measured values and the fuel flow rate.

If the measured values are proportional to the heat release rate, then the ratio between the measured value for a given energy flow rate \dot{H} and the hypothetical area defined by the linear relationship must be proportional to the combustion efficiency.

$$A_{hypothetical} \propto \dot{Q}_{hypothetical} \propto \eta_{hypothetical} \dot{H} \quad (3.5)$$

$$A_{measured} \stackrel{?}{\propto} \dot{Q}_{real} \propto \eta_{real} (\dot{H}) \dot{H} \quad (3.6)$$

$$\frac{A_{measured}}{A_{hypothetical}} \stackrel{?}{\propto} \frac{\eta_{real} (\dot{H}) \dot{H}}{\eta_{hypothetical} \dot{H}} \propto \frac{\eta_{real} (\dot{H})}{\eta_{hypothetical}} \quad (3.7)$$

The ratio between the two areas is shown in *Fig. 3.25*.

At fuel flow rates below the minimum necessary for combustion, the HRR is zero, and so the combustion efficiency is zero. At the same time, the measured area covered by the flame is also zero, giving a ratio of measured to hypothetical of zero. Concerning this point, the observations are compatible with the hypothesis.

To create a double inflection, the efficiency would have to first rise from zero to a high value, and then fall and finally rise again. This would seem unlikely.

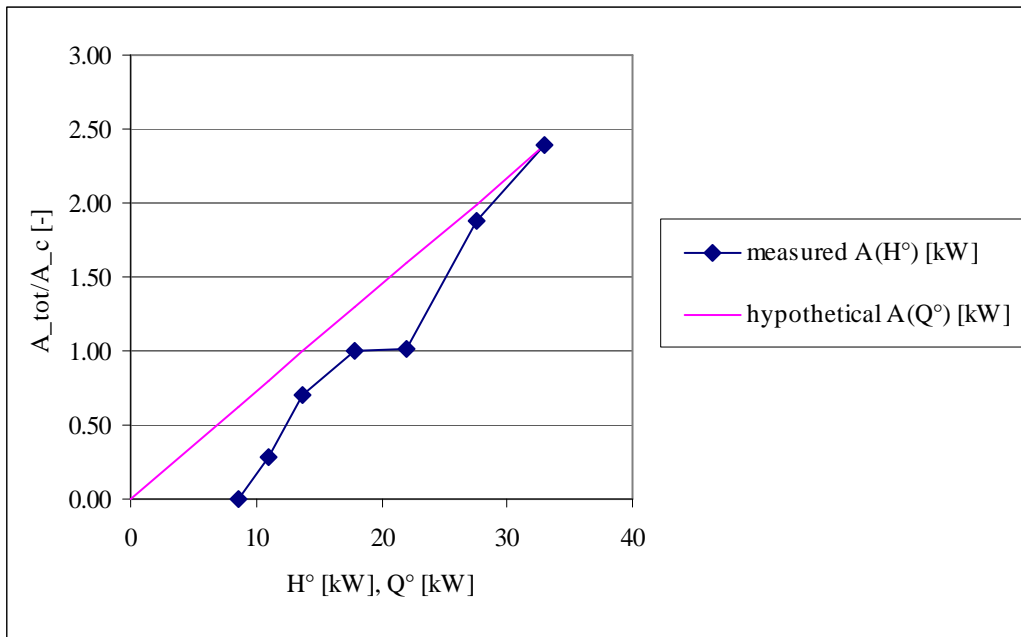


Fig. 3.24: Comparison of the area covered by the flame with a hypothetical area which would be produced if the combustion efficiency were constant and the area were proportional to the heat release rate

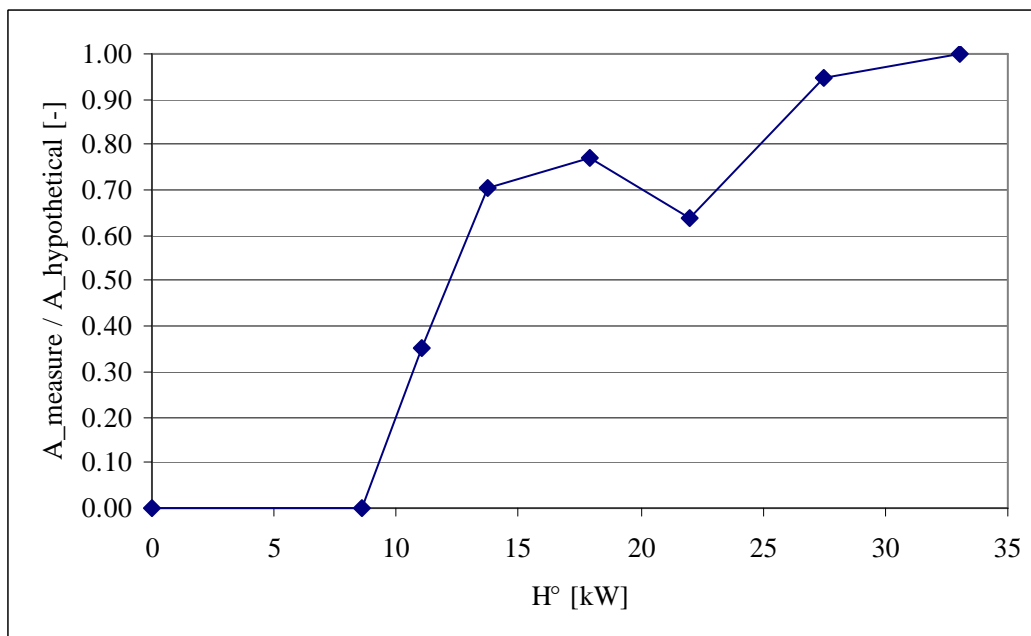


Fig. 3.25: Ratio between the measured area covered by the flame and the hypothetical area one would obtain for a constant ratio between HRR and area and a constant combustion efficiency.

It therefore seems reasonable to conclude that the inflection in the relationship between the area covered by the flame and the fuel flow rate is not, or at least not entirely, due to variations in the combustion efficiency.

Comparison of the Internal and External Parts of the Flame

The discussion in the preceding pages indicates that it is not justified to assume that the area covered by the flame is proportional to the heat release rate.

However, the question can still be raised as to whether in a first approximation the ratio between the area covered by the part of the flame which is inside the compartment and the area covered by the whole of the flame can be taken as an indicator of the ratio between the heat released inside the compartment and the total heat release rate.

This latter can be studied by comparing the internal and total heat release rates which would be witnessed if the ratio between the areas were equal to the ratio between heat release rates. This is illustrated in *Fig. 3.26*. The upper curve is the HRR that would be obtained if the combustion efficiency were unity. The lower curve is this HRR multiplied by the ratio between the internal and total flame lengths. If the ratio between internal and total HRRs is equal to the ratio between internal and total flame areas, then the internal HRR would follow the lower curve, give or take minor variations due to any variations in the combustion efficiency.

As already seen in *Fig. 3.21*, the area covered by the external part of the flame initially remains almost constant and then grows, whereas the area covered by the internal part of the flame initially grows and then levels off. If this behaviour is combined with the hypothesis that $(A_{fl-in}/A_{fl}) \propto (\dot{Q}_{in}/\dot{Q})$ then one obtains heat release rates inside the compartment which initially increase and then drop with increasing fuel flow rate. This would seem unlikely.

The hypothesis that the ratio between the internal and total flame areas is equal to the ratio between the internal and total heat release rates would therefore not seem to be reliable.

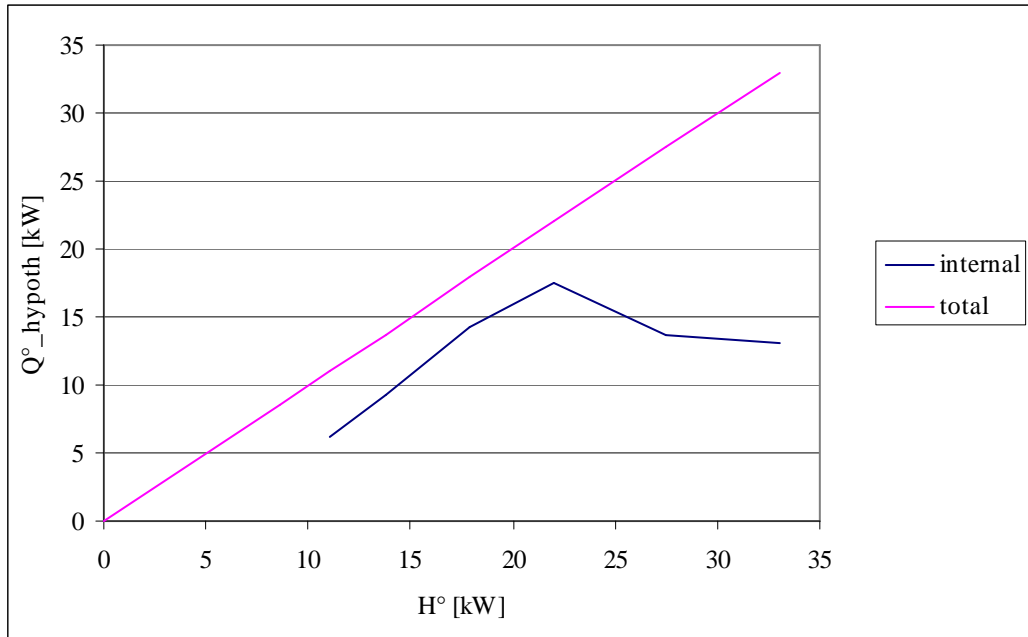


Fig. 3.26: Comparison of the total and internal heat release rates which would be observed if the ratio between the internal and total flame areas were proportional to the total and internal heat release rates.

Relevance of the Minimum Fuel Flow Rate

The question was raised as to whether the area covered by the flame is dependent on the fuel flow rate minus the minimum flow rate necessary to sustain combustion. The idea was that the minimum fuel flow rate may equate to a HRR equal to the heat losses,

$$\dot{m}_{F-\min} \Delta h_c = \dot{Q}_{loss} \quad (3.8)$$

and so a comparison of the A_{fl} to $(\dot{H} - \dot{H}_{\min})$ might equate to comparing the area with the HRR minus the heat losses $(\dot{Q}_{prod} - \dot{Q}_{loss})$. A more clinical definition would be to use the convective heat flow exiting through the vent

$$\dot{Q}_{convective} = \dot{m}_{vent-exit} c_p (T - T_{\infty}) \quad (3.9)$$

rather than $(\dot{Q}_{prod} - \dot{Q}_{loss})$.

A datafit provides

$$\frac{A_{fl}}{A_c} = 362 \cdot 10^{-6} \frac{1}{W^{0.864}} (\dot{H} - \dot{H}_{\min})^{0.864} \quad (3.10)$$

The area of the flame is proportional to $(\dot{H} - \dot{H}_{\min})$ to the power of a factor slightly less than 1, i.e. the area is slightly less than proportional to $(\dot{H} - \dot{H}_{\min})$.

If the area is linked to the convective heat transfer, then the fact that the area increases slightly less than proportionally with the fuel flow rate, would suggest that the conductive and radiative losses increase if the HRR is increased; such behaviour would indeed seem reasonable. It should be noted that the gas temperature in the upper layer is only weakly dependent of the fuel flow rate (as shown by the measurements); because of this, the increase in conductive and radiative losses with increasing \dot{H} is probably only small. Concerning this point, the observations agree with the hypothesis of the area covered by the flame being linked to the convective heat transfer.

$$\frac{A_{fl}}{A_c} = 362 \cdot 10^{-6} \frac{1}{W^{0.864}} (\dot{H} - \dot{H}_{\min})^{0.864}$$

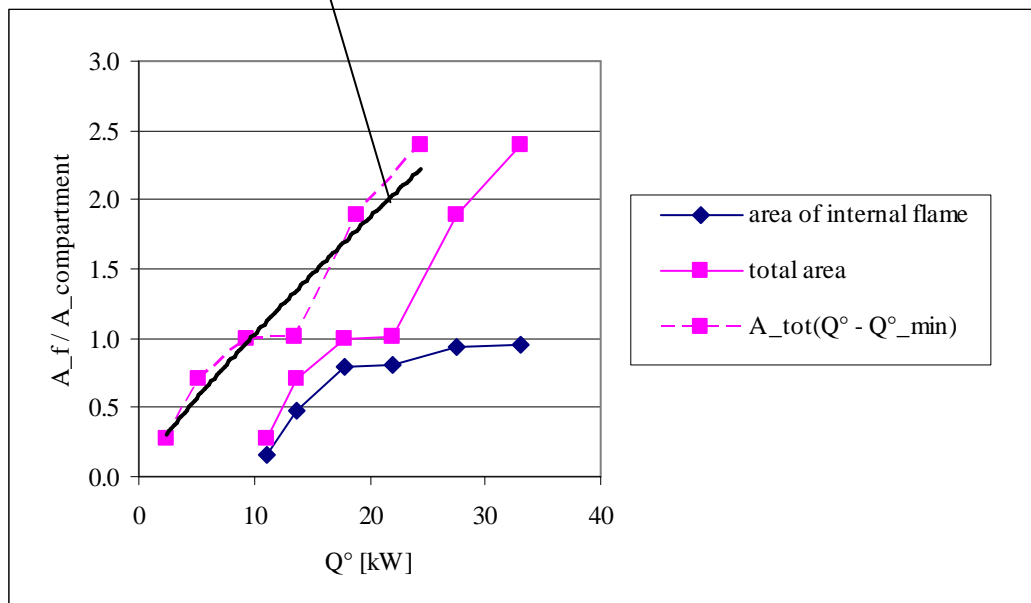


Fig. 3.27: Plot of the area covered by flame together with the area as a function of $(\dot{H} - \dot{H}_{\min})$.

3.4 Influence of the Ventilation on the Behaviour of the Flame

All the results presented so far are from tests with a vent measuring 0.5 m high by 0.4 m wide (ventilation factor $A_V H_V^{0.5} = F_V = 0.14 \text{ m}^{2.5}$). The size of the vent has however a large influence on the behaviour of the flames. This section presents the data obtained while exploring the effect of the vent size.

3.4.1 Description of the Behaviour

The following observations were with a fuel flow rate of 0.71 g/s (which gives an output of 33 kW). The line burner was used, located at $x = 0.31 \text{ m} = 0.5 L$, $y = 0.31 \text{ m} = 0.95 H$, and the deep soffit was installed.

As already mentioned in Section 3.1.2.3, under these conditions, when the vent is unrestricted except for the soffit (vent size 0.5 m high by 0.4 m wide; ventilation factor $F_V = 0.14 \text{ m}^{2.5}$), the upper layer will fill the space from the ceiling to just below the level of the soffit and an amber-yellow cellular flame cover the whole of the interface between the two layers. This is illustrated in *Fig. 3.28*.



Fig. 3.28: View from the side of the flame for a fuel flow rate of 0.71 g/s [$\dot{H} = 33 \text{ kW}$] and a fully open vent

Vertical Slot between 0.2 and 0.05 m wide

In tests which were performed with vents measuring 0.5 m in height, but with widths equal to half, a quarter and an eighth of that of the compartment (vent width 0.2 m, 0.1 m and 0.05 m respectively, ventilation factors F_V 0.71 m^{2.5}, 0.035 m^{2.5} and 0.018 m^{2.5}), the shape and colour of the flames did not noticeably alter. However, the depths of the two layers did change: the smaller the vent, the deeper the upper layer and the closer to the floor the sheet of flames. With decreasing vent width the interface between the upper and lower layers also became more and more inclined: At the rear of the compartment, the interface was closer to the floor than it was at the front of the compartment. This can be seen in the series of images *Fig. 3.29* to *Fig. 3.31*.



Fig. 3.29: View from the side of the flame for a fuel flow rate of 0.71 s/s [$\dot{H} = 33$ kW] and a vent width of 0.2 m = 0.5 W



Fig. 3.30: View from the side of the flame for a fuel flow rate of 0.71 s/s [$\dot{H} = 33$ kW] and a vent width of 0.1 m = 0.25 W



Fig. 3.31: View from the side of the flame for a fuel flow rate of 0.71 g/s [$\dot{H} = 33 \text{ kW}$] and a vent width of $0.05 \text{ m} = 0.125 W$

Vertical Slot 0.025 m wide

When the vent is reduced to 25 mm width (i.e. $\frac{1}{16}$ the width of the compartment; $F_V = 0.009 \text{ m}^{2.5}$), the flame behaviour changes significantly.

Instead of there being distinguishable upper and lower layers, the zone of smoke and combustion gases reaches down to the floor and fills the entire compartment except for a small volume just inside the lower part of the vent.

The flame is visibly more turbulent than the one that is produced at larger vent sizes with the same fuel flow rate.

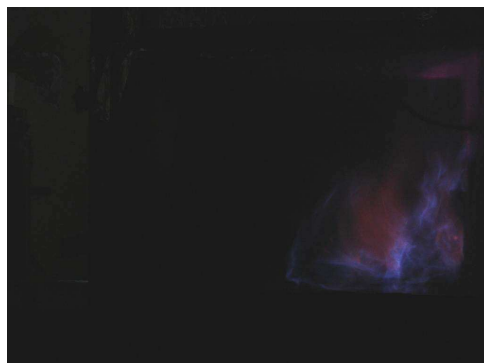


Fig. 3.32: View from the side of the flame for a fuel flow rate of 0.71 g/s [$\dot{H} = 33 \text{ kW}$] and a vent width of $0.025 \text{ m} = 0.063 W$

3.4.2 Layer Depth

As mentioned on the previous page, when the size of the vent is reduced, the upper layer increases in depth. A closer observation of the depth of the layer showed that a similar increase in size of the upper layer also occurs if the fuel flow rate is increased while the size of the vent remains constant, although for safety reasons no tests were performed with fuel flow rates which would have been high enough for the upper layer to be deep enough to reach the floor.

In *Fig. 3.33*, the location of the interface between the two layers is displayed for a range of fuel flow rates between $0.24 \frac{\text{g}}{\text{s}}$ and $0.71 \frac{\text{g}}{\text{s}}$ (\dot{H} between 11 kW and 33 kW) when the deep soffit is installed and the vent is otherwise unrestricted; *Fig. 3.34* shows the location of the interface for a fixed fuel flow rate of $0.71 \frac{\text{g}}{\text{s}}$ (33 kW) when the width of the vent is varied (vent height constant at 0.5 m, F_V ranging from $0.009 \text{ m}^{2.5}$ to $0.14 \text{ m}^{2.5}$). Note that in the case with the smallest vent, the interface between the hot and cold zones does not reach across the whole of the width of the compartment. The cold zone is limited to a small region just inside the vent; the line indicated on the plot shows the intersection between the interface between the zones and the central plane.

Fig. 3.33 shows that within the range of fuel flow rates studied, the increase in depth of the upper layer is only modest. The interface is slightly inclined, with the upper layer being deeper at the rear of the compartment than at the front.

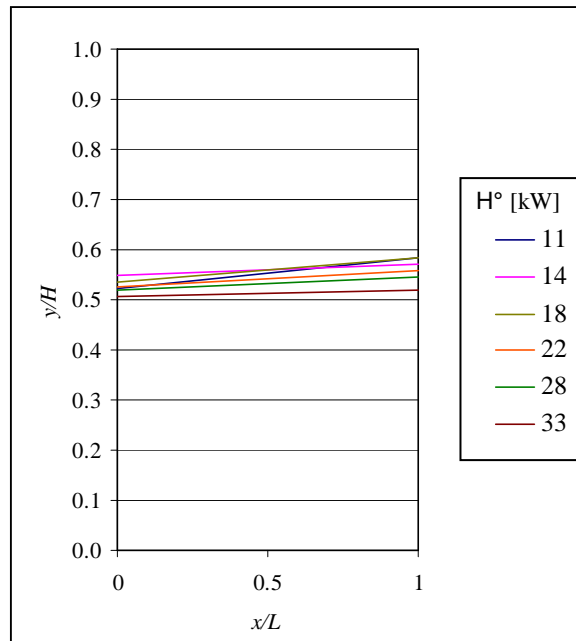


Fig. 3.33: Indication of the location of the interface between the two layers for a range of fuel flow rates. The data stems from cases where the deep soffit is in place and the vent was otherwise unrestricted; the line burner was used, located at $x = 0.32 \text{ m} = 0.5 L$, $y = 0.80 \text{ m} = 0.95 H$.

A reduction in the width of the vent to half the width of the compartment leads to only a slight increase in the depth of the upper layer. However, with further decreases in the width of the vent, the effect on the depth of the layers increases – both in terms of the depth of the upper layer and the inclination of the interface. When the vent is 0.025 m wide, the flame attaches itself to the floor, filling the space just inside the vent, but not reaching far into the compartment. The corresponding line in Fig. 3.34 indicates the intersection of the flame with the central plane – the flame does not lie in a plane perpendicular to the central plane.

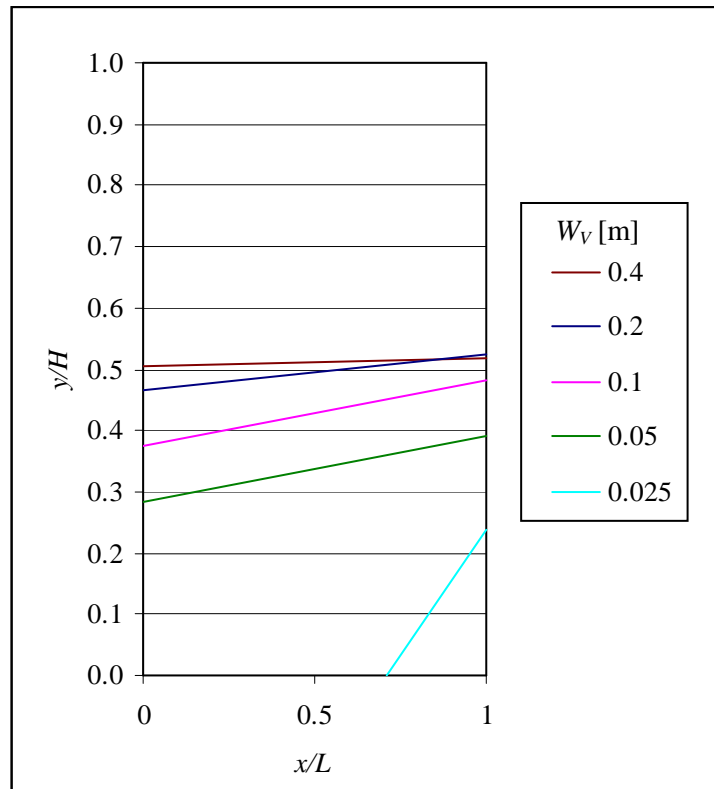


Fig. 3.34: Indication of the location of the interface between the two layers for a range of vent sizes. The data is from cases where the deep soffit is in place; the line burner was used, located at $x = 0.32$ m ($0.5 L$), $y = 0.80$ m ($0.95 H$) with a fuel flow rate of 0.71 s/s , which equates to a value of $\dot{H} = 33$ kW.

From the location of the interface between the two layers, the volumes of the two layers can be estimated. This is depicted in Fig. 3.35. For comparison, the volume of the space between the soffit and the rear wall is also shown. The left-hand plot shows the volume of the layers as a function of the fuel flow rate for several sizes of vent. The right-hand plot shows the volume of the layers as a function of the vent width for two fuel flow rates. The reduced vent sizes did not allow sustained combustion with the lower fuel flow rates, and so the curves in the left-hand plot for the smaller vents cut off at low flow rates, and the curve in the right-hand plot for 22 kW ($\dot{m}_F = 0.47$ s/s) cuts off at low vent sizes.

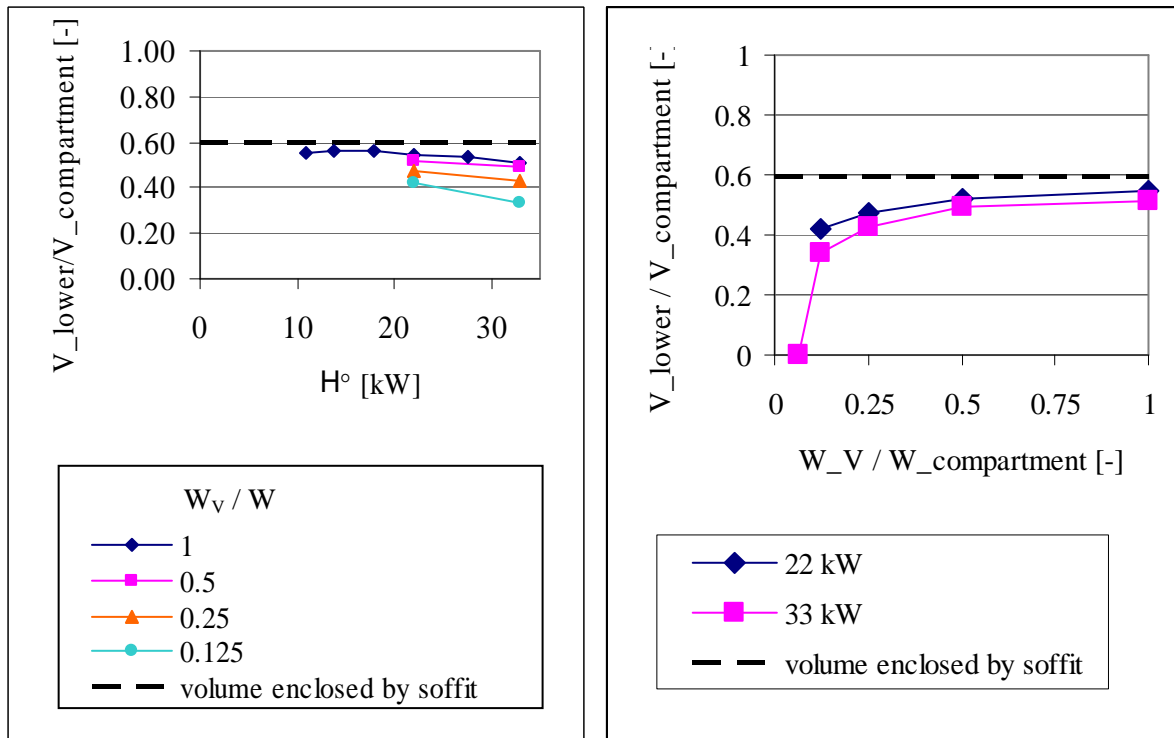


Fig. 3.35: Volume of the two layers – left as a function of the fuel flow rate when the vent is 0.4 m wide, right as a function of the vent width for fuel flow rates of 0.47 %/s and 0.71 %/s (equating to 22 kW and 33 kW respectively). The data stems from cases where the deep soffit is in place; the line burner was used, located at $x = 0.32 \text{ m} = 0.5 L$, $y = 0.80 \text{ m} = 0.95 H$.

The decreasing inclination of the lines on the left-hand plot show that the effect of a given increase in the fuel flow rate is greater at higher fuel flow rates than at low fuel flow rates. Similarly, the increasing inclination of the right-hand plot when the vent is reduced illustrates the increasing influence of the vent size as the size is reduced.

3.4.3 Minimum Fuel Flow Rate

Bertin Apparatus

As mentioned in Section 1.2.4, Coutin showed that when the fuel source is located inside the upper layer, the fuel flow rate must be above a critical value whereby the value depends on the location of the burner and the depth of the soffit: a higher fuel flow rate is required to

sustain combustion when the deeper soffit is installed than with the shallow one, and a higher fuel flow rate is required if the burner is located close to the front or rear walls rather than half-way between the two.

During the current study, observations were made to quantify the minimum fuel flow rate required as a function of the depth of the soffit and the width of the vent when the burner is located half-way between the front and the rear of the compartment. The results are depicted in *Fig. 3.36*.

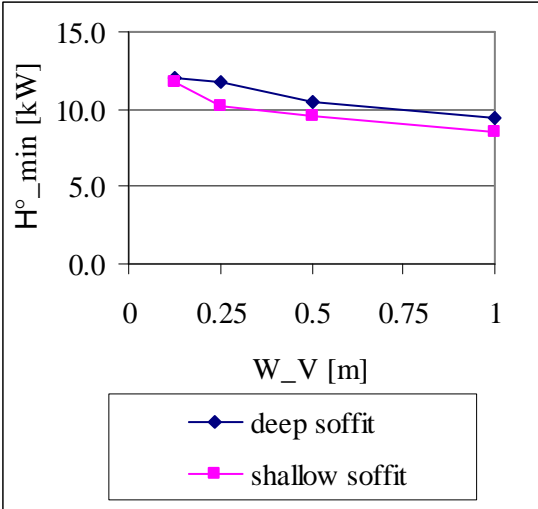


Fig. 3.36: Minimum energy flow rate as a function of the soffit depth and the vent width

The data shows that, the minimum necessary fuel flow rate is increased if the soffit depth is increased and/or the width of the vent decreased.

“Telephone Box”

In the larger installation the minimum required fuel flow rate is roughly 0.3 g/s , which equates to an energy flow rate of 15 kW.

Influence of the History of the Test

During the tests performed to determine the minimum fuel flow rate, an observation was made which influenced the discussion about relative influence of the parameters on the sustainability of the flame. As already explained in Section 2.3.1, the experiments to determine the minimum fuel flow rate were performed by igniting the burner and setting a fuel flow rate which was high enough to sustain combustion, and then by gradually reducing the fuel flow rate. During these tests, the fuel flow rate at which the flame extinguished depended on the fuel flow rates which had previously been set and the length of time that they had been set.

A few examples are given in *Table 3.3*. In the first of the two cases with a vent of 0.05 m width, the test was started with a fuel flow rate which is within about one and a half times the minimum value. After thirty five minutes and three reductions in the fuel flow rate, the fire extinguished when a flow rate equating to 11.9 kW was passing through the burner. In the second case, a much higher initial fuel flow rate was chosen. In this case, the fuel flow rate could be reduced to a value equating to 10.7 kW before the flame extinguished. This is 90 % of the value from the first test.

In the case where the vent was 0.1 m wide, the same initial fuel flow rate was chosen as in the first of the two cases with a narrower vent, but the flow rate was reduced sooner after ignition. The result was that extinction occurred at a higher fuel flow rate than in the cases with the narrower vent, namely the equivalent of 11.6 kW.

0.05 m wide vent:

time [min]	$\dot{m}_F \Delta h_c$ [kW]
0 – 22	13.8
20-32	12.1
32-35	11.9
35	extinction

time [min]	$\dot{m}_F \Delta h_c$ [kW]
0-5	22.0
5-17	16.9
17-32	15.0
32-50	13.4
50-65	12.3
65-82	11.7
82-85	10.7
85	extinction

0.1 m wide vent:

time [min]	$\dot{m}_F \Delta h_c$ [kW]
0 – 20	13.8
20-27	12.1
27-37	11.6
37	extinction

Table 3.3: Three examples of the energy flow rates during tests to determine the minimum flow rate necessary to sustain combustion

3.4.4 Temperatures

Fig. 3.37 and Fig. 3.38 show temperature profiles taken from the rear of the compartment for two different fuel flow rates – 0.47 g/s ($\dot{H} = 22 \text{ kW}$) and 0.71 g/s ($\dot{H} = 33 \text{ kW}$) – taken with a range of vent sizes.

As already seen in Section 3.2.3, the temperatures of the lower layer increase from about 60°C to about 100°C if the fuel flow rate is increased from 0.47 g/s to 0.71 g/s when the vent is 0.4 m wide. The temperature of the upper layer is independent of the fuel flow rate and also independent of the width of the vent.

As would be expected, the increase in the depth of the upper layer, as described in Section 3.4.2, and in particular in Fig. 3.35, is also visible in the temperature data. The increase in depth of the hot zone is clearly visible in the plot for 0.71 g/s (Fig. 3.38). As the vent has less

of an effect on the depth of the layers in the case with 0.47 s/s , little variation is observed in Fig. 3.37 in the height above the floor of the temperature peak produced by the flame.

The plots show that the temperature in the upper layer remains constant at about 550°C , irrespective of the width of the vent. The plots also reproduce the point already presented in Section 3.2.3, that the temperature in the upper layer does not vary with the fuel flow rate, as long as the rate is high enough for the flames to cover the whole of the interface between the two layers.

The temperature of the lower layer does however rise: In the 22 kW case (0.47 s/s) the temperature raises from 70°C when the vent is fully open to 120°C for the $1/4$ -width vent; in the 33 kW (0.71 s/s) case, the value is 130°C for the fully open vent, 190°C for the $1/4$ -width and 240°C for the $1/8$ -width vents.

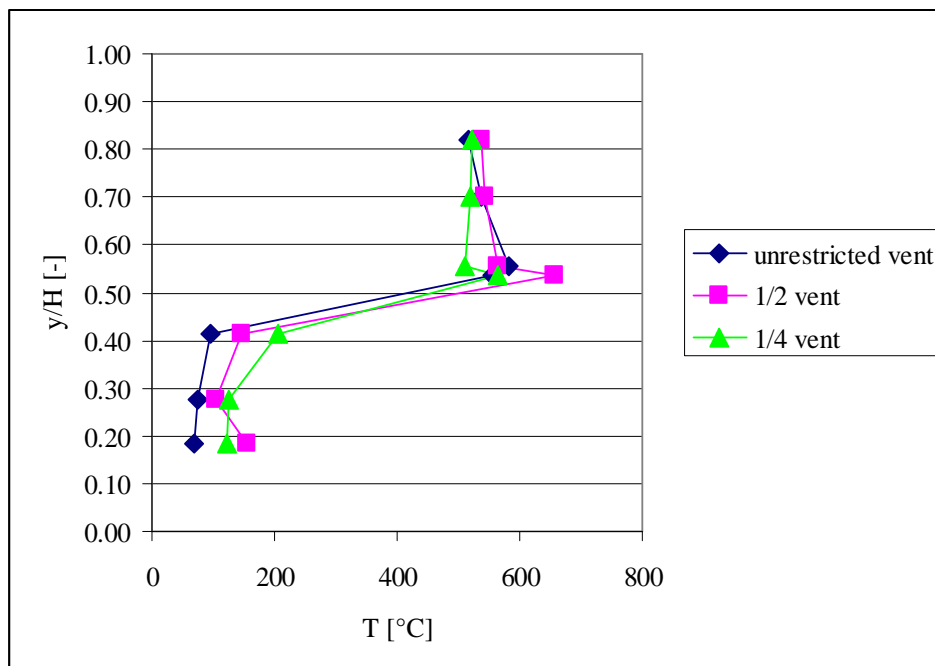


Fig. 3.37: Temperature profiles in the rear of the compartment for a fuel flow rate of 0.47 s/s (equating to 22 kW). Temperatures are shown measured at $x = 0.1 \text{ m}$, $z = 0.04 \text{ m}$, for a range of heights and a range of vent widths. The deep soffit was in place; the line burner was used located at $x = 0.31 \text{ m}$ ($0.5 L$), $y = 0.80 \text{ m}$ ($0.95 H$)

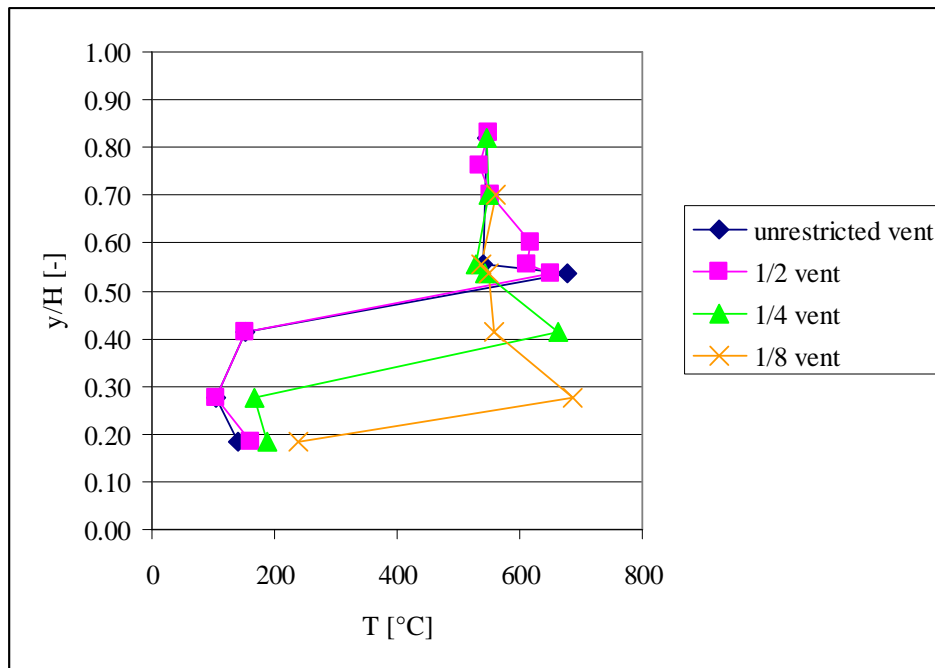


Fig. 3.38: Temperature profiles in the rear of the compartment for a fuel flow rate of 0.71 s/s (equating to 33 kW). Temperatures are shown measured at $x = 0.1 \text{ m}$, $z = 0.04 \text{ m}$, for a range of heights and a range of vent widths. The deep soffit was in place; the line burner was used located at $x = 0.31 \text{ m}$ ($0.5 L$), $y = 0.80 \text{ m}$ ($0.95 H$)

3.4.5 Vent Flow Rate

In order to estimate the flow rate of air into the compartment as a function of the fuel flow rate \dot{m}_F and of the vent width W_V , velocity profiles were measured in the central plane, and from these the flow rates were extrapolated.

Vent Flow Rate as a Function of the Fuel Flow Rate

Velocity profiles through the vent are shown in Fig. 3.39 for the central plane ($z = 0 \text{ m}$) for cases with the deep soffit installed and the line burner located at $x = 0.31 \text{ m}$ ($0.5 L$), $y = 0.80 \text{ m}$ ($0.95 H$), for a range of fuel flow rates between 0.24 s/s ($\dot{H} = 11 \text{ kW}$) and 0.71 s/s ($\dot{H} = 33 \text{ kW}$). Each section of the profiles was calculated from a series of 300 PIV measurements.

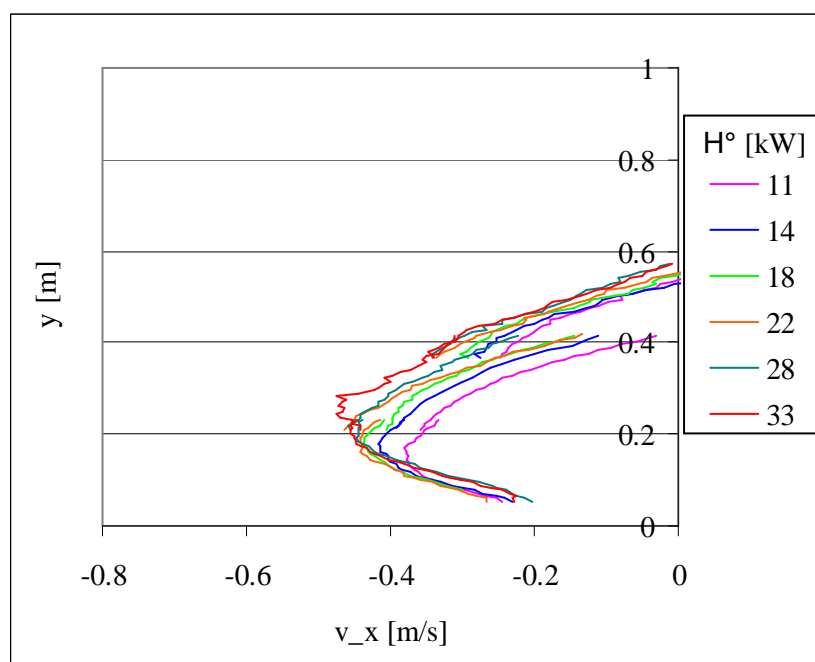


Fig. 3.39: Velocity profiles in the central plane for a range of fuel flow rates. The data stems from cases where the deep soffit is in place and the vent was otherwise unrestricted; the line burner was used, located at $x = 0.32 \text{ m}$ ($0.5 L$), $y = 0.80 \text{ m}$ ($0.95 H$).

The profiles are created by averaging the velocity given by the PIV for the three fields of view described in Fig. 2.9 (Section 2.3.2). It can be seen that the profiles which result for the central field of view for each fuel flow rate follow on well from the profiles for the lower field of view. At the transition between the middle and upper fields of view however, the profiles for all but the highest fuel flow rate ($\dot{H} = 33 \text{ kW}$) are disjointed. However, questions have been raised about the accuracy of the data from the central field of view. If the profiles from the central field of view are extrapolated to determine the location of the neutral plane – the height at which $v = 0 \text{ m/s}$ – one obtains values well below half-way up the vent. This does not agree with the location of the neutral plane indicated by visual observations of the movement of the seeding droplets. In addition, if an extrapolation is created for profiles from the lower and from the upper fields of view for each case, these extrapolations will lie very close to each other. For the calculation of the flow rates, the data from the central field of view were therefore discounted, and an interpolation between the upper and lower fields of view was used.

The flow rate in through the vent was estimated by assuming that the velocity through the vent is proportional to the fourth power of the z -coordinate.

$$v(x, y, z) = v(x, y, 0\text{m}) \left(\left(\frac{x}{W} \right)^4 - 1 \right) \quad (3.11)$$

The resulting velocities are integrated over the width and height of the vent and multiplied by the density of air to give a mass flow rate.

The resulting values are depicted in *Fig. 3.40*. They indicate that the flow rate increases with fuel flow rate for fuel flow rates up to about 0.5 g/s . This value equates to the transition between flames which partially cover the interface and flames which cover the whole of the interface. Further increases in the fuel flow rate do not lead to increases in the flow rate.

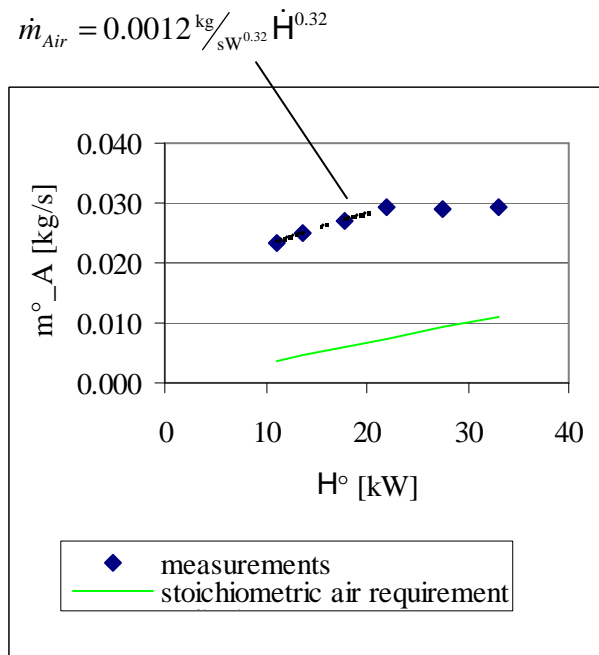


Fig. 3.40: Estimate of the vent flow rate as a function of the fuel flow rate derived from the velocity profiles in Fig. 3.39. Also shown are the flow rate of air required for complete combustion of the fuel and a curve-fit for the flow rate of those cases in which the flame does not cover the whole of the interface between the layers.

The fact that the flow rate is independent of the fuel flow rate providing the flame covers the whole of the surface between the four walls, is probably due to the fact that when the internal part of the flame extends as far as it can, increases in the fuel flow rate do not lead to significant increases in the amount of heat which is released inside the compartment, and thus do not increase the buoyant lift which drives the natural convective flows.

A curve fit for the range where the flow rate increases (\dot{m}_F from 0.2 g/s to 0.47 g/s; \dot{H} from 9.8 kW to 22 kW) delivers a correlation of

$$\dot{m}_{Air} \approx 0.33 \frac{\text{kg}^{0.68}}{\text{s}^{0.68}} \dot{m}_{Fuel}^{0.32} \quad (3.12).$$

In *Fig. 3.40*, the air flow rate required for complete combustion of the fuel is also shown. As already shown by Coutin, the actual flow rate is several times that required to combust all the fuel.

Air Flow Rate as a Function of the Vent Size

Velocity profiles in the central plane for a range of vent widths and a fixed fuel flow rate of 0.71 g/s ($\dot{H} = 33$ kW) are shown in *Fig. 3.41*. The measurements were performed with cases with the deep soffit installed; the width of the vent was varied between 0.4 m (1.0 W) and 0.05 m (0.125 W). Measurements with narrower vents were not possible with the technology used, as the temperature in the lower layer becomes so high that the glycol fog used to seed the flow evaporates.

As the vent is reduced, the velocities increase, although by less than the amount which would lead to the flow rate remaining constant. This means that the flow rate of air through the vent drops.

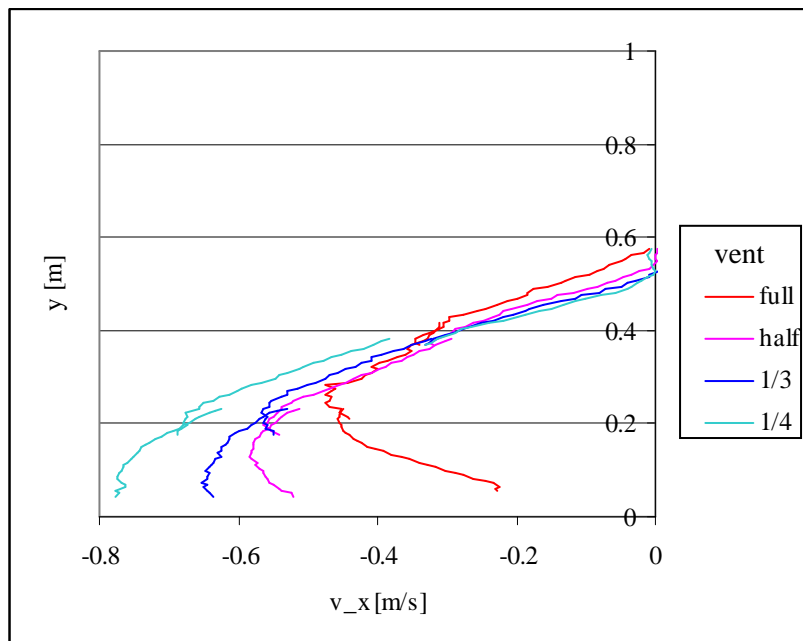


Fig. 3.41: Velocity profiles in the central plane for cases with a fuel flow rate of $0.71 \text{ \%}/s$ and a range of vent widths.

As had been done for the cases with fixed vent size and variable fuel flow rate, the flow rate of air was estimated by assuming that the velocity profile in the horizontal direction describes a fourth-power parabola and by integrating the velocity over the surface of the vent. The resulting flow rates are depicted in Fig. 3.42.

The flow rate is shown to steadily reduce with reducing vent width. A curve fit provides

$$\dot{m}_{Air} \approx 0.055 \frac{\text{kg}}{\text{m}^{0.67} \text{s}} W_V^{0.67} \quad (3.13)$$

Two further curves are shown in Fig. 3.42.

The first is the air flow rate which is required for complete combustion. As the fuel flow rate is constant, this is of course also constant. It can be seen that in all the cases, the flow rate estimated from the velocity measurements is higher than the stoichiometric requirement. However, as the vent flow rate decreases with decreasing vent size, the ratio between the actual air flow rate and the required rate for complete combustion drops from 2.6 to 1.04. Expressed in terms of global equivalence ratios, this equates to an increase from $\phi_{global} = 0.38$ to $\phi_{global} = 0.96$. Any further significant reductions in the vent size would result in the flow rate dropping below that required for stoichiometry.

The second of these curves is the flow rate calculated using the formula presented in Section 1.2.3.2.3 for ventilation-controlled (VC) fires

$$\dot{m}_{Air} \approx 0.5 \frac{\text{kg}}{\text{m}^{2.5} \text{s}} F_V \quad (3.14).$$

This is the flow rate which would be expected to be obtained if a ventilation-controlled fire exists in a compartment when the vent is of the size used in the experiments. In a classical configuration with the fuel source close to the floor, the transition from fuel-control to ventilation control occurs at the vent size at which the stoichiometric requirement intersects the ventilation-controlled flow rate – for larger vent sizes, the air flow rate is higher than that required for stoichiometry; for smaller vent sizes, the air flow rate has the value given by the formula for ventilation-controlled fires and is lower than that required for complete combustion of the fuel. It can be seen that the intersection of these two curves roughly coincides with the intersection of each one and the extrapolated curve from the measurements.

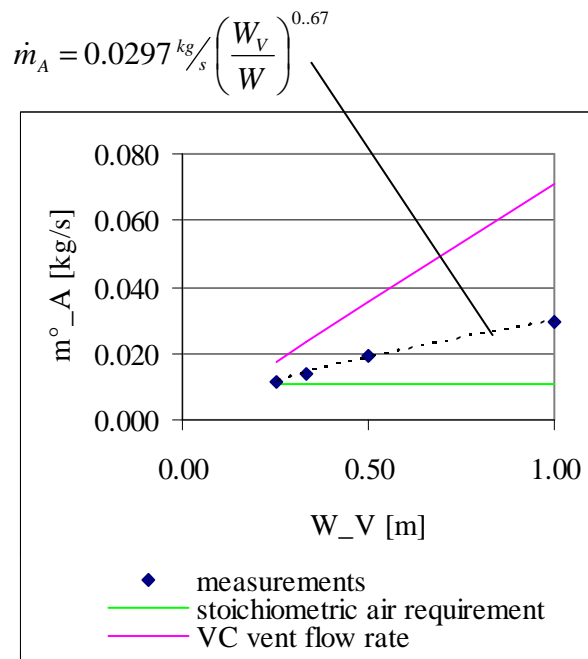


Fig. 3.42: Estimate of the vent flow rate as a function of the vent size for cases with a fuel flow rate of 0.71 s/s (33 kW). Displayed is also the flow rate that would be expected from a VC fire as a function of the vent width for a vent height equating to that in the experiment (0.5 m) and the air requirement for stoichiometric combustion.

3.4.6 Discussion

3.4.6.1 Ventilation Regime

Zone Size and Combustion Regime

As described in Section 3.4.2, the experiments show that the increase of the depth of the upper layer with increasing fuel flow rate or decreasing vent size is only slight at low fuel flow rates and large vent sizes, but is more pronounced at higher fuel flow rates or smaller vent sizes. This is the same behaviour as has been observed and described theoretically for configurations with the fuel source near the floor (see Section 1.2.3.2 and [Prahl, Emmons 1974]).

The results suggest that when the system is running under conditions which create a two-zone behaviour, the vent flow rate is higher than that required for stoichiometry.

Due to the limits of the available seeding technology, no measurements of the vent flow rate could be performed under conditions which lead to the flame descending all the way to the floor, but the results shown here indicate that in such cases the air flow rate is below that required for complete combustion of the fuel. Again, this behaviour is the same as that observed with configurations where the fuel source is close to the floor.

Quantification of the Locus of Transition

It can be noted that the intersection between the extrapolated curve fit for the data and the stoichiometric requirement is almost identical to the intersection between these two curves and the curve describing the vent flow rate under ventilation-controlled conditions for “classical” configurations. This observation led to questions as to whether the conditions for transition between fuel-control and ventilation-control for configurations with fuel sources located near the floor are identical to the conditions which lead to the transition in configurations where the fuel source is near the ceiling.

In the conventional configuration, ventilation-control exists when the flow rate of chemical energy of the gaseous fuel \dot{H} is greater than the heat release rate which is produced from combusting all the oxygen which enters the compartment $\dot{Q}_{prod-VC}$, whereby the amount of oxygen can be calculated using equation (1.14) presented in Section 1.2.3.2.3.

$$\dot{Q}_{prod-VC} = \Delta h_{ox} \dot{m}_{O_2} \approx 13^{MJ/kg} \dot{m}_{O_2} \quad (3.15)$$

$$\dot{m}_{O_2} = 0.23 \dot{m}_{Air} \quad (3.16)$$

$$\dot{m}_{Air} \approx 0.5 \frac{kg}{m^{2.5}s} F_V \quad (3.17).$$

Ventilation-control is therefore present when

$$\dot{m}_F \Delta h_c = \dot{H} > \dot{Q}_{prod-VC} \approx 13^{MJ/kg} \cdot 0.23 \cdot 0.5 \frac{kg}{m^{2.5}s} F_V = 3000^{kJ/kg} \cdot 0.5 \frac{kg}{m^{2.5}s} F_V \quad (3.18).$$

Using this formula, a critical fuel flow rate can be estimated for a given vent geometry or a critical ventilation factor for a given fuel flow rate.

To allow a comparison of the predictions from equation (3.15) with the experimental observations, it is useful to calculate the the critical fuel flow rate for the unrestricted vent and the critical vent size for a fuel flow rate of $0.71 \frac{g}{s}$. For unrestricted vent one obtains

$$\dot{m}_{F-crit} = \frac{3000^{kJ/kg} \cdot 0.5 \frac{kg}{m^{2.5}s} F_V}{\Delta h_c} = \frac{3000^{kJ/kg} \cdot 0.5 \frac{kg}{m^{2.5}s} (0.4m \cdot (0.5m)^{1.5})}{46.5^{MJ/kg}} = 4.5 \frac{g}{s} \quad (3.19)$$

This flow rate (which equates to an energy flow rate of 220 kW) is well above the range used during the present study. Resolving equation (3.15) to obtain the critical vent size for a fuel flow rate of $0.71 \frac{g}{s}$, one obtains

$$W_{V-crit} = \frac{F_{V-crit}}{H_V^{1.5}} = \frac{\dot{m}_F \Delta h_c}{3000^{kJ/kg} \cdot 0.5 \frac{kg}{m^{2.5}s} H_V^{1.5}} \frac{1}{H_V^{1.5}} = \frac{0.71 \frac{g}{s} \cdot 46.5^{MJ/kg}}{3000^{kJ/kg} \cdot 0.5 \frac{kg}{m^{2.5}s} (0.5m)^{1.5}} \frac{1}{H_V^{1.5}} = 0.062m \quad (3.20)$$

This is somewhat larger than the vent size at which the transition is seen in the experiments (two-zone behaviour when $W_{vent} \geq 0.05$ m, one-zone behaviour when $W_{vent} = 0.025$ m). However, it should be borne in mind that during the tests, not all the fuel is combusted inside the compartment. It might therefore be that the fuel flow rate in (3.17) should be reduced, which would then deliver a lower value for the critical vent size, and would bring the calculation into agreement with the observations.

Conclusions

Ventilation-controlled behaviour is possible when the fuel source is located close to the ceiling. All indications are that the behaviour is identical to the ventilation-controlled behaviour when the fuel source is close to the floor.

An identification of the conditions under which the transition occurs will probably require the development of a means to predict the proportion of combustion which occurs inside and outside the compartment.

3.4.6.2 Extinction

As previously mentioned, the conditions under which combustion is no longer sustainable is of fundamental importance.

There is more than one mechanism which plays a role in determining under which conditions combustion is sustainable and under which conditions combustion will extinguish.

Mechanisms of Extinction

The flame can be looked at from two perspectives:

- a premixed flame which propagates against the flow of gas towards the rear wall of the compartment; there is a diffusion flame trailing behind this premixed flame
- a diffusion flame between a layer of fuel-rich/oxygen-lean gas and a layer of oxygen-rich/fuel-lean gas. This diffusion flame is anchored to a premixed flame

Each of these perspectives provides a potential mechanism which can control extinction: the flame will become unsustainable if the premixed flame cannot propagate against the gas flow (*i.e* if $v_e < v_{Gas}$) and/or if the fuel becomes too diluted for the diffusion flame to persist.

Edge Velocity

As long as there exists a flame, then the average velocity of the flame edge relative to the gas must be equal to the average velocity of the gas relative to the apparatus.

As discussed in Section 3.2.2.1, the gas velocity is positively correlated with the fuel flow rate – the higher the flowrate at which fuel is introduced into the system, the higher the velocity of the gas flow along the layer interface.

As discussed in Section 3.2.6.3, it would seem that the average velocity of the flame relative to the gas increases more than the average velocity of the gas relative to the compartment for a given increase in the fuel flow rate; within a limited range of fuel flow rates, the two roughly balance each other out; at fuel flow rates above this range, the premixed flame propagates fast enough to reach the rear wall.

It can be concluded that there must exist a critical value of the fuel flow rate, below which the velocity of the edge relative to the gas is lower than the velocity of the gas relative to the compartment. If the fuel flow rate drops below this critical rate, one would expect the flow to push the flame out through the vent.

Extinction due to Dilution

The concept of flammability limits is more commonly applied to premixed flames than diffusion flames, but several authors – among them Beyler – suggest that the concept of extinction due to dilution can be used for diffusion flames and that they achieve good agreement between prediction and observation [Beyler 1984]. For this, the calculations should be performed with a mixture of the fuel flow and the available oxidant flow in stoichiometric proportions.

This means that there should exist a critical fuel flow rate below which the fuel concentration is too low for a diffusion flame to be sustainable.

As discussed in Section 3.2.6.3, the fuel concentration must be positively correlated to the fuel flow rate, so increases in the flow rate will lead to increases in the concentration. Inversely, if the flow rate is decreased, there must exist a critical rate below which the fuel concentration is too low to sustain combustion.

Influence of Heat Loss and of the Temperature

As shown in the heat balance in the Annexe, the heat losses are in the same order of magnitude as the internal HRR at the minimum fuel flow rate.

There is no conflict between this observation and the concept of extinction due to dilution: the heat losses occur at a distance from the combustion zone, whereas the flammability is determined by local conditions. The heat losses indirectly influence the local temperature, and the temperature is a parameter of the flammability limits. Therefore, the losses play a role, but extinction would better be described in terms of the local conditions, with the losses being a factor which influences the local conditions.

That the temperature plays a role can also be seen from the observations during the warmup phase (Section 2.4), and in particular the fact that sustainable combustion is rarely possible if the burner is located inside the upper part of the compartment from the very start of the test. If the burner is positioned in the lower part of the compartment during the first minutes of a test, two things occur: The gas in the upper layer and the walls are heated and the composition in the upper layer is changed, as oxygen is consumed and fuel and combustion products – both gases and soot – are added. As the flammability limits of a fuel are a function of the temperature [Beyler 1984], it must be assumed that both the heating and the enriching with fuel are important in creating the conditions necessary to permit a flame to stabilise at the interface.

Synthesis

For flammability to be sustainable, the following conditions must be fulfilled:

- the average edge velocity is equal to or greater than the average flow velocity
- the fuel concentration is high enough for the diffusion flame to be sustainable – i.e. high enough for a stoichiometric mixture of the upper layer gases and lower layer gases to be above the LFL

Each set of parameter values corresponds to a value for the edge velocity and a set of values for the species concentrations. If the fuel flow rate is reduced, both the edge velocity and the fuel concentration are reduced.

The question as to which mechanism is dominant equates to the question of which of the two conditions for sustaining combustion is the first to be breached.

Possibly the key to determining which is the dominant mechanism is to observe the behaviour of the flames. If extinction is due to the edge velocity being too low, then the flame will be pushed out through the vent. If extinction is due to dilution, then the flame would be expected to shrink in size as it goes out.

Both behaviour patterns have been observed in the laboratory, although in the vast majority of cases extinction occurs with the flame shrinking in size to zero while it is located inside the compartment. It can therefore be concluded that in the current configuration at the current scale, extinction normally occurs due to dilution, but that critical values of the fuel flow rate associated with each of the two mechanisms are so close to each other for either to be able to occur, depending on the local conditions.

Influence of the Soffit Depth and the Flow Rate per Surface Area

If sustainability is governed by the fuel concentration rather than the total fuel flow rate, then the geometry of the compartment must play a role. This raises the question of what the scaling laws are: if the behaviour is to be reproduced at a larger or smaller scale, then what relationship between fuel flow rate and compartment geometry should be maintained? One suggestion was that the critical fuel flow rate might scale with the area of the interface, which would equate to it being proportional to the floor area of the compartment. However, there is a discrepancy between the values for the two installations.

- in the Bertin compartment, the critical fuel flow rate was determined at 0.20 g/s ($\dot{H} = 9.4 \text{ kW}$) for the deep soffit and 0.18 g/s ($\dot{H} = 8.6 \text{ kW}$). As the floor area is $0.4 \text{ m} \times 0.62 \text{ m} = 0.24 \text{ m}^2$, this leads to values of $0.82 \text{ g/m}^2\text{s}$ (38 kW/m^2) for the deep soffit and $0.72 \text{ g/m}^2\text{s}$ (35 kW/m^2) for the shallow.
- In the “Telephone Box”, the critical fuel flow rate of 0.3 g/s ($\dot{H} = 15 \text{ kW}$) for an area of 0.8 m^2 leads to $0.47 \text{ g/m}^2\text{s}$ (23 kW/m^2).

Influence of the Distance between the Burner and the Walls

As Coutin remarked [Coutin 2000] (see also Section 1.2.4) it is easier to stabilise a flame when the burner is half-way between the rear wall and the soffit than when it is close to the rear or front wall.

A possible explanation as to why a higher fuel flow rate is required if the burner is close to the front or rear wall is that when the horizontal distance between the burner and a wall is significantly less than the depth of the upper layer, it is harder to form a stable vortex to form to lead the fuel from the burner to the reaction zone and combustion products from the reaction zone to the upper layer.

As can be seen from the reproductions of Coutin's maps of the behaviour of the flame, when the shallow soffit was installed:

- when the burner was halfway between the rear and front walls, combustion was not sustainable when the fuel flow rate was below $0.15 \frac{\text{g}}{\text{s}}$ ($\dot{H} = 7 \text{ kW}$) and was sustainable when the fuel flow rate was above $0.19 \frac{\text{g}}{\text{s}}$ ($\dot{H} = 9 \text{ kW}$)
- when the burner was close to the rear wall, combustion was not sustainable when the fuel flow rate was below $0.11 \frac{\text{g}}{\text{s}}$ ($\dot{H} = 5 \text{ kW}$) and was sustainable when the fuel flow rate was above $0.19 \frac{\text{g}}{\text{s}}$ ($\dot{H} = 9 \text{ kW}$)
- when the burner was close to the front wall (the soffit), combustion was not sustainable when the fuel flow rate was below $0.28 \frac{\text{g}}{\text{s}}$ ($\dot{H} = 13 \text{ kW}$) and was sustainable when the fuel flow rate was above $0.99 \frac{\text{g}}{\text{s}}$ ($\dot{H} = 18 \text{ kW}$)

When the deep soffit was installed, the values are

- when the burner was halfway between the rear and front walls, combustion was not sustainable when the fuel flow rate was below $0.19 \frac{\text{g}}{\text{s}}$ ($\dot{H} = 9 \text{ kW}$) and was sustainable when the fuel flow rate was above $0.24 \frac{\text{g}}{\text{s}}$ ($\dot{H} = 11 \text{ kW}$)
- when the burner was close to the rear wall, combustion was not sustainable when the fuel flow rate was below $0.19 \frac{\text{g}}{\text{s}}$ ($\dot{H} = 9 \text{ kW}$) and was sustainable when the fuel flow rate was above $0.28 \frac{\text{g}}{\text{s}}$ ($\dot{H} = 13 \text{ kW}$)

- when the burner was close to the front wall (the soffit), combustion was not sustainable when the fuel flow rate was below 0.19 g/s ($\dot{H} = 9 \text{ kW}$) and was sustainable when the fuel flow rate was above 0.28 g/s ($\dot{H} = 13 \text{ kW}$)

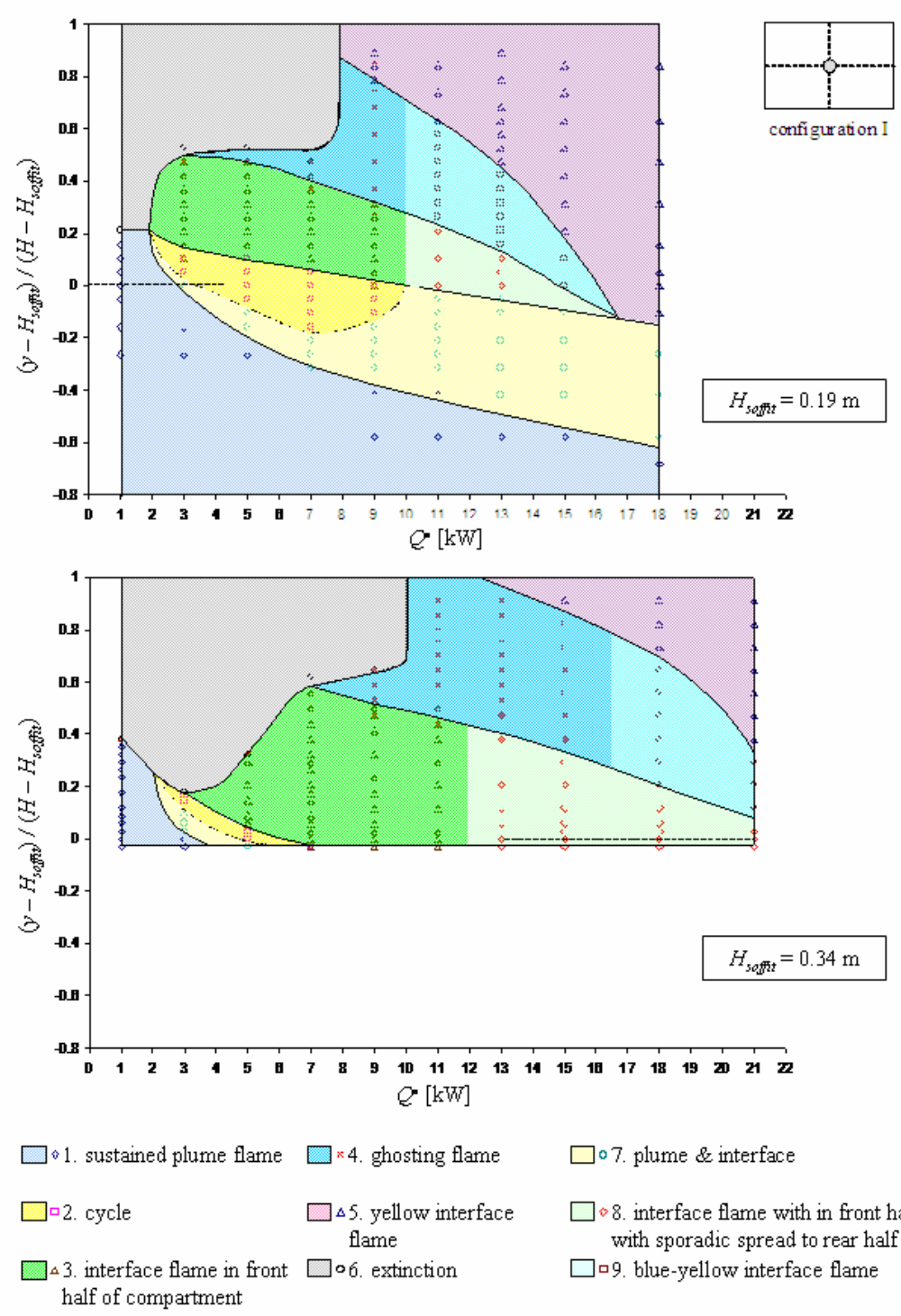


Fig. 3.43: Map of behaviour regimes from Coutin's study for the burner located half-way between the rear wall and the soffit. Top: behaviour when the shallow soffit is installed. Bottom: behaviour for the deep soffit

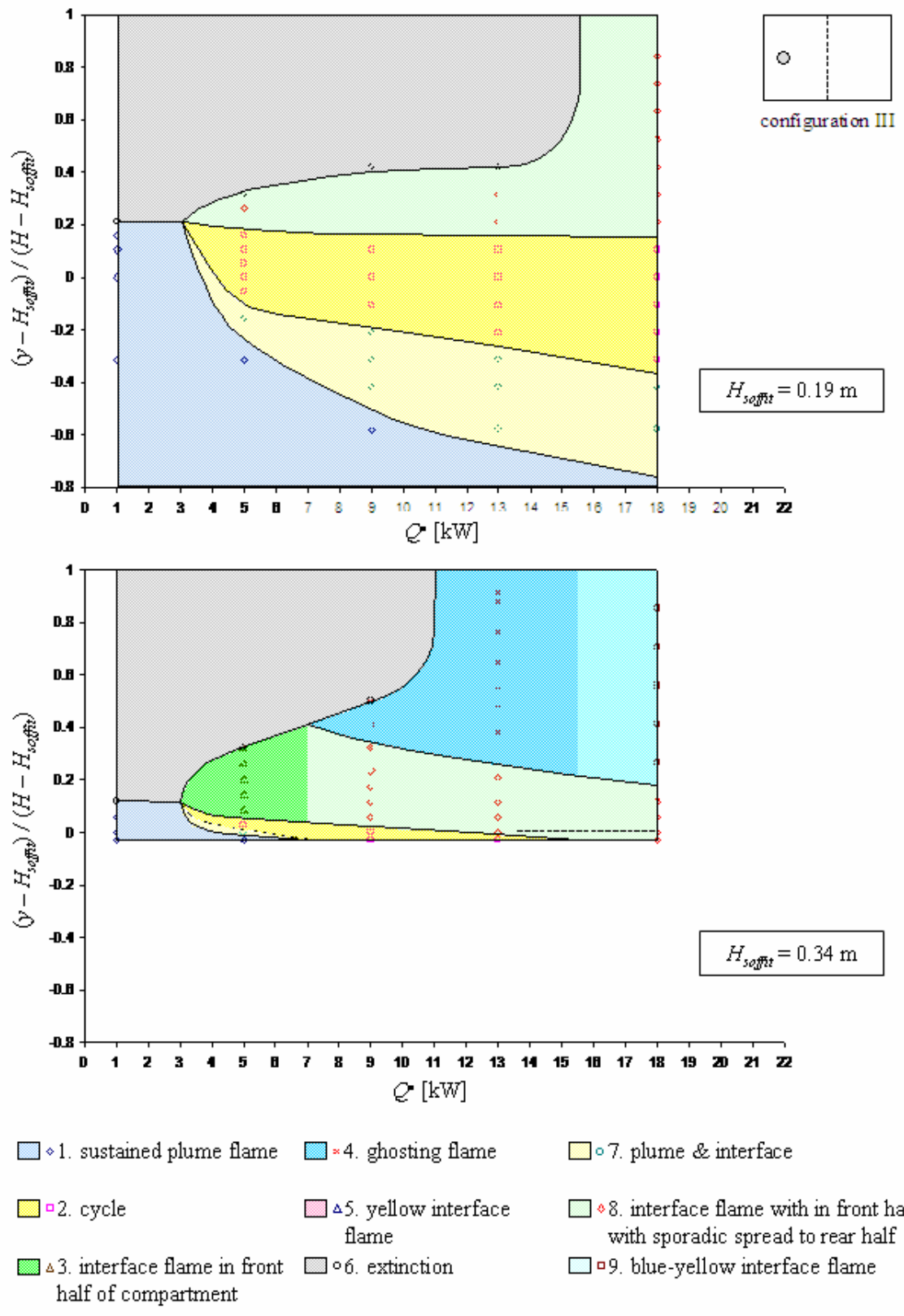


Fig. 3.44: Map of behaviour regimes from Coutin's study for the burner located close to the soffit. Top: behaviour when the shallow soffit is installed. Bottom: behaviour for the deep soffit

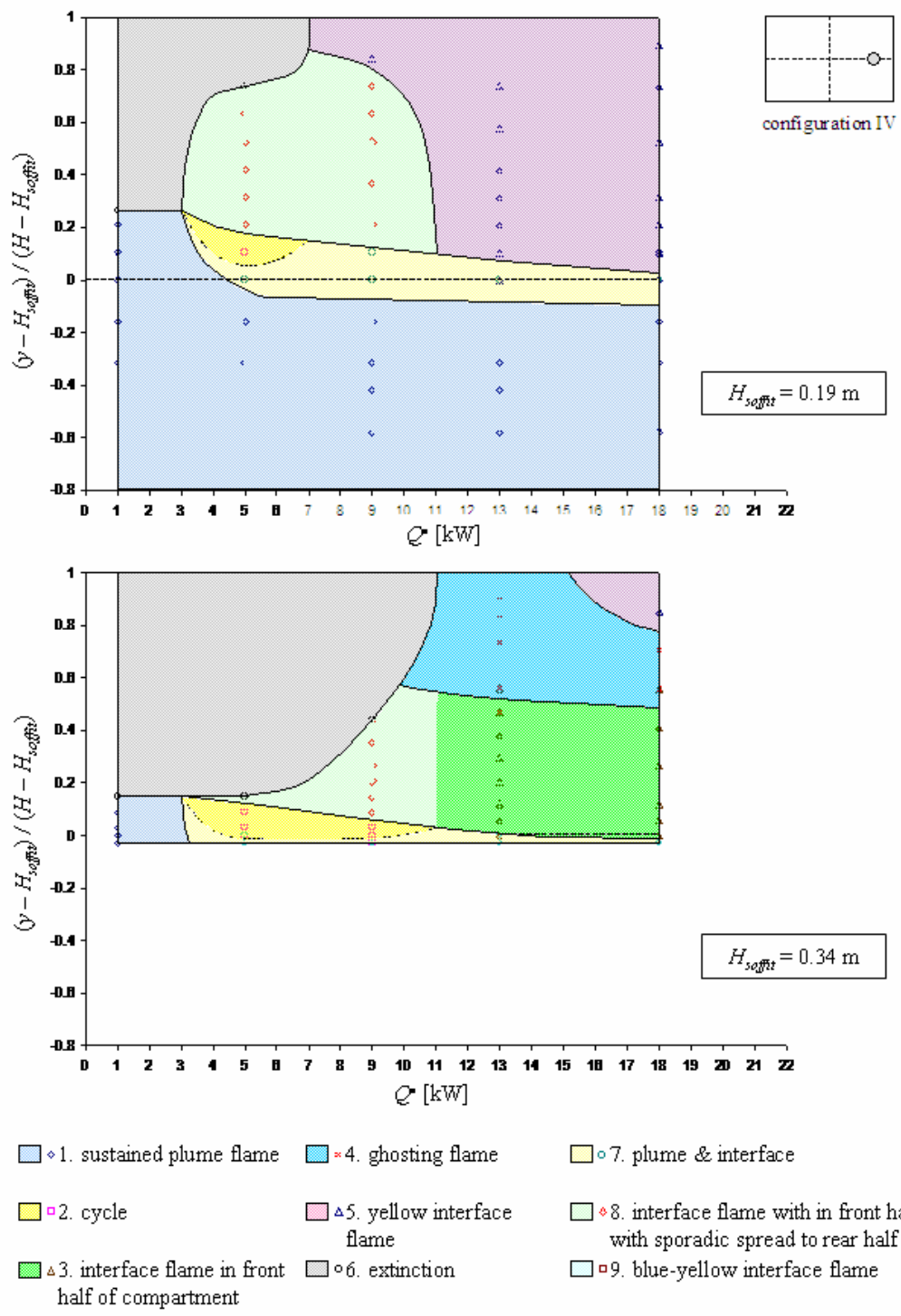


Fig. 3.45: Map of behaviour regimes from Coutin's study for the burner located close to the rear wall. Top: behaviour when the shallow soffit is installed. Bottom: behaviour for the deep soffit

4 Conclusion

An experimental study has been performed into the behaviour of compartment fires when the fuel source is located inside the vitiated zone trapped underneath the ceiling and into the mechanisms which control the behaviour. The influence of the fuel type, fuel flow rate, vent size and soffit depth on the behaviour was also studied.

Recordings of the light emitted by the flame were made to visualise the shape, size and colour of the flame. PIV measurements were performed to study the flow field inside the upper layer and the velocities around the flame and to determine the mass flow rate of air in through the vent. Measurements were performed of the temperature field and of the chemical composition of the upper layer. The minimum fuel flow rate required to sustain combustion was recorded, as was the size and shape of the two zones as a function of the parameters.

Inside the compartment, two clearly distinguishable layers exist – a layer of air in the lower part of the compartment, and above this a layer rich in fuel and combustion products and lean in oxygen. The flame is detached from the burner and is located at the interface between these two layers.

Within the layer of air there is a two-way flow: air enters the compartment through the lower part of the vent and travels towards the rear of the compartment in the lower part of the layer, and in the upper part of the layer it travels from the rear of the compartment forwards towards the vent and out of the compartment through the upper half of the vent.

It was shown that it is possible to sustain a flame irrespective of whether the fuel is heavier or lighter than air. This is in contrast to Morehart's observations [Morehart *et al* 1994a], [Morehart *et al* 1994b] involving a burner underneath a hood with air injected into the upper part of the hood, when combustion was sustainable only with a heavier-than-air fuel, but not with methane; this is probably due to the fact that in Morehart's configuration, a layer enriched with air must have formed above the layer of combustion products – a configuration which did not exist during the current work, where only fuel but no air was introduced into the zone trapped behind the soffit.

At fuel flow rates just above the minimum necessary to sustain combustion, the flame is blue. It partially covers the interface between the layers and extends out through the vent. Its size fluctuates substantially, whereby the fluctuations are aperiodic.

The blue colour is due to the combustion temperature being low, which is itself due to the fact that the fuel is mixed with combustion products as it moves from the burner to the reaction zone.

The velocity measurements and the observation of the shape of the flame show that there is a recirculatory flow inside the upper layer: fuel flows from the burner underneath the ceiling towards the rear of the compartment, then downwards parallel to the rear wall and finally towards the vent along the interface between the two layers until it reaches the reaction zone. Some of the combustion products from the reaction zone are entrained upwards into the upper layer. This recirculatory motion is driven by the thermal instability between the flame and the gases in the upper layer.

Along the interface between the lower layer of air and the upper layer of gas rich in fuel and combustion products and lean in oxygen, some mixing occurs, producing a stratified premixture.

The flame has the structure of a triple flame – a diffusion flame whose edge is made up of two premixed flames – a rich one above the diffusion flame and a lean one below. The premixed flames propagate towards the rear of the compartment through the flammable zone at the interface between the two layers. Fuel and air not consumed by the premixed flames then combust in the trailing diffusion flame.

The fluctuation of the size of the flame is caused by variations in the local flow velocity and species concentrations. These variations are produced, because the transport of air and gases to the flame are driven by buoyancy generated by the instantaneous heat release, but does not occur infinitely fast.

If the fuel flow rate is increased, the average size of the flame will increase and at the same time its colour will change from blue to orange. The average size of the flame is determined by the balance between the flow velocity of the gas and the velocity of the premixed flames propagating against the flow. The colour change is due to an increased temperature due to increased fuel concentration.

Above a certain fuel flow rate, a balance between these two velocities is not possible, and the flame propagates across the whole of the interface and attaches itself to the rear and side walls.

Due to the thermally stable stratification between the layer of air and the vitiated layer above it, mixing of air and fuel occurs by diffusion rather than through turbulence. This limits

the reaction rate and thus explains why the flame extends out through the vent: the fuel is not completely consumed before flowing out of the compartment.

Extinction will occur if the velocity of the premixed flame is too low to allow a balance between this velocity and the flow velocity of the gas.

Extinction will also occur if the concentration of fuel in the stream from the burner to the reaction zone is too low to sustain a diffusion flame.

The minimum flow rate required to sustain combustion increases if the soffit depth is increased or if the burner is located close to the rear or front wall rather than half-way between the two. The former can be attributed to an increase in the dilution of the fuel as it must travel a greater distance to reach the reaction zone, and possibly also to increased heat losses, as the upper layer is enclosed by a larger surface area of wall. The latter can be linked to the stability of the recirculation eddy in the upper zone: if the burner is close to the rear or front wall, a less stable eddy is produced.

The temperature in the upper layer increases with increasing fuel flow rate as long as the fuel flow rate remains lower than the amount necessary to produce flames which cover the whole of the interface between the upper and lower layers. When the flame covers the whole of this interface, the temperature in the upper layer remains constant, independent of further increases in the fuel flow rate or variations of the size of the vent

The study of the vent flow rate as a function of the fuel flow rate showed that the behaviour is different depending on whether the flame covered the whole or only part of the interface. At fuel flow rates which produce a flame partially covering the layer interface, the vent flow rate was found to be proportional to the one-third power of the fuel flow rate. At larger fuel flow rates, when the flame covers the whole of the interface, the vent flow rate is independent of the fuel flow rate. The vent flow is driven by buoyancy induced by the heat released by the flame. The variation in behaviour depending on whether the flame covers the whole or part of the interface must be linked to the fact that a discontinuity exists for the temperature.

The vent flow rate was found to be proportional to the two-thirds power of the width of the vent as long as the flame burns under fuel-controlled conditions.

If the vent is reduced in size, the upper layer increases in depth.

A transition from fuel-control to ventilation-control was observed when vent was too small to allow sufficient air to enter to feed a flame sufficiently large to cover the whole of the interface. This transition coincides with the upper layer being so large as to reach to the floor. This occurs when the internal part of the flame fulfils the criterion $\dot{Q}_{in} = 1500 \frac{\text{kW}}{\text{m}^{2.5}} F_V$.

It was found that the area covered by the flame is not proportional to the heat release rate. When the area is plotted against the fuel flow rate, a double inflection is found: At fuel flow rates below the critical minimum, there is no flame and thus a flame area of zero. With increasing fuel flow rate from the minimum, the area first rises steeply, then levels off, then increases in steepness again. Finally the area covered by the internal part of the flame plateaus as it reaches the extent of the space between the four walls while the external part continues to increase but with a lower rate of growth. The reason for this is unclear. One hypothesis is that it is linked to the increase in radiative heat loss as the flame changes colour, but this is not supported by the fact that the area covered by the flame does not change during the warmup period after ignition despite the fact that the colour of the flame changes during this period.

If the width of the vent is increased, the area covered by the flame remains constant as long as the flow remains laminar. As the flow velocity increases with decreasing vent size, there exists a critical size below which the flow is turbulent; as turbulence enhances the mixing between fuel and air, the fuel burns out more quickly and the flame is shorter.

References

- AUDOUIN, L.; SUCH, J. M.; MALET, J. C.; CASSELMAN, C., 1997: *A Real Scenario for a Ghosting Flame*, Fire Safety Science - proceedings of the fifth international conference, pp 1261-1272, Melbourne, AUS, 3-7 Mar 1997, ed: HASEMI Yuji; International Association for Fire Safety Science, Tsukaba, Japan
- BACKOVSKY, Jana; FOOTE, Kenneth; ALVARES, Norman J., 1989: *Temperature Profiles in Forced-Ventilation Enclosure Fires*; Fire safety science - proceedings of the second international symposium, pp 315-324, Tokyo, 13-17 Jun 1988, International Association for Fire Safety Science; Hemisphere Publishing Corp, New York
- BERTIN, Gilles, 1998: *Mise au Point d'un dispositif pour l'étude d'un feu de compartiment* ("Development of an installation for the study of a compartment fire"), Masters thesis, Conservatoire National des Arts et Métiers, Poitiers
- BERTIN, Gilles; MOST, Jean-Michel; COUTIN, Mickaël, 2002: *Wall behaviour in an under-ventilated room*, Fire Safety Journal; vol 37 (2002), pp 615-630
- BEYLER, Craig L., 1984: *Ignition and Burning of a Layer of Incomplete Combustion Products*, Combustion Science and Technology, vol 39 (1984), pp 287-303
- BEYLER, Craig L., 1986: *Major Species Production by Diffusion Flames in a Two-layer Compartment Fire Environment*; Fire Safety Journal, vol 10 (1986), pp 47-56
- COUTIN, Michael; GAUTIER, Bernard; MOST, Jean-Michel, 2000: *Behaviour of the Combustion of a Fuel Material in the Vitiated Upper Zone of an Open Compartment*, Fire and Explosions Hazards - Proceedings of the Third International Seminar, pp 155-166,
- COUTIN, Mickaël, 2000: *Étude expérimentale et théorique de l'influence de l'entraînement naturel de l'air sur le comportement d'une flamme représentative d'un incendie* ("Experimental and Theoretical Study of the influence of the natural air entrainment on the behaviour of a flame representing a compartment fire"), PhD thesis, Ensmat & Université de Poitiers –Faculté des Sciences Fondamentales et Appliquées, Poitiers
- COUTIN, Mickaël; MOST, Jean-Michel, 2003: *Aerodynamic characterization of a compartment fire as a function of its behaviour*, Fire Safety Science - proceedings of the seventh international symposium, pp 407-418, Worcester, MA, USA, 16-21 June 2002, ed: EVANS, David D., International Association for Fire Safety Science, Worcester, MA, USA
- Dantec Dynamics A/S, 2002: *An overview of the FlowMap systems and the FlowMap Acquisition and Control Units*, Dantec Dynamics A.S., Skovlunde, Denmark, (available under www.dantecmt.com/piv/system)
- DRYSDALE, Dougal, 1995: *Thermochemistry*, SFPE Handbook of Fire Protection Engineering, 2nd ed, pp 1-80 to 1-87, Society of Fire Protection Engineers, Quincy MA, USA
- DRYSDALE, Dougal, 1998: *An Introduction to Fire Dynamics*; 2nd edition, John Wiley & Sons, Chichester, W SUSSEX, UK
- Fire Experimental Unit & Home Office, 1997: *Backdraught*; UK Home Office
- Fire Experimental Unit & Home Office, 1997: *Fire Growth and Flashover*; UK Home Office

- FLEISCHMANN, Charles M.; PAGNI, Patrick J.; WILLIAMSON, R. Brady, 1994: *Exploratory Backdraft Experiments*, Fire safety science - proceedings of the fourth international symposium, pp 298-316, Ottawa, 14-17 Jun 1994, ed: KASHIGAWI, Takashi; International Association for Fire Safety Science, Ottawa
- FLEISCHMANN, Charles M., 1993: *Backdraught Phenomena*, PhD thesis, University of California, Berkley, CA
- Gebäudeversicherung des Kantons Bern, 1992: *Grossschadenanalyse 1986-91 im Kanton Bern*, Gebäudeversicherung des Kantons Bern, Bern, Switzerland
- GLASSMAN, Irwin, 1977: *Combustion*, Academic Press, New York
- GROSS, D.; ROBERTSON, A. F., 1965: *Experimental Fires in Enclosures*, Tenth Symposium (International) on Combustion, pp 931-942, Cambridge, UK, 17-21 Aug 1954, The Combustion Institute, Pittsburgh, PA, USA
- HAYASAKA Hiroshi; KUDOU Yuju; KOJIMA Hideyoshi; HASHIGAMI Tsutomu; ITO Jun; UEDA Takashi, 1998: *Burning rate in a small compartment fire*, Fire Science and Technology - Proceedings of the Third Asia-Oceania Symposium, pp 273-282, Singapore, 10-12 Jun 1998, ed: BUN Ching Chi; SUGAHARA Shinichi, Asia-Oceania Association for Fire Science and Technology, Singapore
- HAYASAKA Hiroshi; KUDOU Yuju; KOJIMA Hideyoshi; UEDA Takashi, 1996: *Backdraft Experiments in a small compartment*, Proceedings of 2nd International Symposium of Scale Modeling, pp97-109
- HINKLEY, P. L.; WRAIGHT, H. G. H.; THEOBALD, C. R., 1984: *The Contribution of Flames under Ceilings to Fire Spread in Compartments*, Fire Safety Journal, vol 7 no 3 (1984), pp 227-242
- KARLSSON, Björn; QUINTIERE, James G, 2000: *Enclosure Fire Dynamics*, CRS Press, Boca Raton,
- LAVISION, 2002: DaVis FlowMaster Manual, LaVision GmbH, Göttingen, Germany
- MOREHART, J. H.; ZUKOSKI, E. E.; KUBOTA, T., 1992: *Characteristics of Large Diffusion Flames in a Vitiated Atmosphere*, Fire Safety Science - Proceedings of third international symposium, pp 575-583,
- MOREHART, J. H.; ZUKOSKI, E. E.; KUBOTA, T., 1992: *Chemical Species Produced in Fires Near the Limit of Extinction*, Fire Safety Journal, vol 19 (1992), pp 177-188
- Office of the Deputy Prime Minister, 2005: *Fire Statistics, United Kingdom, 2003*, Office of the Deputy Prime Minister, London, UK
- OHMIYA, Y.; DELICHATSIOS, M. A.; SUZUKI, J.; KAKEGAWA, S.; HIROTA, M., 2003: *Burning Regimes in Fully Involved Enclosure Fires*, Fourth International Seminar on Fire and Explosion Hazards, pp 121-130, Londonderry, 8-12 Sept 2003, The University of Ulster, Newtownabbey, Co Antrim, N Ireland
- ORLOFF Lawrence, de RIS John, 1982: *Froude Modeling of Pool Fires*; Nineteenth Symposium (International) on Combustion, pp 885-865, Haifa, Israel, 8-13 Aug 1982, The Combustion Institute, Pittsburgh, PA, USA

- PHILLIPS, H., 1965: *Flame in a buoyant methane layer*, Tenth Symposium (International) on Combustion, pp 1277-1283, Cambridge, UK, 17-21 Aug 1954, The Combustion Institute, Pittsburgh, PA, USA
- POIREAULT, Bertrand, 1997: *Mécanisme de combustion dans un brûleur méthane-air de type « swirl » (40 kW): influence de l'intensité de la rotation*, PhD thesis, Ensma & Université de Poitiers - Faculté des Sciences Fondamentales et Appliquées, Poitiers
- PRAHL, J.; EMMONS, H. W., 1975: *Fire Induced Flow Through an Opening*, Combustion and Flame, vol 25 (1975), pp 369-385
- PRÉTREL, H.; SUCH, J. M.; LAZARDEUX, J., 2002: *Ceiling jet in under-ventilated pool fire compartment: experimental study from large scale tests*, Fire Safety Science - proceedings of the seventh international symposium, pp 1173, Worcester, MA, USA, 16-21 June 2002, ed: EVANS, David D., International Association for Fire Safety Science, Worcester, MA, USA
- QUINTIERE, James G., 2001: *Some Aspects of Fire Growth*, Fire and Explosions Hazards - Proceedings of the Third International Seminar, pp 85-102, Lake Windermere, 10-14 Apr 2000, ed: BRADLEY, Derek; DRYSDALE, Dougal; MAKHVILADZE, Georgy, Centre for Research in Fire and Explosion Studies, University of Central Lancashire, Preston, LANCS, 2001
- QUINTIERE, James G.; STECKLER, K.; CORLEY, G., 1984: *An Assessment of Fire Induced Flows in Compartments*; Fire Science and Technology, vol 4 (1984), pp 1-14
- SUGAWA Osami; KAWAGOE Kunio; OKA Yasushi; OGAHARA Ichi, 1989: *Burning Behaviour in a poorly ventilated compartment fire - Ghosting Fire*, Fire Science and Technology, vol 9 no 2 (1989), pp 5-14
- SUGAWA Osami; KAWAGOE Kunio; OKA Yasushi, 1991: *Burning Behaviour in a poorly ventilated compartment fire - Ghosting Fire*; Nuclear Engineering and Design, vol 125 no 3 (Mar 1991), pp 347-352
- SUTHERLAND, B. J., 1999: *Smoke Explosions*, MEng thesis, School of Engineering, University of Canterbury, Christchurch NZ (available under <http://www.firetactics.com/Smoke,%20Sutherland.pdf>)
- TAKEDA Hisahiro; AKITA Kazuo, 1981: *Critical Phenomenon in Compartment Fires with Liquid Fuels*, Eighteenth Symposium (International) on Combustion, pp 519-527, Waterloo, Canada, 17-22 Aug 1980, The Combustion Institute, Pittsburgh, PA, USA
- THOMAS, P. H.; HESELDEN, A. J. M., 1962: *Behaviour of Fully Developed Fire in an Enclosure*, Combustion and Flame, vol 6 (1962), pp 133-135
- WALTON, William D.; THOMAS, Philip H., 1995: *Estimating Temperatures in Compartment Fires*, SFPE Handbook of Fire Protection Engineering, 2nd ed, pp 3-134 to 3-147, Society of Fire Protection Engineers, Quincy MA, USA
- WILMOT, T, 2005: *World Fire Statistics; Information Bulletin of the World Fire Statistics*, The Geneva Association, Geneva, Switzerland

Annexe – Estimate of the Heat Losses

In the following, an estimate for the heat losses through the walls and for the convective heat flow through the vent is presented.

Basic Assumptions and Input Values

Temperatures

The temperature values used in the calculation are listed in *Table 4.1*. The temperature gradient of the wall surfaces in vertical direction is neglected, as the inaccuracy caused by this omission is less than the inaccuracy caused by uncertainty of the temperature measurements.

	temperature of inner surface [K]	temperature of outer surface [K]
ceiling:	650	350
upper part of walls:	650	350
window in upper part of wall	550	400
wall burner	500	300
windows in lower part of wall	400	350
fibreboard on floor	500	300
glass on floor	400	350
smoke layer	800	-
flame	1400	-

Table 4.1: Temperature values used in the calculation of the energy flows

Material Properties

Steel

In the calculations presented in this thesis, the thermal inertia of the steel and its effect on thermal conduction was neglected relative to the properties and effects of the insulation board.

Ceramic Fibreboard

The following values were provided by the manufacturer of the fibreboard [Unifrax, 2004]:

Thermal conductivity

The thermal conductivity is a function of temperature. The following values were provided by the manufacturer.

T [°C]	k [$\frac{W}{mK}$]
400	0.074
600	0.099
800	0.136
1000	0.154

Other values were calculated by linear extrapolation from the values for 400°C and 1000°C:

$$\begin{aligned} k &= (T - 400^\circ\text{C}) \left(\frac{0.154 \frac{W}{mK} - 0.074 \frac{W}{mK}}{1000^\circ\text{C} - 400^\circ\text{C}} \right) + 0.074 \frac{W}{mK} = \\ &= (T - 400^\circ\text{C}) 0.000133 \frac{W}{mK^2} + 0.074 \frac{W}{mK} \end{aligned} \quad (\text{A.1})$$

T [K]	k [$\frac{W}{mK}$]
400	0.04
475	0.05

As there is a temperature gradient inside the layers of fibreboard, there is also a gradient of the conductivity. Because the heat loss through the fibreboard is a lot lower than the loss through the windows, as a first approximation, values are taken for the mean temperature within each panel.

Density

The density of the fibreboard was given by the manufacturer as

$$\rho_{fibreboard} = 240 \text{ kg/m}^3 \quad (\text{A.2}).$$

Emissivity

As the inner surfaces of the fibreboard are covered in soot, a value of unity was used for the emissivity of the fibreboard.

Ceramic Glass

The supplier of the ceramic glass was not able to provide information on the physical properties of this material. In absence of specific data, a typical value for ceramics was taken for the thermal conductivity [Berger *et al*, 1997]

$$k_{glass} = 0.5 \text{ W/mK} \quad (\text{A.3}).$$

For the emissivity, a typical value for glass was taken from [Berger *et al*, 1997]

$$\varepsilon_{glass} = 0.94 \quad (\text{A.4}).$$

Wall Burner

The burner incorporated into the lower part of the rear walls is made up of the plaque of bronze beads, an air chamber, a sheet of steel and a sheet of fibreboard. It is modelled in the following as a sheet of metal of “medium” conductivity, e.g. zink or nickel, of a thickness of 0.1 m. The thermal conductivity was set at [Berger *et al*, 1997]

$$k_{wallburner} = 1.0 \text{ W/mK} \quad (\text{A.5}).$$

The emissivity was set at unity, as the burner is covered in a layer of soot.

Heat Losses through Walls

Heat Loss through the Individual Surfaces

For each surface, the heat conduction was estimated from measured temperatures of the inner and outer surfaces, and from the thermal conductivity.

Floor:

The floor measures 0.62 m in length by 0.4 m in width. It has a window of ceramic glass in its centre, measuring 0.24 m long by 0.18 m wide by 0.005 m thick. The rest of the floor is covered with fibreboard of 0.05 m thickness.

$$\begin{aligned} \dot{Q}_{conv-floor} &\approx (T_{fibreboard-in} - T_{fibreboard-out}) \left(\frac{k_{fibreboard}}{\delta_{fibreboard}} \cdot (L \cdot W - L_{window} \cdot W_{window}) \right) + \\ &\quad + (T_{glass-in} - T_{glass-out}) \left(\frac{k_{glass}}{\delta_{glass}} \cdot (L_{window} \cdot W_{window}) \right) = \\ &= 200 \text{ K} \left(\frac{0.04 \text{ W/mK}}{0.05 \text{ m}} (0.62 \text{ m} \cdot 0.4 \text{ m} + 0.24 \text{ m} \cdot 0.18 \text{ m}) \right) + \\ &\quad + 100 \text{ K} \cdot \left(\frac{0.5 \text{ W/mK}}{0.005 \text{ m}} \cdot (0.24 \text{ m} \cdot 0.18 \text{ m}) \right) = \\ &= 50 \text{ W} + 430 \text{ W} = 480 \text{ W} \quad (\text{A.6}) \end{aligned}$$

Rear Wall:

The lower part of the rear wall is taken up by the wall burner. The upper part is covered in a layer of fibreboard 0.05 m thick and a layer of steel. The presence of the steel is neglected, as its influence is less than that of the inaccuracy of the material properties of the fibreboard of the temperature measurements.

$$\dot{Q}_{conv-rear/upper} \approx 300 \text{ K} \frac{k_{wallburner}}{\delta_{wallburner}} H_{soffit} W = 200 \text{ K} \frac{0.5 \text{ W/mK}}{0.1 \text{ m}} \cdot 0.5 \text{ m} \cdot 0.4 \text{ m} = 200 \text{ W} \quad (\text{A.7})$$

$$\begin{aligned} \dot{Q}_{conv-rear/upper} &\approx 300 \text{ K} \frac{k_{fibreboard}}{\delta_{fibreboard}} (H_0 - H_{soffit}) W = 300 \text{ K} \frac{0.05 \text{ W/mK}}{0.05 \text{ m}} \cdot 0.35 \text{ m} \cdot 0.4 \text{ m} = \\ &= 40 \text{ W} \end{aligned} \quad (\text{A.8})$$

Right Wall:

The lower part of the right wall is made up of a window, 0.62 m long, 0.5 m high, and 0.005 m thick. The upper part is fibreboard, 0.62 m long, 0.34 m high and 0.05 m thick. The steel sheet is neglected in the calculations.

$$\dot{Q}_{conv-right/lower} \approx 50 \text{ K} \frac{k_{glass}}{\delta_{glass}} (H_0 - H_{soffit}) W = 50 \text{ K} \frac{0.5 \text{ W/mK}}{0.005 \text{ m}} \cdot 0.5 \text{ m} \cdot 0.62 \text{ m} = 1550 \text{ W} \quad (\text{A.9})$$

$$\begin{aligned} \dot{Q}_{conv-right/upper} &\approx 300 \text{ K} \frac{k_{fibreboard}}{\delta_{fibreboard}} (H_0 - H_{soffit}) W = 300 \text{ K} \frac{0.05 \text{ W/mK}}{0.05 \text{ m}} \cdot 0.35 \text{ m} \cdot 0.62 \text{ m} = \\ &= 70 \text{ W} \end{aligned} \quad (\text{A.10})$$

Left Wall:

The lower part of the left wall is identical to the lower part of the right wall. The upper part incorporates a window of 0.42 m in length and 0.14 m in height.

$$\dot{Q}_{conv-left/lower} = \dot{Q}_{conv-right/lower} \approx 1550 \text{ W} \quad (\text{A.11})$$

$$\begin{aligned} \dot{Q}_{conv-left/upper} &\approx 300 \text{ K} \frac{k_{fibreboard}}{\delta_{fibreboard}} ((H_0 - H_{soffit}) L - A_{window}) + 150 \text{ K} \frac{k_{glass}}{\delta_{glass}} A_{window} = \\ &= 300 \text{ K} \frac{0.05 \text{ W/mK}}{0.05 \text{ m}} (0.62 \text{ m} \cdot 0.35 \text{ m} - 0.42 \text{ m} \cdot 0.14 \text{ m}) + \\ &\quad + 150 \text{ K} \frac{0.5 \text{ W/mK}}{0.005 \text{ m}} \cdot 0.42 \text{ m} \cdot 0.14 \text{ m} = \\ &= 50 \text{ W} + 880 \text{ W} = 930 \text{ W} \end{aligned} \quad (\text{A.12})$$

Front Wall (Soffit):

The soffit is a sheet of fibreboard, 0.34 m high by 0.4 m wide by 0.05 m thick.

$$\dot{Q}_{conv-soffit} \approx 300 \text{ K} \frac{k_{fibreboard}}{\delta_{fibreboard}} (H_0 - H_{soffit}) W = 300 \text{ K} \frac{0.05 \text{ W/mK}}{0.05 \text{ m}} 0.34 \text{ m} \cdot 0.4 \text{ m} = 40 \text{ W} \quad (\text{A.13})$$

Ceiling:

The soffit is a sheet of fibreboard, 0.62 m long by 0.4 m wide by 0.05 m thick.

$$\begin{aligned} \dot{Q}_{conv-ceiling} &\approx 300 \text{ K} \frac{k_{fibreboard}}{\delta_{fibreboard}} (H_0 - H_{soffit}) W = 300 \text{ K} \frac{0.05 \text{ W/mK}}{0.05 \text{ m}} 0.62 \text{ m} \cdot 0.4 \text{ m} = \\ &= 70 \text{ W} \end{aligned} \quad (\text{A.14})$$

Total

$$\begin{aligned} \dot{Q}_{cond} &\approx \underbrace{480 \text{ W}}_{\text{floor}} + \underbrace{200 \text{ W} + 40 \text{ W}}_{\text{rear}} + \underbrace{1550 \text{ W} + 70 \text{ W}}_{\text{right}} + \underbrace{1550 \text{ W} + 930 \text{ W}}_{\text{left}} + \underbrace{40 \text{ W}}_{\text{soffit}} + \\ &+ \underbrace{70 \text{ W}}_{\text{ceiling}} = 4.9 \text{ kW} \end{aligned} \quad (\text{A.15})$$

Sensitivity Analysis

The losses through the surfaces covered by fibreboard make less than 10 % of the total. Inaccuracies in these components, such as inaccurate temperature measurements, are of little consequence.

In contrast the flow of heat through the windows in the lower part of the compartment makes up over half the total. The input data for these components is of very limited reliability – the temperature has not been measured directly and the conductivity is estimated from that for other materials rather than from manufacturer's data. Inaccuracies in the input values cause large errors in the resulting value: a variation of the temperatures by 20 K or a variation of the conductivity by 25 % would alter the total heat loss by over a kilowatt

Discussion

The calculated value for the heat losses is in the order of half the heat release rate. The largest contribution is made by the windows; over half the total heat loss is through the side windows, roughly 20 % through the window in the upper half and about 10 % is through the window in the floor.

It has not yet been possible to determine what proportion of the heat release occurs within the compartment, but the conductive heat losses must equate to a large proportion of the heat released inside the compartment. As the accuracy available data on the surface temperatures and the heat conductivity of the ceramic glass is limited, it may be that a more accurate estimate of the conductive heat losses would be obtained by calculating the convective heat transfer through the vent and estimating the heat release inside the compartment.

Convective Heat Transfer through the Vent

The convective heat transfer can be divided up into the parts linked to the flow of uncombusted fuel, the flow of air and the flow of combustion products.

$$\begin{aligned}\dot{Q}_{conv} &= \dot{Q}_{conv_F} + \dot{Q}_{conv_CP} + \dot{Q}_{conv_A} = \\ &= -\dot{m}_{F-vent}c_{p_F}\Delta T_F - \dot{m}_{CP-vent}c_{p_CP}\Delta T_{CP} - \dot{m}_{A-vent-exit}c_{p_A}\Delta T_A\end{aligned}\quad (\text{A.16})$$

The mass balance dictates the following relationships:

$$\dot{m}_{F-vent} = \dot{m}_{F_burner} - \dot{m}_{F_react-in}\quad (\text{A.17})$$

$$\dot{m}_{A-vent} = \dot{m}_{Ain_burner} - \dot{m}_{A_react-in}\quad (\text{A.18})$$

$$\dot{m}_{CP-vent} = \dot{m}_{F_react-in} + \dot{m}_{A_react-in}\quad (\text{A.19})$$

Therefore:

$$\begin{aligned}\dot{Q}_{conv} &= -(\dot{m}_{F_Burner} - \dot{m}_{F_react-in})c_{p_F}\Delta T_F - \dot{m}_{F_react-in}(1+r)c_{p_CP}\Delta T_{CP} - \\ &\quad -(\dot{m}_{A-in} - \dot{m}_{F_react-in}r)c_{p_A}\Delta T_A\end{aligned}\quad (\text{A.20})$$

The proportion of fuel which is combusted inside the compartment is not yet known, and consequently it is currently only possible to estimate orders of magnitude. If the fuel flow rate

is in the order of $0.3 \frac{\text{g}}{\text{s}}$ and about half of this is combusted inside the compartment, and if the flow rate of air entering the compartment is taken as $30 \frac{\text{g}}{\text{s}}$, we obtain:

$$\begin{aligned} \dot{Q}_{conv} = O & \left(-0.15 \frac{\text{g}}{\text{s}} \cdot 1.7 \frac{\text{kJ}}{\text{kmolK}} \cdot 480 \text{K} - 0.15 \frac{\text{g}}{\text{s}} \cdot (1 + 15.6) \cdot 1 \frac{\text{kJ}}{\text{kmolK}} \cdot 480 \text{K} - \right. \\ & \left. - 30 \frac{\text{g}}{\text{s}} \cdot 1 \frac{\text{kJ}}{\text{kgK}} \cdot 30 \text{K} \right) = O(-0.1 \text{kW} - 1.2 \text{kW} - 0.9 \text{kW}) = O(-2.1 \text{kW}) \quad (\text{A.21}). \end{aligned}$$

Conclusions

If we combine the assumption that about $0.15 \frac{\text{g}}{\text{s}}$ of fuel is combusted inside the compartment, this gives an internal heat release rate of about 7 kW. If about 2 kW are convected out of the compartment, then the conductive heat losses must be about 5 kW. The fact that this figure is so close to the value obtained in (A.21) is probably to a certain extent coincidental rather than being any indicator that the assumptions made on the previous pages.

References

- BERGER, C.; BURR, A.; HABIG, K.-H.; HARSCH, G.; KLOOS, K. H.; SPECKHARDT, H., 1997;
 STEPHAN, K, 1997: *Werkstofftechnik, Dubbel – Taschenbuch für den Maschinenbau*, 19th
 ed, Springer, Berlin
- UNIFRAX, 2004: *Panneau Isofrax® 1260 C*, Unifrax, Paris

RÉSUMÉ

Ce travail a pour but d'identifier les régimes de combustion se développant lors d'un feu de compartiment, la source de combustible étant située dans la zone piégée par un linteau. Le comportement de la flamme est étudié en fonction de la géométrie de l'enceinte, du débit et du type de combustible, et du facteur de ventilation. Une enceinte est réalisée, des visualisations de l'émission de la flamme, des mesures de vitesse, de température et de composition des espèces chimiques sont effectuées.

Une flamme se stabilise à l'aide d'une *flamme triple* à l'interface entre les zones ventilées du compartiment et non ventilée au dessus du niveau du linteau. Cette structure réactive ainsi que la mesure d'aire de la flamme permet de dégager des comportements du feu en fonction des conditions expérimentales. La flamme est stable dès que la vitesse de propagation de la flamme prémélangée devient supérieure ou égale à la vitesse de convection naturelle. Deux régimes de combustion sont observés, l'un est contrôlé par le combustible disponible (fort débit injecté), l'autre par l'air entrant dans l'enceinte pour les faibles facteurs de ventilation. La transition de ce régime de flamme vers un embrasement de cibles combustibles est également abordée.

ABSTRACT

This study aimed at identifying the combustion regimes which develop during a compartment fire with a fuel source located in the zone trapped behind a soffit. The behaviour of the flame was studied as a function of the geometry of the compartment, the flow rate and type of fuel and the ventilation factor. An experimental compartment was built, and visualisations of the light emitted by the flame, and measurements of velocity, temperature and chemical composition were performed.

A flame is stabilised by a triple flame at the interface between the ventilated zone in the lower part of the compartment and the unventilated zone above the level of the soffit. This reactive structure, together with the measurement of the area of the flame, allows the behaviour of the fire to be determined as a function of the experimental conditions. The flame is stable when the propagation velocity of the premixed flame is higher or equal to the velocity of the convective flow. Two combustion regimes are observed, one controlled by the available fuel (flowrate introduced), the other controlled by the air entering the compartment, occurring when the ventilation factor is low. The transition from this flame regime to involvement of flammable targets is studied.

Mots clé :

combustion

bâtiments incendies et prévention des incendies

flamme de diffusion